

# **A Method to Prioritize Sources for Reducing High PM<sub>2.5</sub> Exposures in Environmental Justice Communities in California**

Joshua S. Apte (principal investigator)  
Sarah E. Chambliss  
Christopher W. Tessum  
Julian D. Marshall

Contract Number: 17RD006

Contractor Organization:  
The University of Texas at Austin  
301 E. Dean Keeton St. Stop C1700,  
Austin, Texas 78712-0273  
(512) 232-6039

November 21, 2019

Prepared for the California Air Resources Board and the California  
Environmental Protection Agency

The statements and conclusions in this Report are those of the contractor and not necessarily those of the California Air Resources Board. The mention of commercial products, their source, or their use in connection with material reported herein is not to be construed as actual or implied endorsement of such products.

## Prepared By:

Joshua S. Apte, Principal Investigator  
Department of Civil, Architectural, and Environmental Engineering  
The University of Texas at Austin

Sarah E. Chambliss  
Department of Civil, Architectural, and Environmental Engineering  
The University of Texas at Austin

Christopher W. Tessum  
Department of Civil and Environmental Engineering  
University of Washington

Julian D. Marshall  
Department of Civil and Environmental Engineering  
University of Washington

Suggested citation: Apte, J. S., Chambliss, S. E., Tessum, C. W., Marshall, J.D. (2019). *A Method to Prioritize Sources for Reducing High PM<sub>2.5</sub> Exposures in Environmental Justice Communities in California*. Sacramento, CA: California Air Resources Board and California Environmental Protection Agency.

## Acknowledgements

Thank you to key personnel associated with the project:  
Contract managers: Qunfang “Zoe” Zhang and Patrick Wong, California Air Resources Board

This Report was submitted in fulfillment of Contract Number: 17RD006, A Tool to Prioritize Sources for Reducing High PM<sub>2.5</sub> Exposures in Environmental Justice Communities in California by the University of Texas at Austin under the sponsorship of the California Air Resources Board. Work was completed as of November 30, 2019.

## Table of Contents

<b>ACKNOWLEDGEMENTS</b> .....	<b>III</b>
<b>LIST OF FIGURES</b> .....	<b>VII</b>
<b>LIST OF TABLES</b> .....	<b>IX</b>
<b>ABSTRACT</b> .....	<b>X</b>
<b>EXECUTIVE SUMMARY</b> .....	<b>XI</b>
BACKGROUND .....	XI
OBJECTIVES AND METHODS .....	XI
RESULTS .....	XII
CONCLUSIONS .....	XII
<b>INTRODUCTION</b> .....	<b>1</b>
PUBLIC HEALTH AND PM <sub>2.5</sub> EXPOSURE METRICS .....	1
METHODS FOR DEVELOPING INTAKE FRACTION VALUES .....	1
INTAKE METRICS AND ENVIRONMENTAL JUSTICE .....	3
THE IF DATABASE: SCREENING TOOL FOR POLICY AND ENVIRONMENTAL JUSTICE ISSUES....	4
<b>METHODS</b> .....	<b>7</b>
THE INTERVENTION MODEL OF AIR POLLUTION (INMAP) .....	7
<i>Source-Receptor Matrix</i> .....	10
DEMOGRAPHIC DATA .....	12
<i>Joining Census Data to InMAP Model</i> .....	14
EJ METRIC CALCULATION .....	15
EMISSIONS DATA .....	19
TOOL LIMITATIONS .....	19
EXAMPLE APPLICATION OF IF DATABASE TO EVALUATE ENVIRONMENTAL JUSTICE CONCERNS	
.....	20
<i>Step 1: Assemble emissions inventory</i> .....	20
<i>Step 2: Align emissions location with iF grid</i> .....	20
<i>Step 3: Look up relevant iF values for pollutant species and height</i> .....	20
<i>Step 4: Calculate intake and population-weighted metrics</i> .....	21
<b>RESULTS</b> .....	<b>22</b>
SUMMARY OF INTAKE FRACTION DATABASE .....	22
<i>Intake Fraction Differences by Demographic Group</i> .....	25
<i>Localized Intake Fraction Patterns</i> .....	27
VISUAL REPRESENTATION OF INTAKE CALCULATION FROM EMISSIONS AND INTAKE FRACTION	
.....	29
SECTOR-SPECIFIC ENVIRONMENTAL JUSTICE IMPACTS .....	31
<i>Effects across all sectors</i> .....	31
<i>Agriculture</i> .....	36
<i>Construction</i> .....	38
<i>Cooking</i> .....	40
<i>Electricity Generation</i> .....	42

<i>Fugitive Dust</i> .....	44
<i>Industrial Sources</i> .....	46
<i>Miscellaneous</i> .....	49
<i>Natural Gas and Petroleum</i> .....	51
<i>Off-Road Mobile Sources</i> .....	53
<i>On-Road Mobile Sources</i> .....	55
<i>Residential Sources</i> .....	57
<b>DISCUSSION</b> .....	<b>59</b>
FINDINGS FROM THE IF SPATIAL DATABASE .....	59
SECTOR-SPECIFIC ENVIRONMENTAL JUSTICE IMPACTS .....	61
<b>SUMMARY AND CONCLUSIONS</b> .....	<b>62</b>
<b>RECOMMENDATIONS FOR FURTHER RESEARCH</b> .....	<b>63</b>
<b>REFERENCES</b> .....	<b>64</b>
<b>GLOSSARY OF TERMS, ABBREVIATIONS, AND SYMBOLS</b> .....	<b>67</b>

## **APPENDIX A: BENCHMARK INTAKE FRACTION VALUES**

Appendix A includes three tables and a brief description of intake fraction estimates from peer-reviewed literature.

## **APPENDIX B: MODEL EVALUATION AND UNCERTAINTY**

Appendix B describes sources of uncertainty from the InMAP model and provides comparisons against other modeling and empirical measurements of PM<sub>2.5</sub>

OUTLIER EXCLUSION.....	B1
OMISSION OF NON-CALIFORNIA AND BIOGENIC EMISSIONS .....	B2
METRICS FOR MODEL EVALUATION.....	B2
MODEL ERROR AND BIAS .....	B3
<i>Satellite remote sensing</i> .....	B3
<i>Monitoring network</i> .....	B4
BASELINE CONCENTRATION DIFFERENCES.....	B5
IMPLICATIONS FOR SOURCE-SPECIFIC EJ COMPARISONS .....	B6

## **APPENDIX C: SECTOR CATEGORY DESCRIPTIONS AND EMISSIONS BREAKDOWN**

Appendix C provides tables of emission totals within the modeling domain for each source category based on the input data from the US NEI. It also describes in more detail the specific source types and emission-generating activity within each of the source categories.

## **APPENDIX D: IN-DEPTH INTAKE FRACTION DATABASE**

Appendix D provides ten tables with additional intake fraction summary values, including population-weighted intake fraction for all demographic groups, emissions-weighted intake fraction for all demographic groups, and source-specific emissions-weighted intake fraction by sector and subsector.

## **APPENDIX E: ENVIRONMENTAL JUSTICE METRIC TABLES**

Appendix E provides 144 additional tables of EJ metrics supporting the graphics shown in the main report: population-weighted exposure concentration totals, absolute difference in population-weighted exposure concentration, and percent difference in population-weighted exposure concentration from the population as a whole. Tables are divided by sector and demographic groupings.

## **APPENDIX F: DESCRIPTION OF ADDITIONAL DATA**

Appendix F includes a list and description of data files created for this project which are available from the California Air Resources Board

## List of Figures

Figure 1: InMAP model domain for California. ....	9
Figure 2: Inset of the InMAP domain for the San Francisco Bay Area.....	10
Figure 3: Illustration of Source-Receptor Matrix.....	11
Figure 4: InMAP grid overlaying census block groups in the San Francisco area. ....	14
Figure 5: Illustration of intake calculation from an S-R matrix. ....	16
Figure 6: Location of example facility in Richmond, in the north east Bay Area (left) and the location of the facility within the iF grid (right). ....	20
Figure 7: Intake fraction in Los Angeles for ground-level emissions of primary PM <sub>2.5</sub> . ...	27
Figure 8: Intake fraction in Los Angeles for formation of particulate NO <sub>3</sub> from emissions of NO <sub>x</sub> at an elevation of 57 – 140 meters. ....	28
Figure 9: Area charts showing total population intake of PM <sub>2.5</sub> from each emitted species as the product of annual sector ground-level emissions and sector-specific intake fraction. ....	30
Figure 10: Contribution of all sectors to population-weighted average exposure concentration for different demographic categories. ....	31
Figure 11: All-sector relative percent differences in population-weighted average PM <sub>2.5</sub> concentration compared to total population average, shown by race-ethnicity (colored circle icons) and by each income quintile in each racial-ethnic category (gray square icons). ....	35
Figure 12: Agricultural sector: contribution of sector categories to population-weighted average exposure concentration for different demographic groups. ....	36
Figure 13: Agricultural sector: relative percent differences in population-weighted average PM <sub>2.5</sub> concentration compared to total population average for categories. ....	37
Figure 14: Construction sector: contribution of construction sector categories to population-weighted average exposure concentration for different demographic groups. ....	38
Figure 15: Construction sector: relative percent differences in population-weighted average PM <sub>2.5</sub> exposure concentration compared to total population average for categories. ....	39
Figure 16: Cooking: contribution to population-weighted average exposure concentration for different demographic groups. ....	40
Figure 17: Cooking: relative percent differences in population-weighted average PM <sub>2.5</sub> concentration compared to total population average. ....	41
Figure 18: Electricity generation: contribution of sector categories to population-weighted average exposure concentration for different demographic groups.....	42
Figure 19: Electricity generation: relative percent differences in population-weighted average PM <sub>2.5</sub> concentration compared to total population average for categories. ....	43
Figure 20: Fugitive dust: contribution of fugitive dust categories to population-weighted average exposure concentration for different demographic groups. ....	44
Figure 21: Fugitive dust: relative percent differences in population-weighted average PM <sub>2.5</sub> concentration compared to total population average.....	45
Figure 22: Industrial sector: contribution of industrial sector categories to population-weighted average exposure concentration for different demographic groups.....	46
Figure 23: Industrial sector: relative percent differences in population-weighted average PM <sub>2.5</sub> concentration compared to total population average.....	48

Figure 24: Miscellaneous sources: contribution to population-weighted average exposure concentration for different demographic groups. ....	49
Figure 25: Miscellaneous sources: relative percent differences in population-weighted average PM <sub>2.5</sub> concentration compared to total population average. ....	50
Figure 26: Natural gas and petroleum: contribution to population-weighted average exposure concentration for different demographic groups. ....	51
Figure 27: Natural gas and petroleum: relative percent differences in population-weighted average PM <sub>2.5</sub> concentration compared to total population average. ....	52
Figure 28: Off-road mobile sources: contribution to population-weighted average exposure concentration for different demographic groups. ....	53
Figure 29: Off-road mobile sources: relative percent differences in population-weighted average PM <sub>2.5</sub> concentration compared to total population average. ....	54
Figure 30: On-road mobile sources: contribution to population-weighted average exposure concentration for different demographic groups. ....	55
Figure 31: On-road mobile sources: relative percent differences in population-weighted average PM <sub>2.5</sub> concentration compared to total population average. ....	56
Figure 32: Residential sector: contribution to population-weighted average exposure concentration for different demographic groups. ....	57
Figure 33: Residential sector: relative percent differences in population-weighted average PM <sub>2.5</sub> concentration compared to total population average. ....	58

## List of Tables

Table 1: Summary of 2016 American Community Survey demographic data within the modeling domain. ....	13
Table 2: Racial-ethnic composition of each income quintile.....	13
Table 3: Share of racial-ethnic group in each income quintile* .....	14
Table 4: Metrics for population exposure. ....	15
Table 5: Metrics for environmental justice analysis.....	18
Table 6: Ground-level iF values for facility in Richmond. ....	21
Table 7: Example impact metrics for Richmond facility. ....	21
Table 8: Population-weighted iF summary values (ppm) for the total population.....	23
Table 9: Emissions-weighted iF summary values (ppm) for the total population. ....	24
Table 10: Emissions-weighted intake fraction (ppm) by income quintile .....	24
Table 11: Emissions-weighted intake fraction (ppm) by racial-ethnic group .....	25
Table 12: Relative percent difference in emissions-weighted per-capita intake fraction (% difference from total population per-capita iF) by income quintile.....	26
Table 13: Relative percent difference in emissions-weighted per-capita intake fraction (% difference from total population per-capita iF) by racial-ethnic group .....	26
Table 14: Difference in population-weighted exposure concentration to PM <sub>2.5</sub> by race-ethnicity (units: µg/m <sup>3</sup> , relative percent difference). ....	33
Table 15: Difference in population-weighted exposure concentration to PM <sub>2.5</sub> by income category (units: µg/m <sup>3</sup> , relative percent difference).....	33
Table 16: Difference in population-weighted exposure concentration to PM <sub>2.5</sub> by age category (units: µg/m <sup>3</sup> , relative percent difference).....	34
Table 17: Difference in population-weighted exposure concentration to PM <sub>2.5</sub> by other socioeconomic status categories (units: µg/m <sup>3</sup> , relative percent difference).....	34

## Abstract

This study developed and utilized a method based on intake fraction for evaluating inequality in exposure to fine particulate matter (PM<sub>2.5</sub>). The method utilizes a spatial database built from a reduced-complexity chemical transport model and census data for groups of different ages, income levels, and race/ethnicity. Given information on location and emission rates of PM<sub>2.5</sub> or precursor emissions (NO<sub>x</sub>, SO<sub>2</sub>, NH<sub>3</sub>, or VOCs), one can calculate, for a specific source, the amount of PM<sub>2.5</sub> inhaled by the total population and exposure differences among demographic groups. Applying this method to an inventory of anthropogenic emissions sources in California shows differences in per-capita exposure concentration of up to 15% by income and 35% by race-ethnicity. The two top sources of exposure, on-road vehicles and industrial activity, contribute most to exposure concentration disparity by race-ethnicity in absolute terms. Some minor sources, such as petroleum refining and outdoor emissions from commercial cooking, result in higher percentages of exposure differences among demographic groups. Patterns in exposure disparity vary among population groups, with some source categories most severely affecting one particular group. This impact-oriented evaluation of emission sources can help decision makers to screen emission-reduction targets for further investigation in order to achieve environmental justice goals.

## Executive Summary

### Background

Long-term exposure to PM<sub>2.5</sub> increases the risk of heart disease, lung disease, stroke, and numerous other health problems. Improving public health by reducing levels of PM<sub>2.5</sub> is a goal shared by policymakers and community leaders in California. Although policies in California have effectively reduced PM<sub>2.5</sub> pollution, not all communities have benefitted equally from improvement in air quality. Seeking a more equitable distribution of benefits is a matter of environmental justice (EJ).

Policymaking guided by environmental justice principles aims to find pollution reduction strategies that specifically benefits groups that are most vulnerable to air pollution health risks due to high exposure levels and other socioeconomic factors. EJ-oriented policy making also aims to involve members of vulnerable communities in the decision-making process.

The first EJ policy goal, is to reduce emissions from sources with a disproportionate impact on low-income groups, racial-ethnic minority groups, or other communities with lower socioeconomic status. Determining which sources to target requires highly technical research. A vast array of sources contribute to PM<sub>2.5</sub> concentrations, resulting in a complex spatial pattern of pollution. Once pollutants enter the atmosphere they are subjected to complex physical and chemical processes that transport and/or transform them into the PM<sub>2.5</sub> concentrations measured at air quality monitoring stations. To trace local air pollution back to its source requires sophisticated modeling based on complex Chemical Transport Models (CTM).<sup>1</sup> A second EJ policy goal is to involve members of affected communities in the decision-making process. Making the results of technical modeling more accessible to a lay audience helps facilitate community engagement.

### Objectives and Methods

In this project we develop a methodology to aid EJ-oriented decision making for PM<sub>2.5</sub> reduction. The method uses a reduced-form air pollution model that requires much less computational power than a traditional CTM, allowing for both high spatial resolution and broad geographic coverage and allowing for many repeated model runs to evaluate the effects of a large set of emission source categories. A key model output is the intake fraction (iF) metric,<sup>2</sup> which integrates both air pollution modeling and demographic data into a single summary value. The iF database we produced can be used to directly calculate PM<sub>2.5</sub> intake<sup>3</sup> for each demographic group from emissions data. We apply this model to a subset of the 2014 US National Emissions Inventory for California and the surrounding areas and perform sector-by-sector analysis to identify categories of sources (e.g. passenger vehicles, refineries, power plants) that contribute to higher exposure rates for disadvantaged and minority communities.

---

<sup>1</sup> Some determination of pollution sources can be made with a chemical analysis of PM<sub>2.5</sub> components, but this approach provides less detailed source specifications and is not easily scaled up to an analysis of a large number of communities.

<sup>2</sup> The fraction of emissions emitted by a specific source that are inhaled by the population

<sup>3</sup> Total amount of an air pollutant emitted by a specific source that is inhaled by the population

## Results

The modeling results find that groups of lower socioeconomic status – non-white, low-income, low educational attainment, or linguistically isolated groups – systematically experience higher PM<sub>2.5</sub> exposure concentrations from all emissions categories in California. On average, white populations experience 18% lower PM<sub>2.5</sub> exposure concentrations than the population average, while Hispanic, black, and Asian populations experience 17%, 15%, and 6% higher-than-average exposure concentrations, respectively. Exposure concentration in the lowest income group is 15% higher than in the highest income group. We find that while exposure concentration varies by income within a racial-ethnic group, the within-group variation is generally small compared to the differences among racial-ethnic groups

Comparing intake attributable to different emission source categories, we find that industry and on-road vehicles are the two highest-impact sectors in California, each contributing 24% of total PM<sub>2.5</sub> exposure concentration. Both sources disproportionately impact non-white and low-income groups. A ranking of sector-specific impacts highlights subsectors that may be potentially effective targets for emission reductions to lower exposure concentration levels for specific groups: metals manufacturing for Asian and black communities, waste disposal and incineration for Hispanic and Asian communities, and petroleum refining for black communities. Some minor sectors showed high disparity in impacts – for example, outdoor emissions from commercial cooking, agriculture, and off-road mobile sources – with mixed effects among different racial-ethnic, income, and other socioeconomic groupings.

The iF database showed high spatial heterogeneity and a significant difference between population-weighted and emissions-weighted iFs, emphasizing the importance of emissions location in determining their health impact. In subsets of the spatial data, we see distinct intraurban patterns in iF by racial-ethnic category, demonstrating that the iF tool is sensitive to localized demographic differences. This is true for tall stack precursor emissions as well as primary emissions. We demonstrate a visualization technique that combines total emissions and source-specific iF to highlight sectors with a large total impact and high potential for exposure disparity reduction.

## Conclusions

This work presents a comprehensive analysis of sector-specific PM<sub>2.5</sub> impacts from an EJ-perspective, including all anthropogenic sources and covering the entire state of California. The rankings of major and minor sectors by total impact and exposure concentration disparity can inform research and policy priorities. The iF database produced from this modeling can also be applied to emissions data compiled by other agencies or organizations and can serve as an accessible means for groups with more limited technical capacity to explore the EJ impacts of different sources of PM<sub>2.5</sub>. The ongoing application of the iF database with new emissions data or with a more targeted focus on specific demographics can continue to serve both public agencies and community groups hoping to improve air quality, public health, and environmental justice in California.

## Introduction

### Public Health and PM<sub>2.5</sub> Exposure Metrics

Exposure to fine particulate matter (particles with aerodynamic diameter  $\leq 2.5 \mu\text{m}$ , or PM<sub>2.5</sub>) increases the risk of a range of adverse health outcomes. Risks for chronic or recurring health problems include increased rates of asthma attacks in sensitive individuals, reduced lung development and increased asthma rates in children, and increased hospital visits for respiratory problems (Meng et al., 2010; Patel et al., 2009). Chronic exposure also increases the risk of death from respiratory infections, heart attack, lung cancer, stroke, and obstructive lung diseases such as emphysema (Burnett et al., 2014; Krewski, 2009; Laden et al., 2006).

Restrictions on emissions from PM<sub>2.5</sub> sources have succeeded in reducing ambient PM<sub>2.5</sub> concentrations in California in the past two decades. However, these reductions have not benefitted all communities equally. Low-income communities and communities of ethnic or racial minorities in California are still exposed to higher-than-average levels of PM<sub>2.5</sub> (Marshall, 2008; Marshall et al., 2014; Su et al., 2012). Reducing this exposure disparity is an aspect of environmental justice (EJ), i.e., a fair distribution of environmental benefits or risks across all groups of people. In accordance with AB 2312, California Air Resources Board (CARB) seeks to include EJ considerations in setting emission control priorities, selecting emission control targets based on both (i) reducing aggregate population exposures and (ii) reducing disparity in impacts by race-ethnicity, income or socioeconomic status. This additional criterion introduces the need for additional metrics describing the impacts of emission sources and source categories on exposure and health.

The health impact of a PM<sub>2.5</sub> source is determined by the amount that it contributes to exposure, not the total mass it emits. This is largely a function of location: a ton of PM<sub>2.5</sub> emitted in the middle of a city, increasing pollution levels for millions, is a much greater concern for public health than a ton of PM<sub>2.5</sub> released in a remote location. The metrics of intake and intake fraction help describe emission sources on terms most relevant to public health. The intake metric, in units of mass per time, describes the total amount of PM<sub>2.5</sub> from a source that is ultimately inhaled. Intake is calculated cumulatively across an entire exposed population. Intake fraction (iF) is a unitless metric that normalizes intake to emissions rates, describing the intake that results from a single unit of emissions. Both intake and iF are calculated for a defined population, which may be as broad as the entire population within a specific air basin or as specific as the group of passengers waiting at a bus stop. Calculating an array of intake and iF values for a given source based on its impact on different demographic groups provides a basis for evaluating control measures from both an intake and EJ perspective.

### Methods for Developing iF Values

The iF concept, which links source emissions to population exposures, had been described as other terms, including “exposure efficiency,” in publications starting in the mid-1980s until the 2002 work by Bennett and colleagues formalized the term “intake

fraction” (Bennett et al., 2002; Evans et al., 2002). Intake fraction quantifies the efficiency of a source in causing  $PM_{2.5}$  exposure; reducing a ton of emissions from source with a high iF provides greater reductions of exposure than the same amount of emission reduction from a source with a lower iF. The utility of the iF metric is documented in the literature and iF has been recommended as one of the best-practice indicators for the exposure impacts of particulate matter (Evans et al., 2002; Hauschild et al., 2013; Lai et al., 2011). A panel of scientific experts and stakeholders, organized by the European Joint Research Centre, reviewed and evaluated a wide set of metrics as candidates for a set of ISO standard indicators for life-cycle assessment. Intake fraction was found to be the best indicator for evaluating the health impacts of particulate matter based on the completeness of its scope, its environmental relevance, its scientific robustness, its transparency and reproducibility, and its applicability (Hauschild et al., 2013). In California, CARB has successfully used iF to inform programs and facilitate source control prioritizations (Marshall and Nazaroff, 2002; 2004). The 2005 findings of Marshall and Behrentz regarding high iF values of self-pollution from school buses motivated and supported CARB’s school bus retrofit programs (Marshall and Behrentz, 2005).

Intake fractions may be highly specific or highly generic, depending on research goals. At one extreme are iFs estimated for a single source at a single location at a specific time, e.g., the exposure at a bus stop to diesel PM from municipal buses during rush hour or exposure to bus emissions during transport (Marshall and Behrentz, 2005; Xu et al., 2015). Less specific iFs, estimated using mechanistic models, may represent a category of sources in a specific area, e.g., ground-level sources of primary  $PM_{2.5}$  within a chosen city or county (Greco et al., 2007; Marshall et al., 2006). At the other extreme are intentionally generic “archetypical” iFs used in life cycle assessments that draw from multiple modeling studies to provide values that can be extrapolated to similar circumstances (Fantke et al., 2017; Humbert et al., 2009, 2011). It is desirable to use more specific iFs when possible, as there is high variability among iFs in different locations due to both population distribution and meteorological patterns. Intake fraction values can vary by orders of magnitude among sources, source categories, and source locations (Apte et al., 2012; Fantke et al., 2017; Marshall and Nazaroff, 2004).

Mechanistic models provide the means to calculate intake fraction for many sources in a single study using consistent methodology. The simplest modeling framework is a one-compartment box model that assumes uniformly distributed emissions and pollution removal via advection (Apte et al., 2012; Marshall et al., 2005). These require very little input data and provide rough estimates of primary pollutant iF within the modeled compartment. Other studies have estimated intake fraction using variety of more complex mechanistic models (Lamancusa et al., 2017; Marshall et al., 2014; Tainio et al., 2014), including steady-state plume models (e.g. AERMOD), non-steady-state plume models (e.g. CALPUFF), and Eulerian chemical transport models (e.g. WRF-Chem, CMAQ). These models integrate more complex meteorological patterns and photochemistry, allowing the calculation of iFs of precursor species along with primary  $PM_{2.5}$ , providing coverage over a larger spatial domain, and in some cases also providing higher spatial resolution. However, complex models rely on detailed

meteorological inputs and a spatially explicit emissions inventory. The uncertainty of these inputs is compounded with the uncertainty inherent in the model. Poor quality or highly uncertain inputs can make the sophistication of the model irrelevant, but high-quality input data may not be available in some situations. Another disadvantage of complex models is that running such models requires substantial training and is computationally expensive, often requiring access to a research-scale computing cluster. The computational intensity limits the scale at which these models can be run, restricting it to a smaller high-resolution domain (e.g., 1 km<sup>2</sup> grid cells within a single city) or a low-resolution larger domain (e.g., 150 km<sup>2</sup> grid cells within an entire country).

Source-Receptor modeling grew from the desire to apply a reduced-form model derived from more complex atmospheric chemistry modeling that could be used quickly and required fewer inputs. This modeling method uses source-receptor (S-R) matrices, multidimensional data tables that contain the predicted change in PM<sub>2.5</sub> concentration (units:  $\mu\text{g m}^{-3}$ ) resulting at any location from a unit of emission increase or decrease (units: tons y<sup>-1</sup>) in one specified location. The meteorology and atmospheric chemistry are built into the S-R matrix so it can be used as a stand-alone tool for estimating concentration surfaces and iF. Well-cited iF studies have used S-R models derived from AERMOD and the Climatological Regional Dispersion Model (Greco et al., 2007; Lobscheid et al., 2012). Source-Receptor modeling has the advantage of providing values with a fair degree of specificity over a wide range of source locations, as well as emissions source categories if it is paired with an emissions inventory. This study employs a source-receptor modeling approach, described in detail in the methods section.

Although there are very few semi-empirical studies that provide benchmark iF values to be used to validate or adjust model-based estimates, the range of iF values included within the overall body of iF research can serve as a broad indicator of whether a given model is producing reliable iF estimates. A collection of these values is included in Appendix A and compared with our results in the results section of this report.

### Intake, iF, and Environmental Justice

A small but growing body of literature presents EJ impacts of emissions alongside intake and iF for particulate matter in California. We present a limited review of results from five such studies (Cushing et al., 2016; Marshall et al., 2006, 2014; Nguyen et al., 2018; Su et al., 2012). Most of these have focused on one or more discrete areas within the state (air basins or counties) and used diesel particulate matter (DPM) or traffic-related air pollution as the pollutants of interest.

In 2006, Marshall et al. reported that per-person DPM intake in the South Coast Air Basin was higher for non-whites and for individuals in low-income households than for the population as a whole in the South Coast Air Basin. The 2012 work of Su and colleagues investigated pollution exposure and environmental justice in three California counties: Alameda, Los Angeles, and San Diego. Using a statistical technique that compares the observed distribution of exposure against a hypothetical “equality line,” they found that within-county inequality was highest for diesel PM exposure throughout

the domain, but inequality followed a less consistent pattern across counties for total PM exposure.

The 2014 analysis by Marshall, Swor, and Nguyen divided diesel burning into five subcategories, including four mobile sources and one stationary source category, and considered environmental justice impacts in the South Coast Air Basin. They found that there are potential trade-offs among the goals of reducing intake, targeting high-iF sources, and seeking outcomes that improve EJ; their findings indicated that while reductions in train emissions are optimal for iF and EJ, reductions from off-road mobile sources rate higher for overall intake reduction.

Complementing these peer-reviewed journal articles, a detailed report was published in 2015 evaluating the EJ impacts of California's cap-and-trade program (Cushing et al. 2016). This report found that the co-emitted PM<sub>10</sub> at major GHG-emitting facilities tended to impact neighborhoods with lower-income residents and a higher share of people of color. Some of these facilities maintained or increased localized pollution and purchased out-of-state offset credits, losing potential EJ co-benefits of the policy. This case study demonstrates the importance of considering multiple metrics to meet policy goals.

The location of emissions from a source category are as important for EJ outcomes as they are for iF, but the spatial pattern of EJ metrics may vary substantially from that for iF. Sites that rank high in iF may rank lower in impacts on exposure disparity (Nguyen et al., 2018). For example, emissions from a location near a medium-density, low-income neighborhood may have a lower iF than the same amount of emissions in a high-density, high-income urban neighborhood. However, the lower-iF emissions have a higher EJ impact because they disproportionately affect a low-income neighborhood. By considering an array of metrics, decision-makers can identify emissions reductions that are effective at improving EJ and reducing overall exposure.

### [The iF Database: Screening Tool for Policy and Environmental Justice Issues](#)

Source-specific intake and iF metrics have great potential to reveal existing inequality in PM<sub>2.5</sub> exposure concentrations among demographic groups and inform future pollution control policy. This report describes the creation and application of a methodology that focused on intake and iF. This methodology can provide several advantages relevant to public health decision-making:

#### **1. Broad coverage with high spatial resolution**

The iF tool is a spatial database – an organized collection of data tables that are indexed to spatial locations. The spatial locations are arranged in a grid that covers an area of 1296 km by 960 km, including California and parts of the surrounding states. Grid cells are variably sized based on population density, so the spatial resolution in urban areas is 1 km<sup>2</sup>. This allows the tool the breadth to evaluate intake throughout the entire state rather than in select counties, and the detail to evaluate within-county and within-city differences in intake fraction.

## **2. Inclusion of PM<sub>2.5</sub> precursors**

Emission sources contribute to PM<sub>2.5</sub> in two ways: direct emissions of PM<sub>2.5</sub> (primary PM<sub>2.5</sub>) and emissions of chemicals that form PM<sub>2.5</sub> in the atmosphere, known as precursor species. Primary PM<sub>2.5</sub> is emitted 100% in the particle phase. Precursor species include ammonia (NH<sub>3</sub>), sulfur dioxide (SO<sub>2</sub>), oxides of nitrogen (NO<sub>x</sub>), and volatile organic compounds (VOCs). These species are emitted as gases and form particle-phase PM<sub>2.5</sub> via physical or chemical reactions. The major reactions for NH<sub>3</sub>, SO<sub>2</sub>, and NO<sub>x</sub> result in particle-phase ammonium sulfate ((NH<sub>4</sub>)<sub>2</sub>SO<sub>4</sub>) and ammonium nitrate (NH<sub>4</sub>NO<sub>3</sub>).<sup>4</sup> Previous studies of EJ impacts in California have focused on DPM or other primary particulate emissions, which proves a major limitation to a comprehensive comparison of impacts among sources: the majority of ambient PM<sub>2.5</sub> is composed of secondary aerosol species, and most source categories contribute more to exposure concentrations via precursor emissions than via primary emissions (Bell et al., 2007). We include the four major precursor species in our database and investigate the importance of different species in the impacts of different source categories.

## **3. Detailed demographic categories**

For the sake of simplicity, studies often present results along simplified demographic divides, e.g., white vs. nonwhite or highest vs. lowest income. This tool provides the flexibility to make more detailed comparisons among five racial/ethnic categories, five income quartiles, five age group categories, two additional groups associated with lower socioeconomic status, and SB 535 Disadvantaged Communities as determined by the CalEnviroScreen 3.0 environmental health screening tool (Faust et al. 2017). In addition, it separates each racial category by income level so that the tool can show the interaction between income and race-ethnicity in exposure levels.

## **4. Application to comprehensive inventory of anthropogenic emissions**

To demonstrate this methodology, we apply it to the 2014 US EPA National Emissions Inventory, grouped into 11 sector categories containing 59 subcategories. Intake and iF for each subcategory are calculated for each demographic group, allowing a rich analysis of sector-specific impacts across socioeconomic groups.

This screening tool is designed to provide a rapid assessment of disparity in PM<sub>2.5</sub> exposure concentration. Because it runs based on pre-calculated chemical transport

---

<sup>4</sup> In our discussion of intake and intake fraction we refer to particulate species resulting from each gaseous species separately, as pNH<sub>4</sub> (particulate ammonium), pSO<sub>4</sub> (particulate sulfate), and pNO<sub>3</sub> (particulate nitrate). Volatile organic compounds (VOCs) include an array of carbon-containing chemicals that are emitted in the gas phase but undergo physical processes (condensation) and/or complex reactions and chemical transformations in the atmosphere that then cause them to condense into the particle phase. We refer to the particle-phase species resulting from VOC emissions as secondary organic aerosol (SOA).

modeling parameters, it requires a small fraction of the computing power required for a more complex model (Tessum et al., 2017). It is accessible as a spatial database, so use of this tool requires a limited degree of expertise. More complex analyses can be automated using a scripting language (e.g., MATLAB, R, Python), but do not depend on an additional program to run. However, simplicity of use requires simplifying assumptions that limit model accuracy compared to more complex models. The strength of this tool is its ability to compare the relative effects of emissions from different areas or sources, and it is designed to complement but not replace existing complex models for calculating total  $PM_{2.5}$  concentrations or absolute  $PM_{2.5}$  exposure concentration. Model uncertainty and limits on model precision should be taken into account when interpreting small differences among groups or emission sources in model output. In this light, the database and results presented should be considered as a guiding tool for identifying high-impact sources and generating hypotheses that can be further investigated with other assessment methods.

## Methods

### The Intervention Model of Air Pollution (InMAP)

The Intervention Model of Air Pollution (InMAP) is a reduced-complexity alternative to comprehensive chemical transport models (CTMs). It operates by modeling annual-average changes in primary PM<sub>2.5</sub> concentration directly emitted from sources and secondary PM<sub>2.5</sub> concentrations attributable to annual changes in precursor emissions. InMAP uses pre-processed physical and chemical information from the output of a state-of-the-science CTM (i.e., WRF-Chem) and a variable spatial resolution computational grid to perform simulations that are several orders of magnitude less computationally intensive than comprehensive model simulations. Typical state-of-the-science CTMs create a three-dimensional Eulerian grid and simulate changes in pollutant concentration in each cell at a high temporal resolution (<1 hour) based on physical transport via wind flow and plume rise, emissions, physical removal mechanism (e.g., deposition), and interdependent nonlinear physicochemical transformation pathways. InMAP uses time-averaged transport and reaction rates in its algorithms for emissions, plume rise, transport, transformation, and removal of atmospheric pollution. To reduce computational intensity, the algorithms are in some cases simplified as compared to similar algorithms in a comprehensive CTM.

InMAP takes as an input a previously generated data file containing information on meteorological and background parameters to provide transport and reaction rates. In this case results generated at 12 km resolution from WRF-Chem v3.4 based on year 2005 inputs (Tessum et al., 2015). InMAP uses a set of emergent atmospheric properties generated as model outputs (Tessum et al. 2015, Supplemental Information Table 1) to inform the parametric equations used in each grid cell for advection, mixing, chemistry, and deposition (Tessum et al., 2017). Due to nonlinear dynamics in the transformation of gaseous to aerosol species, concentration estimates for secondary species are sensitive to base-year concentrations and have higher errors and biases than primary PM<sub>2.5</sub>, as discussed in Appendix B.

Instead of solving for pollutant concentrations at specific points in time using temporally explicit input data as CTMs does, InMAP directly estimates annual average pollutant concentrations using annual average input data and numerical integration. This simplification reduces the computational intensity of running InMAP and produces metrics relevant to exposure and health risk calculations (annual average PM<sub>2.5</sub> exposure concentration). Model limitations due to this assumption are explained in Tessum et al. 2017:

*Many of the chemical and physical processes important to the fate and transport of air pollution vary with the time of day and the season. A steady-state, annual-average model risks being unable to represent the results of these temporally explicit phenomena. InMAP mitigates this potential limitation by using temporally explicit information wherever possible when calculating annual average input properties. For instance, the gas-phase oxidation of SO<sub>2</sub> to SO<sub>2</sub><sup>-</sup> is represented*

*as the product of the  $\text{SO}_2$  concentration and a reaction rate constant, but the reaction rate constant has a non-linear dependence on temperature and on the concentration of hydroxyl radical ( $\text{HO}^*$ ), both of which are temporally variable. To represent the formation of particulate  $\text{SO}_4$  ( $\text{pSO}_4$ ), InMAP needs an annual average rate constant. To capture some of the effects of temporal variability, instead of calculating the rate constant using annual average values for temperature and  $\text{HO}^*$ , we instead use temporally explicit temperatures, solar radiation intensities, and  $\text{HO}^*$  concentrations to then calculate rate constants for every hour during the year, and then take the average of these 8760 rate-constant values. Thus, the reaction rate InMAP uses for a given grid cell is an annual-average rate, not a rate calculated using annual-average values for input parameters.*

InMAP uses the annual average reaction rates and meteorological data to model the concentrations resulting from any given emissions inventory, including inventories for a smaller subset of the model domain or inventories from different years. These emissions inventories must be spatially explicit, specifying emissions amounts and locations, and stack parameters if appropriate. The emissions shapefile may specify emissions at a single location or at many locations. This study used the most recent comprehensive national emissions inventory available from the U.S. EPA, compiled for the year 2014 (U.S. EPA 2014).

The performance of InMAP has been validated against four commonly used models: WRF-Chem, a full chemical transport model; COBRA and AP2 (Air Pollution Emission Experiments and Policy), two reduced-complexity models based on a Source-Receptor Matrix framework; and EASIUR (Estimating Air pollution Social Impacts Using Regression), a reduced-complexity model produced using regression analysis on multiple CTM runs (Gilmore et al., 2019; Tessum et al., 2017). A comparison of outputs across models has shown satisfactory agreement for all pollutant species considered for this project.

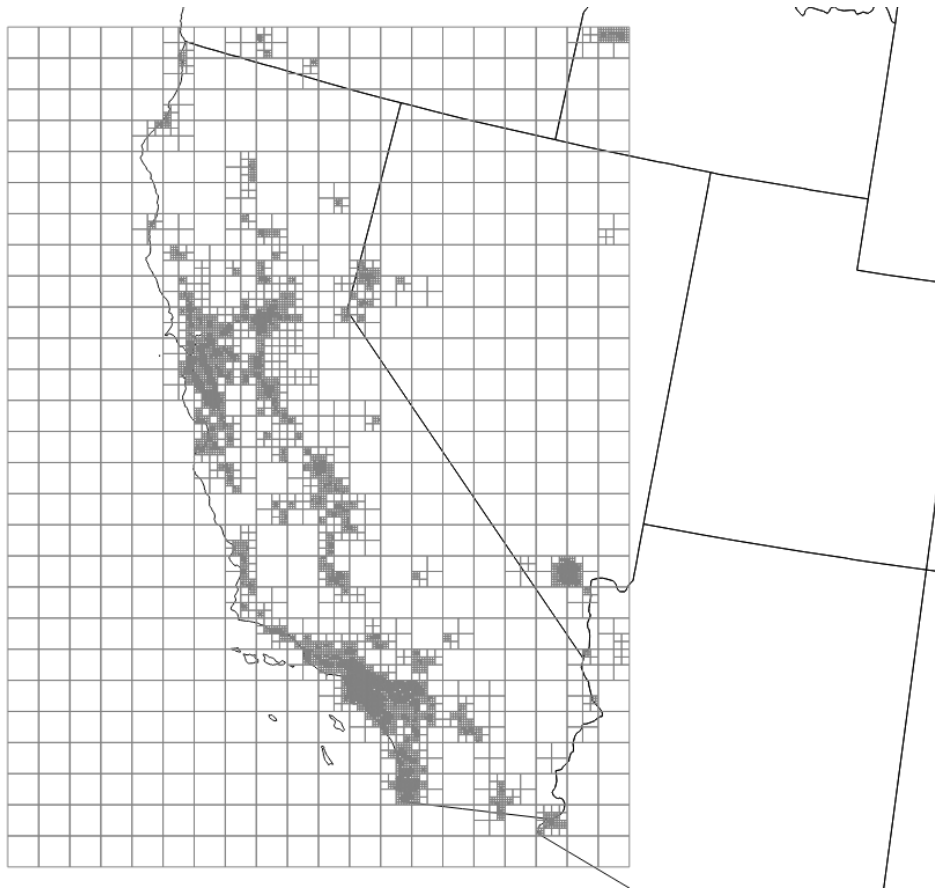


Figure 1: InMAP model domain for California.

*The largest grid cells, used to cover sparsely populated regions, have an area of 2,304 km<sup>2</sup> (48 km per side). In densely populated urban areas, the resolution is increased, with the finest resolution being one cell per km<sup>2</sup>. Variable grid sizing provides computational efficiency and greater power to distinguish effects among city neighborhoods.*

InMAP models the concentration of PM<sub>2.5</sub> resulting from five pollutant categories: primary PM<sub>2.5</sub> and four precursor gaseous species: oxides of nitrogen (NO<sub>x</sub>), sulfur dioxide (SO<sub>2</sub>), ammonia (NH<sub>3</sub>), and volatile organic carbon species (VOCs). Concentrations are modeled for 21,705 variably sized grid cells covering the state of California and portions of the surrounding states, shown in Figure 1. The size of each grid cell is determined based on population density. The largest grid cells, used to cover sparsely populated regions, have an area of 2,304 km<sup>2</sup> (48 km per side). In densely populated urban areas, the resolution is increased, with the finest resolution being one cell per km<sup>2</sup>. The algorithm ensures that no grid cell larger than 1 km<sup>2</sup> has a total population of greater than 20,000 people and that no grid cells larger than 1 km<sup>2</sup> contain a census block group with population density greater than 2,500 people/km. As shown in Figure 2, a subset of the national grid centered on the Bay Area of California, the algorithm used to create this grid leads to most urbanized areas having much of their land area covered with 1 km<sup>2</sup> grid cells. Variable grid sizing provides computational efficiency and greater power to distinguish effects among city neighborhoods.

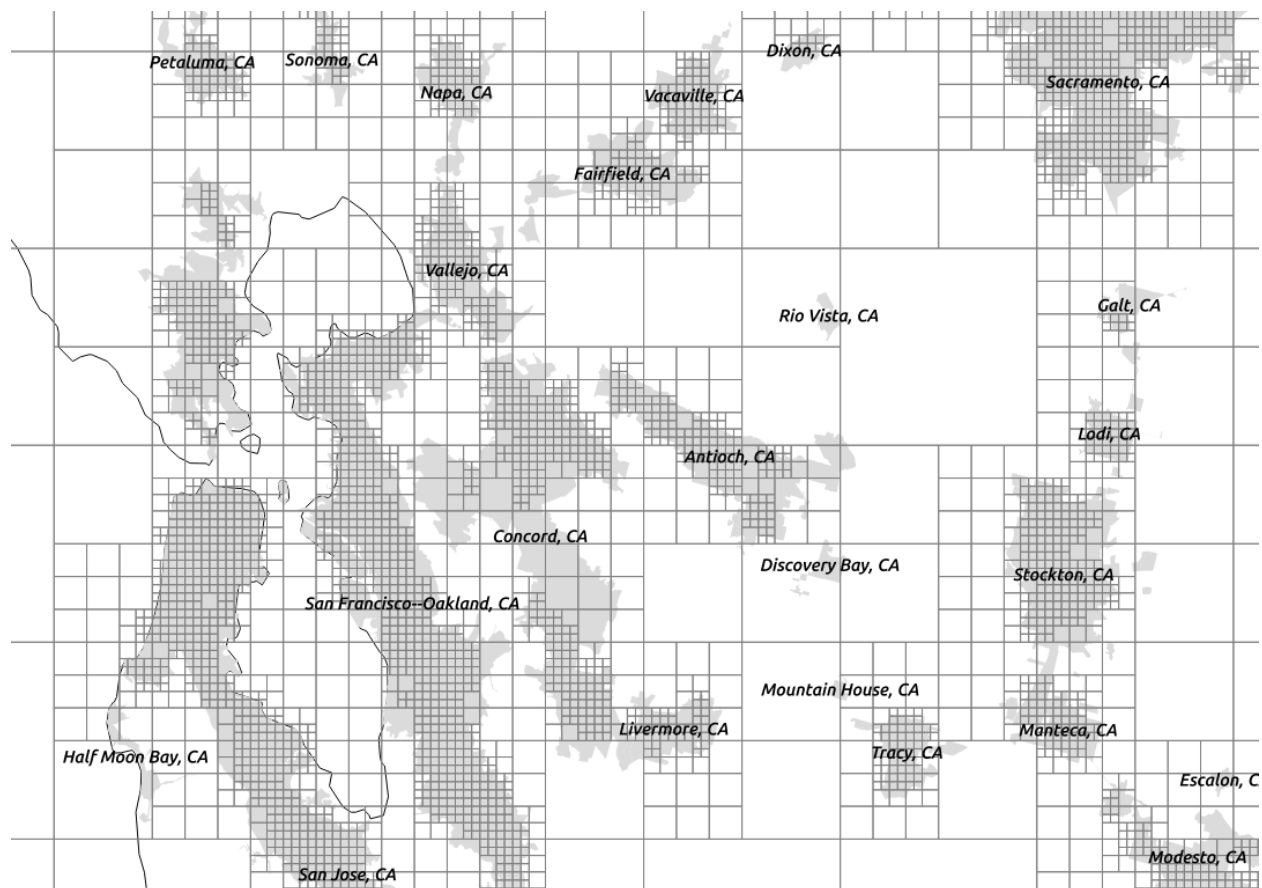


Figure 2: Inset of the InMAP domain for the San Francisco Bay Area.

This figure illustrates the increased model resolution in urban areas. Light grey areas with black labels indicate US Census-defined urban areas. The smallest of the dark grey grid cells are 1 km<sup>2</sup> in area.

### Source-Receptor Matrix

To calculate iF and other EJ metrics we rely on an intermediate product of the InMAP model called the Source-Receptor (S-R) matrix. The source-receptor relationships included in the S-R matrix quantify the marginal change in concentration at each receptor site resulting from a unit increase of emissions at the source site. In other words, if primary PM<sub>2.5</sub> emissions at a specified source grid cell (**S**, illustrated in Figure 3) were to increase by 1 kg per year, the S-R matrix would provide the resulting change in annual average concentration (units: µg/m<sup>3</sup>) at any receptor grid cell (**R**), including the source grid cell itself. If the total emissions change at **S** is known, the change in concentration at each **R** can be scaled up or down linearly. In addition to changes in concentration with primary PM<sub>2.5</sub> emissions, the relationships included in the S-R matrix cover changes in pNH<sub>4</sub> concentration per unit NH<sub>3</sub> emitted, pSO<sub>4</sub> concentration per unit SO<sub>2</sub> emitted, pNO<sub>3</sub> concentration per unit NO<sub>x</sub> emitted, and SOA concentration per unit VOC emitted.

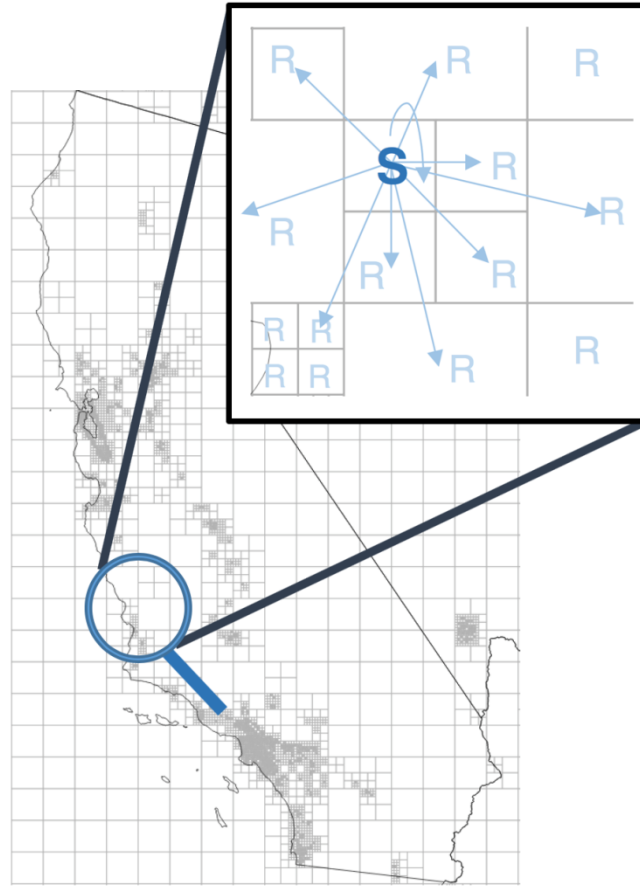


Figure 3: Illustration of Source-Receptor Matrix.

We use the InMAP capability to efficiently calculate the results of marginal emission changes to perform the many repeated model simulations required to create a S-R matrix. Each simulation assumes an emissions change of 1 short ton per year of each pollutant in a single location, and then evaluates the resulting change in  $PM_{2.5}$  concentration in every location within the domain. The S-R matrix includes the per-unit change in  $PM_{2.5}$  concentration for each of the five pollutants at three effective plume heights<sup>5</sup> and 21,705 emission locations. To reduce computational cost, this method makes the simplifying assumption that the impacts of unit emission change of  $PM_{2.5}$ , VOCs,  $SO_2$ ,  $NO_x$ , and  $NH_3$  on ambient  $PM_{2.5}$  concentrations are independent of each other. This means that the model does not adjust secondary  $PM_{2.5}$  formation rates based on changes in emissions of other precursor species, which could lead to modeling error in some cases (e.g., the interaction between  $NO_x$  concentrations and  $pNH_4$  formation (Schiferl et al., 2014)). This limitation is discussed further in Appendix B.

<sup>5</sup> Ground level and low stack, 0-57 meters; medium and high stack, 57-140 meters; and high elevation plume emissions, above 760 meters. It is rare that plume heights fall between high stack and high elevation plume; in those cases, model values are based on a linear interpolation between high and low elevation values.

## Demographic Data

Environmental justice issues can occur on several dimensions: by race-ethnicity, by income level, by age group, and by other factors that lead to differences in socioeconomic status. In this work we include a wide range of demographic groups to identify specific subgroups most affected by different sectors, and to allow users of this tool to select specific groups of interest to them. The total population and population share of each demographic group are provided in Table 1.

Demographic data were obtained for the year 2016 from the American Community Survey: 5-Year Data [2012-2016], downloaded from the National Historical Geographical Information System (NHGIS), a service that curates US Census and census-based data (nhgis.org). Wherever possible, demographic data resolution is at the block group level (the level above the smallest unit, census blocks, in the geographic hierarchy). The size of block groups relative to the InMAP grid is shown in Figure 4. Block group data includes race-ethnicity, age, education, and income data. County-level data were used for income levels within racial-ethnic groups and linguistic isolation, defined as the share of the population reporting that household members spoke English less than “very well.”

A final population group is included based on the CalEnviroScreen 3.0 tool (Faust et al., 2017). This tool uses twelve pollution burden metrics and eight population characteristic metrics to rank communities within California by degree of vulnerability to environmental injustice. The highest-ranking groups are designated as SB 535 Disadvantaged Communities. Two of the pollution burden metrics used in CalEnviroScreen are  $PM_{2.5}$  and Diesel PM levels, so it is expected that this analysis will show elevated per-capita  $PM_{2.5}$  intake and population-weighted exposure concentration within Disadvantaged Communities. CalEnviroScreen statistics are reported at the census tract level (the level above block groups in the census geographic hierarchy). The total population of block groups within tracts identified by CalEnviroScreen as SB 535 Disadvantaged Communities compose the “Disadvantaged Communities” category. Although impacts in this category may be further divided by race-ethnicity, age, and income, that level of detail was not included in this analysis.

Table 1: Summary of 2016 American Community Survey demographic data within the modeling domain.

	<b>Group</b>	<b>Total population</b>	<b>% of total</b>
<i>Total</i>		42,748,417	
<i>Racial-ethnic groups</i>	White <sup>1</sup>	17,207,869	40.3%
	Hispanic	15,956,888	37.3%
	Asian <sup>1</sup>	5,518,299	12.9%
	Black <sup>1</sup>	2,404,572	5.6%
	Other Race <sup>2</sup>	1,660,788	3.9%
<i>Age groups</i>	Under 5	2,758,101	6.5%
	Under 18	10,101,687	23.6%
	Over 25	28,322,235	66.3%
	Women of Childbearing Age <sup>3</sup>	9,401,850	22.0%
	65 and over	5,597,726	13.1%
	85 and over	741,749	1.7%
<i>Income Quintiles</i>	Q1: < \$25,000	8,278,553	19.4%
	Q2: \$25k - \$45k	7,324,192	17.1%
	Q3: \$45k - \$75k	8,731,699	20.4%
	Q4: \$75k - \$125k	9,063,866	21.2%
	Q5: > \$125,000	9,117,258	21.3%
<i>Other groups</i>	Linguistic Isolation	7,592,076	17.8%
	Under High School Level of Education	4,794,092	11.2%
	Disadvantaged Communities	9,742,626	22.8%

<sup>1</sup> The white, black, and Asian categories include only non-Hispanic identifying individuals in those categories.

<sup>2</sup> The “other race” racial-ethnic category includes non-Hispanic multiracial, Native American, Pacific Islander, and other races not otherwise specified.

<sup>3</sup> Childbearing age is considered to be between the ages of 18 and 49

Table 2: Racial-ethnic composition of each income quintile.

	<b>Q1</b>	<b>Q2</b>	<b>Q3</b>	<b>Q4</b>	<b>Q5</b>
<i>White</i>	2,826,268	2,467,318	3,290,095	3,865,778	4,758,410
<i>Hispanic</i>	3,381,470	3,485,794	3,894,334	3,280,991	1,914,299
<i>Asian</i>	888,291	645,729	936,705	1,234,834	1,812,740
<i>Black</i>	748,835	447,519	462,060	429,598	316,561
<i>Other Race</i>	348,760	289,636	344,655	349,451	328,285

Table 3: Share of racial-ethnic group in each income quintile\*

	% Q1	% Q2	% Q3	% Q4	% Q5
White	16.4%	14.3%	19.1%	22.5%	27.7%
Hispanic	21.2%	21.8%	24.4%	20.6%	12.0%
Asian	16.1%	11.7%	17.0%	22.4%	32.8%
Black	31.1%	18.6%	19.2%	17.9%	13.2%
Other Race	21.0%	17.4%	20.8%	21.0%	19.8%

\*Rows sum to 100%

Joining Census Data to InMAP Model

Figure 4 shows an example of the size and spatial arrangement of census block groups compared with the InMAP modeling grid in SF area. Because several block groups overlap each grid cell and most block groups were not fully contained by one grid cell, we used an area-weighting approach to assign population counts to each grid cell. We calculated the share of the area of each block group contained in all overlapping grid cells, applied that proportion to the population within the block group and assigned the resulting share of the population to the grid cell. Data validation was performed to assure that all population was assigned to a grid cell and that no block groups were double counted.

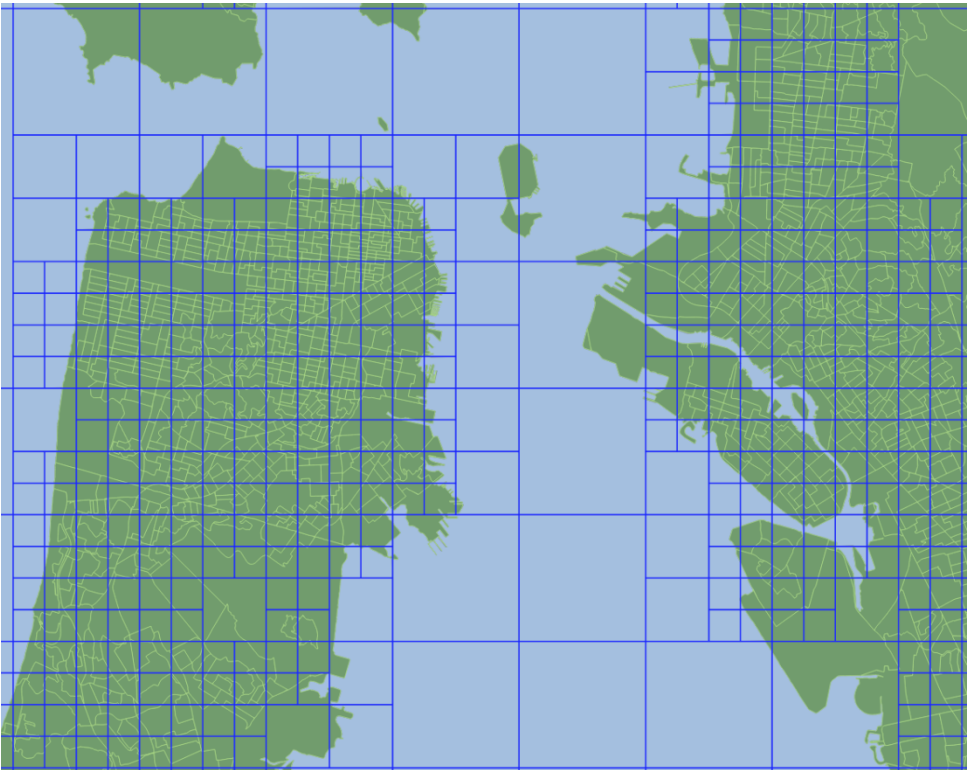


Figure 4: InMAP grid overlaying census block groups in the San Francisco area.

## EJ Metric Calculation

The two metrics relevant for overall population exposure in this analysis are  $iF$  and intake, described in Table 4. The first metric, intake, is defined here as the total mass of  $PM_{2.5}$  emitted by a given source that is inhaled each day by the entire exposed population. An intake of 380 grams per day would mean that emissions of a particular pollutant from a particular source category result in 380 grams of  $PM_{2.5}$  being inhaled throughout the entire modeling domain.

Table 4: Metrics for population exposure.

Metric	Equation	Example
<p><b>(1)</b> Intake: the total amount of an air pollutant emitted by a specific source that is inhaled by the population per day</p> <p>This study assumes a constant breathing rate of <math>14.5 \text{ m}^3 \text{ d}^{-1}</math>, or <math>5,292.5 \text{ m}^3 \text{ yr}^{-1}</math></p>	$intake = \sum_{i=1}^n C_i Q_i$ <p><math>C_i</math>, concentration (<math>\mu\text{g m}^{-3}</math>) for person <math>i</math>  <math>n</math>, number of people  <math>Q_i</math>, breathing rate (<math>\text{m}^3 \text{ yr}^{-1}</math>) for person <math>i</math></p>	<p>380 <math>\text{g d}^{-1}</math></p>
<p><b>(2)</b> Intake fraction: the fraction of emissions emitted by a specific source that are inhaled by the population</p> <p>Intake fraction is dimensionless but conventionally reported in parts per million (ppm). If a source has an intake fraction of 1 ppm then one millionth of the mass emitted from that source is inhaled, or one milligram is inhaled per kilogram emitted.</p>	$iF = \frac{1}{E} \sum_{i=1}^n C_i Q_i$ <p><math>C_i</math>, concentration (<math>\mu\text{g m}^{-3}</math>) for person <math>i</math>  <math>n</math>, number of people  <math>Q_i</math>, breathing rate (<math>\text{m}^3 \text{ yr}^{-1}</math>) for person <math>i</math>  <math>E</math>, total emissions (<math>\text{ton yr}^{-1}</math>)</p>	<p>15 ppm</p>

Calculation of intake from an S-R matrix is illustrated in Figure 5. Intake from source location **S** for a single receptor location **R** is calculated by modeling the annual average concentration of  $PM_{2.5}$  (units:  $\mu\text{g}/\text{m}^3$ ) in **R** attributable to emissions (units: metric ton/year) in **S**. That concentration is multiplied by the size of the total population within that grid cell<sup>6</sup> and the average annual volume of air breathed by each individual (units:  $\text{m}^3/\text{year}$ ). The result is the total mass of emissions inhaled in **R** from emissions in **S**. The total intake for **S** is the sum of intake in all receptor locations (21,705 total **R** cells). The intake calculation for a specific subpopulation proceeds the same way, but the size of the subpopulation within the cell is substituted for the total population.

<sup>6</sup> Using census-based grid cell population counts to calculate intake and intake fraction relies on the assumption that a person's exposure is determined by their residence address. In reality, personal daily exposure may include intake that occurs while commuting, at work, and at locations of other daily activities.

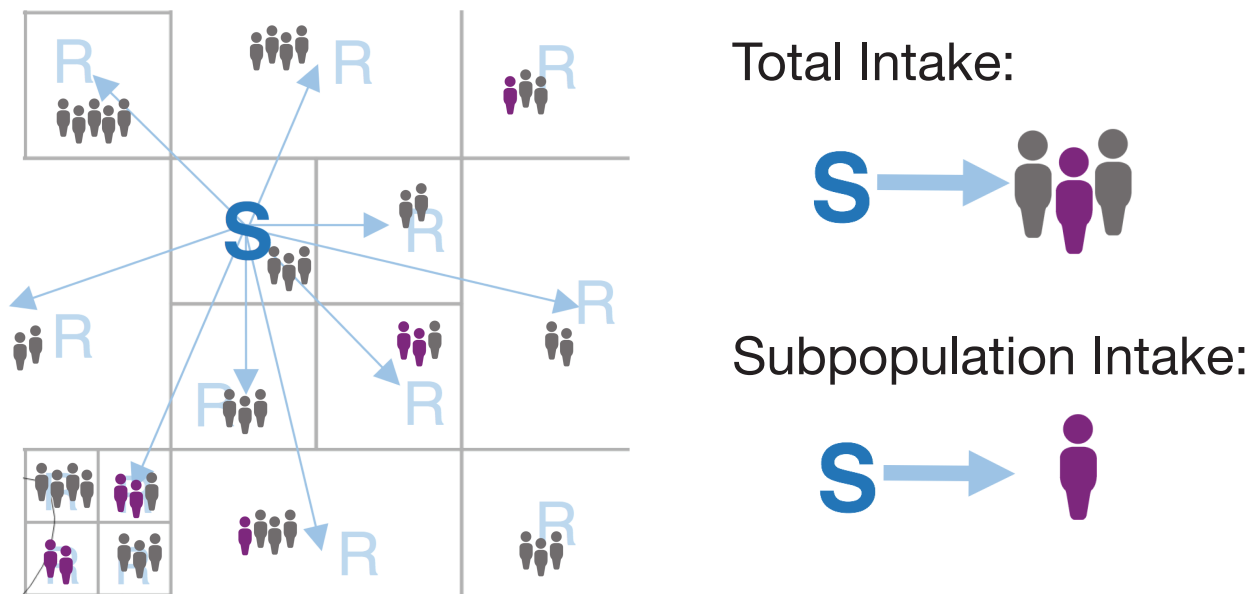


Figure 5: Illustration of intake calculation from an S-R matrix.

The second metric,  $iF$ , is used to compare the relative importance of sources in terms of the impact caused by each ton emitted from a given source. An  $iF$  of 15 ppm, for example, would mean that 15 grams of  $PM_{2.5}$  are inhaled for every million grams of primary  $PM_{2.5}$  or precursor pollutant emitted. A higher  $iF$  means that per mass emitted, the portion inhaled is greater and thus results in a greater impact on exposure concentration per mass emitted. For primary  $PM_{2.5}$  an  $iF$  of 1 ppm means that one milligram of  $PM_{2.5}$  is inhaled for each kilogram of  $PM_{2.5}$  emitted. For precursor species an  $iF$  of 1 ppm means that for each kilogram of the precursor gas emitted ( $VOC$ ,  $NH_3$ ,  $NO_x$ , or  $SO_2$ ), one milligram of particulate matter formed from that gas is inhaled ( $SOA$ ,  $pNH_4$ ,  $pNO_3$ , or  $pSO_4$ ).

The  $iF$  calculation from the S-R matrix proceeds in a similar way as the intake calculation, with one change in the units. The concentration in  $R$  is expressed as  $\mu g/m^3$  per unit emissions in  $S$ . Absent an S-R matrix,  $iF$  can also be calculated by dividing the intake metric described above by the total mass of emissions from a specific source.

The data needs for calculating  $iF$  are the S-R matrix and a map of the population distribution. To calculate intake, a spatially explicit emissions inventory is also required. The inventory must include that location of each point source, and for non-point sources, e.g. motor vehicles, estimate the approximate spatial distribution of the emissions. "Approximate spatial distribution" refers to the fact that for non-point sources, proxy variables are used in place of exact measurements of emissions-generating activity. In the case of mobile sources, for example, total emissions based on state- or county-level fuel consumption data may be distributed throughout the domain based on a combined weighting of location characteristics such as road type, total miles of road within an area, and average traffic counts.

The EJ metrics included in Table 5 are derived from the intake metric calculated for different demographic groups. The first, total intake difference, compares the total intake for one population group against another. Intake difference is not normalized for population size, so intake for a larger population will likely be higher than for a smaller population even if intake is higher for individual members of the smaller population. Population-normalized or per-capita metrics are recommended for comparisons among differently sized groups (including most racial-ethnic and age-based categories). The second, third, and fourth metrics are population normalized and calculated by comparing a specific group against the value for the total population. Per-capita intake difference is calculated directly from intake values divided by population size and is given in units of mass per time. Per-capita exposure concentration and exposure concentration difference are given in more intuitive units of mass per volume, comparable to air quality standards. It may be calculated by dividing annual intake by the per-capita annual breathing rate of 5292.5 m<sup>3</sup>/year. Relative percent difference expresses the difference in per-capita intake (or exposure concentration) between two groups, or one group and the total population, relative to the per-capita intake (or exposure concentration) of the total population. Emission sources with low total per-capita intake may still be useful targets for EJ goals if the relative percent difference is high.

Two additional metrics used throughout the report are the population-weighted average and the emissions-weighted average. Population-weighted average is calculated as the sum of the product of grid-cell population and the value to be averaged, divided by the sum of the population of all grid cells, or

$$\frac{\sum_i^N C_i \times \text{Pop}_i}{\sum_i^N \text{Pop}_i}$$

where N is the total number of grid cells, Pop<sub>i</sub> is the population of grid cell i, and C<sub>i</sub> is the value of interest (iF, concentration, etc.) in that grid cell. Similarly, emissions-weighted average is calculated as the sum of the product of grid-cell emissions and the value to be averaged, divided by the sum of the emissions of all grid cells,

$$\frac{\sum_i^N C_i \times E_i}{\sum_i^N E_i}$$

where N is the total number of grid cells, E<sub>i</sub> is the emissions in grid cell i, and C<sub>i</sub> is the value of interest.

Table 5: Metrics for environmental justice analysis.

Metric	Equation	Example
<p><b>(1) Intake difference:</b> the absolute difference in intake between two specific demographic groups (group of interest and control).</p>	$\begin{aligned} & \textit{intake difference} \\ & = \sum_{i=1}^{n_G} C_{iG} Q_i - \sum_{i=1}^{n_O} C_{iO} Q_i \end{aligned}$ <p><math>C_{iG}</math>, <math>C_{iO}</math>, annual average concentration (<math>\text{g m}^{-3}</math>) that person <math>i</math> within the group of interest (<math>iG</math>) and within another control group (<math>iO</math>) are exposed to  <math>n_G</math>, <math>n_O</math>, number of people in group of interest (<math>iG</math>) and control group (<math>iO</math>)  <math>Q_i</math>, breathing rate (<math>\text{m}^3 \text{d}^{-1}</math>) for person <math>i</math>, assumed equal across groups</p>	<p>400 <math>\text{g d}^{-1}</math></p>
<p><b>(2) Per-capita intake difference:</b> the absolute difference in mean per-capita intake between a specific demographic group and the mean per-capita intake for the total population.</p>	$\begin{aligned} & \textit{per - capita intake difference} \\ & = \frac{\sum_{i=1}^{n_G} C_{iG} Q_i}{n_G} - \frac{\sum_{i=1}^{n_T} C_{iT} Q_i}{n_T} \end{aligned}$ <p><math>C_{iG}</math>, <math>C_{iT}</math>, annual average concentration (<math>\mu\text{g m}^{-3}</math>) that person <math>i</math> within the group of interest (<math>iG</math>) and within population as a whole (<math>iT</math>) are exposed to  <math>n_G</math>, <math>n_T</math>, number of people in group of interest (<math>G</math>) and total population (<math>T</math>)  <math>Q_i</math>, breathing rate (<math>\text{m}^3 \text{d}^{-1}</math>) for person <math>i</math>, assumed equal across groups</p>	<p>10 <math>\mu\text{g d}^{-1}</math></p>
<p><b>(3) Per-capita exposure concentration difference:</b> the absolute difference in population-weighted average exposure concentration between a specific demographic group and the total population.</p>	$\begin{aligned} & \textit{exposure difference} \\ & = \frac{\sum_{i=1}^{n_G} C_{iG}}{n_G} - \frac{\sum_{i=1}^{n_T} C_{iT}}{n_T} \end{aligned}$ <p><math>C_{iG}</math>, <math>C_{iT}</math>, annual average concentration (<math>\mu\text{g m}^{-3}</math>) that person <math>i</math> within the group of interest (<math>iG</math>) and within population as a whole (<math>iT</math>) are exposed to  <math>n_G</math>, <math>n_T</math>, number of people in group of interest (<math>G</math>) and total population (<math>T</math>)  <math>Q_i</math>, breathing rate (<math>\text{m}^3 \text{d}^{-1}</math>) for person <math>i</math>, assumed equal across groups</p>	<p>0.5 <math>\mu\text{g}/\text{m}^3</math></p>
<p><b>(4) Relative percent difference</b></p>	$RPD = \frac{ \mu_{CG} - \mu_{VP} }{\mu}$ <p><math>\mu_{CG}</math>, mean per-capita intake in comparison group  <math>\mu_{VP}</math>, mean per-capita intake in specified vulnerable population  <math>\mu</math>, population mean per-capita intake</p>	<p>25%</p>

## Emissions Data

To calculate total intake and sector-specific impacts we use the most recent US EPA National Emissions Inventory. A description of sources included in each category and a summary of source-specific emissions is provided in Appendix C. Emissions data are available in a spatially explicit file format (ArcGIS shapefiles) with all sources assigned to specific point coordinates (longitude and latitude pairs). Area sources are represented in the NEI files as a grid of point coordinates. Emissions shapefiles were projected to match the InMAP model datum and coordinate reference system. Emissions were allocated to each grid cell using a point-in-polygon joining technique. When an emissions source point fell on the boundary between one or more grid cells, emissions were divided equally among those grid cells to avoid double-counting of emissions.

## Tool Limitations

This methodology relies on simplifying assumptions used to improve model efficiency, a reduced scope of emissions input data, and simplifying assumptions in calculating exposure concentration. The results are recommended for use as a screening-level analysis for investigating the relative magnitude of disparities from different sources, sectors, and release environments. However, due to modeling limitations, we advise against the use of this data for certain other types of analyses. These results are not a substitute for more complex modeling of total  $PM_{2.5}$  concentrations and exposure concentrations. The source-receptor matrix simplifies meteorology and atmospheric physicochemical transformation rates, which limits the accuracy of absolute  $PM_{2.5}$  concentration values. The rate of transformation of precursors to secondary  $PM_{2.5}$  is derived from a fixed baseline and is not adjusted based on changes to the emissions inventory. While the assumption has a small effect for minor perturbations in emissions, uncertainty increases for large changes. This tool's performance in predicting absolute concentrations is only fair compared to more complex models, and limits to the modeling domain result in systematic underestimation of exposure concentration due to long-range transport (See Appendix B).

The model uses annual average modeling parameters, so it does not produce time-resolved results. While this tool works well with annual emissions estimates, it is not recommended that the tool be used with seasonal or time-varying emissions data, or to analyze short-term high concentration events. This tool assumes exposure concentration levels based only on place of residence. Estimates do not account for activity patterns (time spent traveling, at work, etc.) that affect the exact locations and microenvironments where an individual is exposed to  $PM_{2.5}$  throughout the day. The model does not support time-resolved concentrations, so it is not appropriate to apply time-varying activity patterns or diurnal variation in breathing rate. This simplification increases uncertainty in exposure concentration estimates, although other studies have found that activity patterns and breathing rate cause a relatively small change in estimates of individual exposure to Diesel  $PM_{2.5}$  (Marshall et al., 2006). It was not within the scope of this project to account for indoor/outdoor concentration ratios which may differ among buildings of different type and age and may be relevant to exposure disparity.

## Example Application of iF Database to Evaluate Environmental Justice Concerns

To illustrate the use of the iF spatial database, we use the hypothetical example of a facility (point source) located in Richmond, California, shown in Figure 6.



Figure 6: Location of example facility in Richmond, in the north east Bay Area (left) and the location of the facility within the iF grid (right).

### Step 1: Assemble emissions inventory

The first step in using the iF tool is to evaluate the total annual emissions from the source of interest. For our example, we assume that the facility generates **258 metric tons of VOCs and 1.4 metric tons of primary PM<sub>2.5</sub> per year**, emitted at a low height (between ground level and a height of 57 m).

Note on units: iF values are reported in units of ppm, which translates to 1 µg inhaled per 1 g emitted, or 1 g inhaled per metric ton emitted. For simplicity, emission values should be converted to metric units before iF values are applied (conversion: 1 US ton = 0.9072 metric tons). In addition, population-weighted concentration values are based on annual intake. To calculate concentrations correctly, emission values should express total annual emissions from the sources of interest.

### Step 2: Align emissions location with iF grid

The iF values applied to the emissions source must correspond to the source location. For our point source example, we use the coordinates of the facility generating the emissions (see Figure 6). The process is more complex for non-point sources that are spread over an area that covers multiple grid cells. In that case, the user must determine the share of emissions that occur in each grid cell and either perform the intake calculation for each cell or calculate a weighted average iF based on the proportion of emissions in each cell. This can be accomplished using GIS tools or automated using a scripting language.

### Step 3: Look up relevant iF values for pollutant species and height

As described above, iF is highly pollutant- and height-specific. Our example facility emits both primary PM<sub>2.5</sub> and VOCs at the lowest height category (< 57 m). Based on these details, the relevant values from the iF database are those shown in Table 6. The iF for the total population is the sum of the iF values for the full set of race-ethnicity categories. The magnitude of the iF for each group depends on the size

of the total population within that group and the proximity of communities within each group to the emissions location. The iF of primary PM<sub>2.5</sub> is higher and more strongly dependent on the population in close proximity to emissions. We observe in this table that the iF for SOA from VOC emissions is of similar magnitude for White and Hispanic populations, reflecting the size of both populations in the wider Bay Area, while the primary PM<sub>2.5</sub> iF is higher for the Hispanic population, due to the demographic make-up of the neighborhoods directly surrounding the refinery.

Table 6: Ground-level iF values for facility in Richmond.

	Total	White	Black	Asian	Hispanic/Latinx	Other
<b>VOC</b>	0.23	0.08	0.03	0.03	0.08	0.01
<b>Primary PM<sub>2.5</sub></b>	6.2	1.9	0.8	0.9	2.3	0.3

#### Step 4: Calculate intake and population-weighted metrics

Intake for each population category is calculated by multiplying VOC emissions by VOC iF, primary emissions by primary iF, and adding together the results. Here, the values have been converted to units of grams per day. This value is the cumulative intake of the whole population: on average, a total of 0.19 grams of PM<sub>2.5</sub> is inhaled per day or 69.4 grams inhaled per year. To calculate the population-weighted average exposure concentration, divide the annual intake by the breathing rate (5292.5 m<sup>3</sup> per year) and the size of the population (see Table 1).

The population-weighted average exposure concentration values in row two vary by demographic group based on the proximity of the source to where people of different races/ethnicities live. When values are normalized by population size, we see that per-capita exposure concentrations in minority groups (e.g., Black) is higher than in larger groups (e.g., White and Hispanic), even though total intake is lower. The final results show that on the whole, the refinery results in higher intake for the Hispanic population than for any other group. Per-capita, however, we see that black, Asian, and Other Race communities are exposed at higher rates than either white or Hispanic populations. The results shown in the final row of the table combine the effects of different pollutant species, so they reflect both the local emissions inventory and iF values for the area.

Table 7: Example impact metrics for Richmond facility.

	Total	White	Black	Asian	Hispanic	Other
<b>Intake (g/day)</b>	0.19	0.06	0.02	0.03	0.07	0.01
<b>Pop. wtd avg. exposure concentration (ng/m<sup>3</sup>)</b>	0.31	0.25	0.64	0.35	0.29	0.42
<b>Total difference</b>	-	-0.06	0.34	0.04	-0.01	0.11
<b>% difference</b>	-	-19%	109%	14%	-5%	35%

## Results

### Summary of IF Database

The complex spatial patterns of iF for different pollutants and populations in the iF database are critical for evaluating source impacts and are also difficult to describe succinctly. We offer several summary descriptions of iF values within the database so that a user may better understand and interpret the results of iF-based modeling. More in-depth iF summary metrics are presented in Appendix D.

Three of the main sources of variation in iF are, in general order of importance, (1) the pollutant species, either primary or precursor: the iF for primary PM<sub>2.5</sub> is generally more sensitive to local population density resulting in steeper spatial gradients, while precursor iFs show more gradual changes in space. (2) the population density near the source location: for all species, iF values are highest in dense urban areas and lowest in rural or unpopulated areas. (3) the height at which the pollutant is emitted: increased stack height generally results in iF values that are lower and less sensitive to local population density.

A summary of population-weighted average iF values across the entire modeling domain for the total population is provided in Table 8, including the mean, median, and interquartile range (IQR) which reports the 25<sup>th</sup> and 75<sup>th</sup> percentile values. Population-weighting is often chosen as the best metric for summarizing iFs (Fantke et al., 2017; Humbert et al., 2009). Care should be taken in understanding the purpose of population-weighting in the iF context, as iF is a metric specific to a pollution source and not to the population exposed. Population weighting makes the assumption that the distribution of emissions is roughly equivalent to the distribution of the population; this assumption may not hold for some source categories, such as agriculture or electricity generation. Additional population-weighted iF values specific to each demographic group are included in Appendix D, as well as population-weighted mean per-capita values. These may be used to calculate the change in intake resulting from a generic, distributed increase or decrease in emissions, as well as the relative percent difference among demographic groups following that change.

Primary PM<sub>2.5</sub> emissions have the highest population-weighted iF, as primary emissions contribute directly to local pollution levels. The mean primary PM<sub>2.5</sub> iF value of 12 ppm falls within the range of values reported in the literature for the United States: 2 to 16 ppm overall, and 4 to 25 for urban areas (see Appendix A). Precursor species iFs are 1/10<sup>th</sup> to 1/20<sup>th</sup> the magnitude of primary PM<sub>2.5</sub> iFs, with the exception of NH<sub>3</sub>. For both pNO<sub>3</sub>/NO<sub>x</sub> and pSO<sub>4</sub>/SO<sub>2</sub>, mean values in the model fell within the range of values cited in other studies, 0.05 to 0.22 ppb for NO<sub>x</sub> and 0.3 to 1.3 ppb for SO<sub>2</sub>. Values for NH<sub>3</sub> are considered more uncertain than other precursor iFs due to base year sensitivity issues (see note on page 6). Few studies include iF values for NH<sub>3</sub>, but the one comparison value of 1.9 ppm suggests that our estimates may be high but are the correct order of magnitude (Humbert et al., 2011). Intake fractions based on formation of SOA from VOC emissions were not found in the literature.

Elevated emissions have significantly lower population-weighted iF values, as high emission plumes travel away from high population areas before they descend to breathing height. The mean iF values for primary PM<sub>2.5</sub> and NH<sub>3</sub> are greater than median values, indicating that there are some areas where the iF of these pollutants is atypically high due to a combination of meteorological, chemical, and demographic factors.

Table 8: Population-weighted iF summary values (ppm) for the total population.

	Height <sup>7</sup>	Mean	Median	25 <sup>th</sup> percentile	75 <sup>th</sup> percentile
<b>Primary PM<sub>2.5</sub></b>	Height 1	12	9.3	4	17
	Height 2	4.5	2.8	1.3	7.2
	Height 3	1	0.68	0.36	1.7
<b>VOC/SOA</b>	Height 1	0.48	0.43	0.22	0.66
	Height 2	0.19	0.14	0.076	0.3
	Height 3	0.049	0.041	0.022	0.074
<b>NH<sub>3</sub>/pNH<sub>4</sub></b>	Height 1	5.6	3.8	1.4	8.4
	Height 2	2.2	1.2	0.52	3.6
	Height 3	0.53	0.31	0.18	0.91
<b>NO<sub>x</sub>/pNO<sub>3</sub></b>	Height 1	0.44	0.41	0.2	0.6
	Height 2	0.19	0.17	0.09	0.27
	Height 3	0.055	0.055	0.028	0.078
<b>SO<sub>2</sub>/pSO<sub>4</sub></b>	Height 1	0.85	0.61	0.22	1.4
	Height 2	0.88	0.61	0.23	1.4
	Height 3	0.41	0.3	0.14	0.69

Emissions-weighted summary iF values are shown in Table 9. This weighting is based on the spatial data associated with emissions included in the US EPA National Emissions Inventory, and reflects the spatial distribution of pollutants aggregated across all source categories. This spatial weighting differs from population weighting: for some source categories, emissions occur in remote areas far from population centers. For this reason, emissions-weighted iF values are lower than population-weighted values. Emissions-weighted average iFs for each emissions sector and subsector are included in Appendix D. These source-specific metrics are useful for comparing which source categories tend to pollute more in highly populated areas and thus have a greater effect on public health. They may also be used to calculate the change in state-wide intake that might be expected from a reduction in emissions from a specific source category. Source- and demographic-specific iF values are not reproduced in print but are available in the accompanying spreadsheet referenced in Appendix E. These values may be used to calculate the state-wide EJ impacts of emissions changes from specific source categories.

<sup>7</sup> Height 1: ground level and low stack emissions (0-57m), Height 2: medium and high stack emissions (57-140m), Height 3: high plume emissions (>760m).

Table 9: Emissions-weighted iF summary values (ppm) for the total population.

	Height <sup>8</sup>	Mean	Median	25 <sup>th</sup> percentile	
<b>Primary PM<sub>2.5</sub></b>	Height 1	6	2.4	0.49	
	Height 2	2.5	0.9	0.24	
<b>VOC/SOA</b>	Height 1	0.35	0.27	0.068	
	Height 2	0.16	0.097	0.049	
<b>NH<sub>3</sub>/pNH<sub>4</sub></b>	Height 1	1.2	0.42	0.27	
	Height 2	2.5	1.5	0.49	
<b>NO<sub>x</sub>/pNO<sub>3</sub></b>	Height 1	0.27	0.16	0.036	
	Height 2	0.11	0.076	0.017	
<b>SO<sub>2</sub>/pSO<sub>4</sub></b>	Height 1	0.39	0.16	0.066	
	Height 2	0.53	0.21	0.057	

Table 10: Emissions-weighted iF (ppm) by income quintile

<b>Primary PM<sub>2.5</sub></b>	Height 1	1.3	1.1	1.2	1.2	1.1	6
	Height 2	0.51	0.44	0.52	0.52	0.48	2.5
<b>VOC/SOA</b>	Height 1	0.071	0.061	0.072	0.072	0.068	0.35
	Height 2	0.031	0.027	0.032	0.033	0.032	0.16
<b>NH<sub>3</sub>/pNH<sub>4</sub></b>	Height 1	0.25	0.22	0.26	0.26	0.25	1.2
	Height 2	0.48	0.42	0.51	0.53	0.52	2.5
<b>NO<sub>x</sub>/pNO<sub>3</sub></b>	Height 1	0.056	0.048	0.055	0.056	0.052	0.27
	Height 2	0.022	0.019	0.023	0.024	0.022	0.11
<b>SO<sub>2</sub>/pSO<sub>4</sub></b>	Height 1	0.072	0.063	0.077	0.082	0.089	0.39
	Height 2	0.1	0.093	0.11	0.11	0.11	0.53

<sup>8</sup> Height 1: ground level and low stack emissions (0-57m), Height 2: medium and high stack emissions (57-140m). Although a plume-rise algorithm was integrated into the source-specific concentration modeling, it was not used for calculating these emission-weighted averages so iFs for high-elevation plume emissions (>760 m) are not included here.

Table 11: Emissions-weighted iF (ppm) by racial-ethnic group

	Height	White	Hispanic	Asian	Black	Other	Total
<b>Primary PM<sub>2.5</sub></b>	Height 1	1.9	2.6	0.85	0.42	0.21	6
	Height 2	0.78	1.1	0.34	0.16	0.082	2.5
<b>VOC/SOA</b>	Height 1	0.12	0.15	0.048	0.023	0.012	0.35
	Height 2	0.052	0.068	0.021	0.0097	0.0052	0.16
<b>NH<sub>3</sub>/pNH<sub>4</sub></b>	Height 1	0.41	0.55	0.17	0.075	0.041	1.2
	Height 2	0.78	1.1	0.36	0.14	0.075	2.5
<b>NO<sub>x</sub>/pNO<sub>3</sub></b>	Height 1	0.092	0.12	0.034	0.017	0.0095	0.27
	Height 2	0.039	0.048	0.013	0.0062	0.0039	0.11
<b>SO<sub>2</sub>/pSO<sub>4</sub></b>	Height 1	0.14	0.15	0.058	0.024	0.014	0.39
	Height 2	0.17	0.23	0.074	0.034	0.018	0.53

### Intake Fraction Differences by Demographic Group

The iF for the total population can be broken down by population divisions such as income quintile (Table 10) and race-ethnicity (Table 11). Intake fraction values for population subgroups are included in the iF spatial database and are used to calculate the EJ metrics described in Table 5. The iF for a specific group depends on the total size of that population. Because the size of the population is consistent across income quintiles, the total magnitude of iFs shown in Table 10 is also consistent. In contrast, the iF for some racial-ethnic minority groups – Asian, black, and other races – is considerably lower than for larger groups – white and Hispanic (see Table 1)

Differences in iFs among demographic groups are also driven by factors beyond the size of the population. Emissions-weighted iFs for people of different races and ethnicities, income level, or other SES groups also differ if people in those groups tend to live closer to emission sources. To isolate the effect of emissions proximity, we control for population size. We calculate the per-capita iF value for each group by dividing the emissions-weighted mean by the size of the population of that group. Table 12 and Table 13 show the difference in per-capita emissions-weighted mean iF of each group relative to the value for the total population. There is a moderate trend across income quintiles shown in Table 12. For most pollutants, per-capita iF decreases with an increase in income, reflecting a closer proximity to pollution sources in lower income brackets. The trend is stronger for racial-ethnic groups. The major non-white populations (excluding “Other Race”) show higher per-capita iF values for most pollutants, indicating that more emissions occur near those populations than near others.

Table 12: Relative percent difference in emissions-weighted per-capita iF (% difference from total population per-capita iF) by income quintile

	Height <sup>9</sup>	Income Q1	Income Q2	Income Q3	Income Q4	Income Q5
Primary PM <sub>2.5</sub>	Height 1	9%	5%	1%	-3%	-10%
	Height 2	5%	4%	2%	-1%	-10%
VOC/SOA	Height 1	7%	4%	1%	-2%	-8%
	Height 2	3%	2%	1%	0%	-5%
NH <sub>3</sub> /pNH <sub>4</sub>	Height 1	5%	2%	1%	-1%	-6%
	Height 2	-1%	0%	1%	1%	-1%
NO <sub>x</sub> /pNO <sub>3</sub>	Height 1	8%	4%	1%	-2%	-9%
	Height 2	2%	3%	2%	1%	-7%
SO <sub>2</sub> /pSO <sub>4</sub>	Height 1	-4%	-4%	-3%	0%	8%
	Height 2	2%	2%	2%	0%	-6%

Table 13: Relative percent difference in emissions-weighted per-capita iF (% difference from total population per-capita iF) by racial-ethnic group

	Height	White	Hispanic	Asian	Black	Other
Primary PM <sub>2.5</sub>	Height 1	-19%	15%	9%	23%	-9%
	Height 2	-22%	21%	6%	15%	-15%
VOC/SOA	Height 1	-16%	14%	7%	16%	-10%
	Height 2	-16%	16%	4%	10%	-14%
NH <sub>3</sub> /pNH <sub>4</sub>	Height 1	-18%	18%	3%	7%	-14%
	Height 2	-22%	22%	12%	-3%	-22%
NO <sub>x</sub> /pNO <sub>3</sub>	Height 1	-15%	16%	-2%	14%	-9%
	Height 2	-12%	16%	-9%	0%	-9%
SO <sub>2</sub> /pSO <sub>4</sub>	Height 1	-11%	5%	16%	10%	-5%
	Height 2	-19%	17%	8%	15%	-11%

<sup>9</sup> Height 1: ground level and low stack emissions (0-57m), Height 2: medium and high stack emissions (57-140m). Although a plume-rise algorithm was integrated into the source-specific concentration modeling, it was not used for calculating these emission-weighted averages so iFs for high-elevation plume emissions (>760 m) are not included here.

### Localized IF Patterns

The summary statistics provided above integrate the wide-scale spatial patterns in the iF database, but the database also includes more localized patterns of iF driven by fine-scale differences in population density of different races, income groups, or other EJ-relevant groupings. These patterns are most apparent when viewing the iF database at a relatively fine spatial scale in highly populated areas. Figure 7 shows the heterogeneity of ground-level, primary  $PM_{2.5}$  iF for different racial-ethnic groups within the greater Los Angeles area. The highest iF values occur in densely populated central Los Angeles, and these are driven mostly by localized exposure in Black and Hispanic communities who make up the majority of residents in that area. Intake fraction at the periphery of the urban core is lower by ~50%, although there are localized peaks near smaller population centers. Often these peaks appear across groups, but some are most dramatic for a single race-ethnicity.

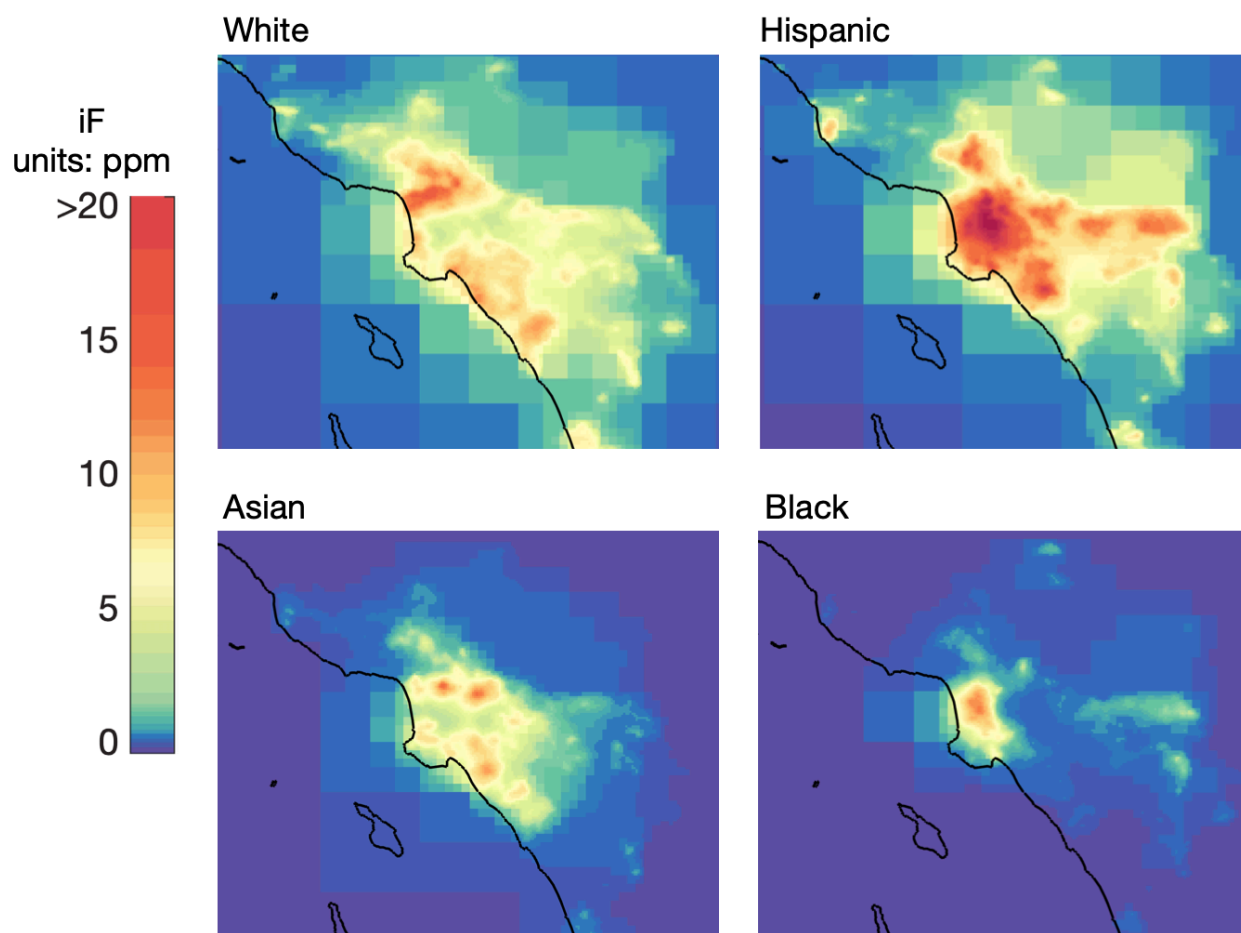


Figure 7: Intake fraction in Los Angeles for ground-level emissions of primary  $PM_{2.5}$ .

Patterns for primary  $PM_{2.5}$  can be further compared against iF patterns for elevated emissions of  $NO_x$ , shown in Figure 8. The iF values shown are not specific to a single emissions source category, but apply to any source of emissions of that species and in that location. Absolute iF values are much lower for  $NO_x$ , they show shallower gradients

from the urban core to surrounding areas, and exhibit less distinct localized differences among races/ethnicities. Based on this contrast in patterns, we can expect that highly localized sources of primary  $PM_{2.5}$  are more likely to result in high exposure concentration disparity among races/ethnicities than sources of  $NO_x$ . However, even elevated precursor emissions do have the potential to cause exposure concentration disparity.

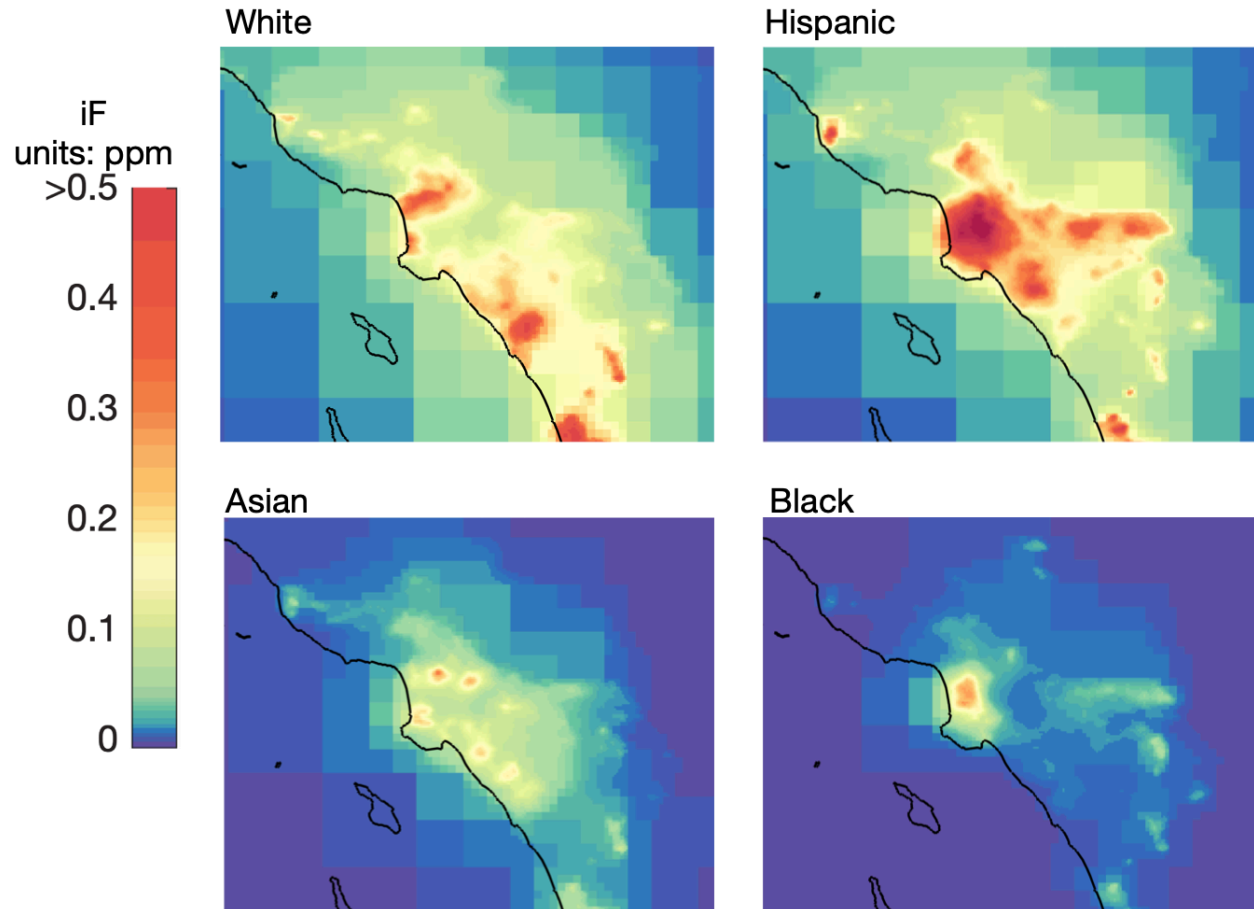


Figure 8: Intake fraction in Los Angeles for formation of particulate  $NO_3$  from emissions of  $NO_x$  at an elevation of 57 – 140 meters.

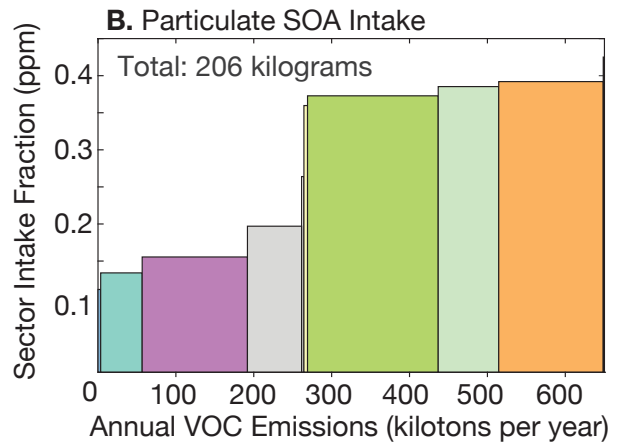
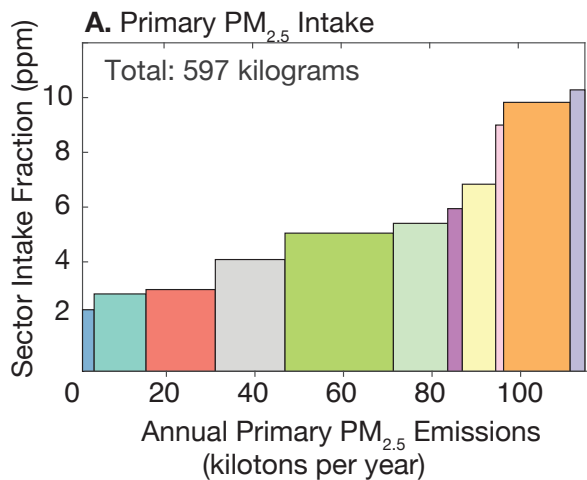
## Visual Representation of Intake Calculation from Emissions and IF

The basic calculation underlying the sector-specific impact analysis that follows this section is:  $iF \times \text{Emissions} = \text{Intake}$ . Figure 9 provides a visual representation of that calculation, integrating both ground-level and elevated emissions. Each panel corresponds to either primary  $\text{PM}_{2.5}$  or a precursor pollutant. The total intake for a pollutant is the sum of the intake contributions from each emission sector, shown as colored rectangles. For each sector's rectangle, the width of the base indicates the total mass of annual emissions from the sector. The height indicates the  $iF$  for that sector, determined by the spatial distribution of sector emissions. The product of the base (emissions) and height ( $iF$ ), the area of the rectangle, represents the total intake from that sector.<sup>10</sup>

A sector may result in high intake if either its emissions or  $iF$  are high. As one example, total emissions of primary  $\text{PM}_{2.5}$  from the industrial sector (panel A, rectangle shown in green) are greater than emissions of primary  $\text{PM}_{2.5}$  from on-road mobile sources (rectangle shown in orange), shown by the greater width of the green rectangle relative to the orange one. However, the  $iF$  for on-road mobile sources is much higher than for the industrial sector because driving tends to occur most in areas with high population density. As a result, the total intake from on-road mobile source primary  $\text{PM}_{2.5}$  emissions is higher than that from the industrial sector (146 and 100 kilograms, respectively). As another example, the agricultural sector is the dominant source of  $\text{NH}_3$  emissions (panel C, rectangle shown in teal), but has a lower  $iF$  than most other sectors. Agriculture causes greater intake of particulate  $\text{NH}_4$  than any other source, but a small increase in mobile-source or industrial emissions would cause more intake than a large increase in agricultural emissions.

---

<sup>10</sup> The scale of the axes is different for each panel, so the area of a sector's rectangle in one panel should not be compared with the area of a rectangle in another panel.



Sector	
Elec. Gen	Residential
Agriculture	Misc. Fuel Comb
Fugitive Dust	Construction
Industrial	On-road Mob. Srcls
Nat. Gas & Petr.	Cooking
Off-road Mob. Srcls	

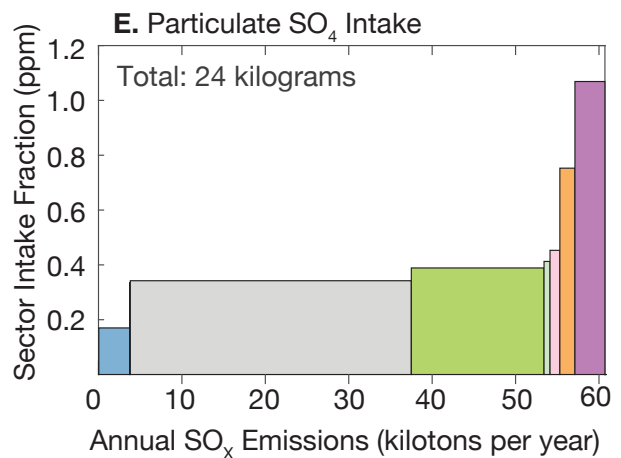
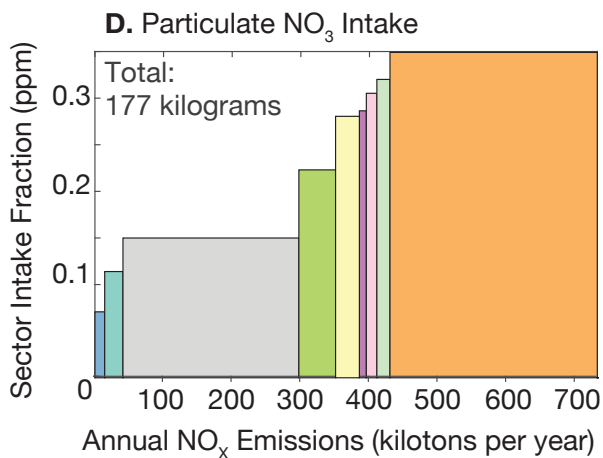
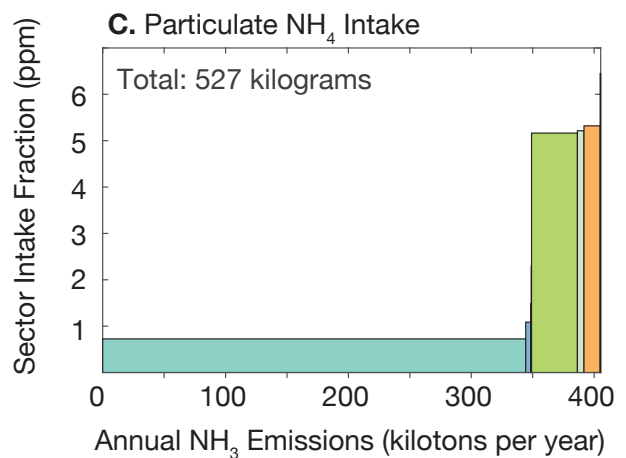


Figure 9: Area charts showing total population intake of PM<sub>2.5</sub> from each emitted species as the product of annual sector ground-level emissions and sector-specific iF.

The total population intake of PM<sub>2.5</sub> from each source and precursor is equal to the area of that sector's rectangle. The scale varies among panels, so the area of a source in one panel should not be compared with that source in another. In each chart, the sectors are sorted from lowest to highest iF. This order varies by sector.

## Sector-Specific Environmental Justice Impacts

### Effects across all sectors

In the sector-by-sector analysis we examine the relative impact of each category on the total population as well as disparity by race-ethnicity, income, age, and other socioeconomic factors. Figure 10 shows the population-weighted average exposure concentration for each major demographic group, represented as the sum of exposure concentrations from each of the 11 sectors. These exposure concentration values combine both primary and precursor emissions. The exposure concentration level for the total population is included in the top bar and marked with a vertical grey line so that subgroup values could be easily compared against the average. At the beginning of each individual sector description we include a copy of the top bar and highlight the relevant sector to place that sector within the context of total exposure concentration levels.

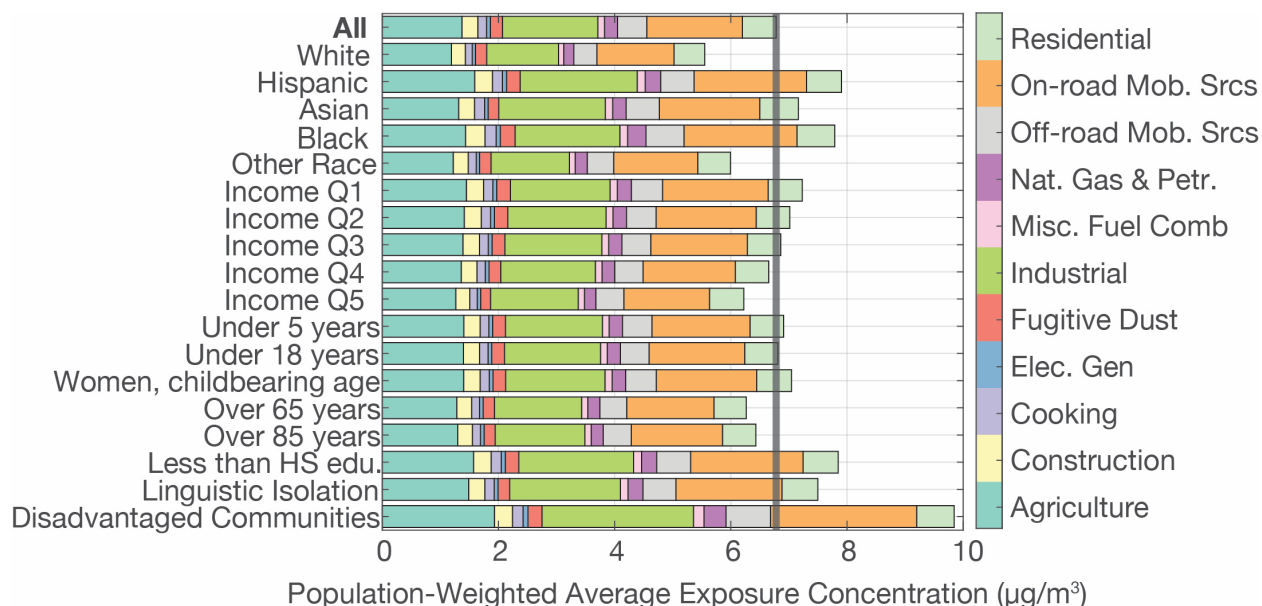


Figure 10: Contribution of all sectors to population-weighted average exposure concentration for different demographic categories.

The overall population-weighted average exposure concentration from anthropogenic emissions in the modeling domain is  $6.78 \mu\text{g}/\text{m}^3$  of  $\text{PM}_{2.5}$ .<sup>11</sup> Disadvantaged Communities experience the highest average exposure concentrations, in line with the  $\text{PM}_{2.5}$  and

<sup>11</sup> These exposure concentration values are useful for comparing the relative importance of different sources, but do not reflect the total population-weighted  $\text{PM}_{2.5}$  exposure in California, as this analysis does not include natural sources of  $\text{PM}_{2.5}$  (e.g., wildfires, biogenic VOC emissions, sea salt), nor does it include the long-range transport of anthropogenic pollution from beyond the bounds of the model domain. Monitoring data from 2014 indicates that annual average  $\text{PM}_{2.5}$  concentrations in California air basins ranged from  $4.0\text{--}22.8 \mu\text{g}/\text{m}^3$ , with an average of  $10.9 \mu\text{g}/\text{m}^3$  across all basins.

DPM exposure criteria used by the CalEnviroScreen 3.0 tool (Faust et al. 2017). These communities experience higher average impacts from every sector, resulting in 45% higher average exposure concentrations compared with the average for the total population. The highest overall exposure concentration disparity results from the industrial sector, followed by on-road mobile sources, and the highest relative disparity results from the natural gas and petroleum sector (see Table 17 and Table E8).

Among races and ethnicities, Hispanic and black populations are most exposed, and Asian population exposure concentration also exceeds the overall average. There is a linear decrease in total exposure concentration by income quintile, although the difference is less marked than among racial groups. Younger segments of the population tend to be more exposed than the elderly. Both lower educational status and linguistic isolation are associated with higher exposure concentrations.

The sectors that contribute most to population exposure concentrations across demographic groups are on-road mobile sources and the industrial sector, each contributing 24% to average population exposure concentration. The industrial sector emits more than twice the mass of primary  $PM_{2.5}$  and  $NH_3$  than on-road sources but has iF values for  $PM_{2.5}$  and  $NH_3$  of 6 ppm and 4 ppm, respectively, compared with 10 ppm and 5 ppm for on-road mobile sources, resulting in a magnified effect from the on-road mobile source sector. In addition, the large total on-road  $NO_x$  emissions result in substantial additional  $PM_{2.5}$ , despite the lower iF for  $NO_x$  compared to other precursors (see Appendices C and D). This specific case illustrates the importance of integrating multiple pollutants and using source-specific iFs when comparing sector contributions to population exposure concentration. The third largest contributor is the agricultural sector, contributing 20% to average exposure concentration. Agriculture generates 90% of total anthropogenic  $NH_3$  emissions, which drives its high ranking. Residential and off-road mobile sources contribute 9% and 7% respectively. Total emissions by off-road mobile sources are comparable to on-road sources, but their distance from highly populated areas results in substantially lower exposure concentrations. The final six sectors contribute 5% or less to total population exposure concentration.

Table 14 and Table 15 show the relative difference in exposure concentrations among races and income quintiles by sector. Average exposure concentration among the white population is lower for all categories, ranging from 7% to 25% below average. The reverse is true for the Hispanic population, with exposure concentrations ranging from 3% to 23% above average. Exposure concentration disparity is most dramatic for the black population, with some minor categories like off-road mobile sources, natural gas and petroleum, and outdoor emissions from commercial cooking resulting in exposure concentrations 30% to 40% higher than the population average. Exposure concentration disparity by sector is mixed for the Asian population, and those in the “other race” group tend to be less exposed than the population average.  $PM_{2.5}$  exposure concentration decreases with an increase in income for all sectors except residential sources of outdoor emissions (e.g., woodstoves, fireplaces, and lawn and garden equipment).

Table 14: Difference in population-weighted exposure concentration to PM<sub>2.5</sub> by race-ethnicity (units: µg/m<sup>3</sup>, relative percent difference).

	Average	Δ White	Δ Hispanic	Δ Asian	Δ Black	Δ Other
Agriculture	1.37	-13%	16%	-4%	5%	-11%
Construction	0.28	-12%	11%	0%	21%	-6%
Cooking	0.15	-21%	14%	16%	30%	-8%
Elec. Gen	0.06	-15%	18%	-5%	9%	-11%
Fugitive Dust	0.21	-7%	10%	-13%	20%	-7%
Industrial	1.64	-25%	23%	12%	10%	-18%
Miscellaneous	0.12	-20%	18%	9%	13%	-12%
Nat. Gas & Petr.	0.22	-23%	19%	3%	42%	-8%
Off road Mob. Srcs	0.50	-21%	14%	14%	30%	-9%
On road Mob. Srcs	1.65	-19%	18%	5%	18%	-12%
Residential	0.58	-9%	3%	14%	12%	-3%
<b>Grand Total</b>	<b>6.78</b>	<b>-18%</b>	<b>17%</b>	<b>6%</b>	<b>15%</b>	<b>-12%</b>

Table 15: Difference in population-weighted exposure concentration to PM<sub>2.5</sub> by income category (units: µg/m<sup>3</sup>, relative percent difference)

	Average	Δ Q1	Δ Q2	Δ Q3	Δ Q4	Δ Q5
Agriculture	1.37	6%	3%	1%	-1%	-8%
Construction	0.28	7%	7%	4%	-2%	-13%
Cooking	0.15	8%	6%	2%	-3%	-11%
Elec. Gen	0.06	4%	3%	1%	-1%	-10%
Fugitive Dust	0.21	11%	10%	6%	-3%	-19%
Industrial	1.64	5%	3%	2%	-1%	-8%
Miscellaneous	0.12	9%	3%	0%	-3%	-8%
Nat. Gas & Petr.	0.22	8%	4%	2%	-2%	-12%
Off road Mob. Srcs	0.50	7%	1%	-1%	-3%	-4%
On road Mob. Srcs	1.65	10%	5%	1%	-3%	-10%
Residential	0.58	1%	-1%	-1%	-1%	2%
<b>Grand Total</b>	<b>6.78</b>	<b>7%</b>	<b>3%</b>	<b>1%</b>	<b>-2%</b>	<b>-8%</b>

Relative exposure concentration disparity for age groups and other SES groups are shown in Table 16 and Table 17. Those over the age of 65 and 85 tend to be less exposed than the population as a whole at a fairly consistent level of 5-10% across sources. This is desirable, as those of advanced age are more susceptible to the chronic health effects of PM<sub>2.5</sub> exposure. Women of childbearing age are more exposed than the population average, presenting a possible concern for adverse prenatal and neonatal health effects, but the elevation in exposure concentration is minor. The two additional markers for low socioeconomic status, adults over 25 with less than a high school education and linguistic isolation (households self-reporting as speaking English less than “very well”), are both associated with higher PM<sub>2.5</sub> exposure concentrations. Disparity rates for those with less than a high school education are larger than for any

other demographic group apart from Disadvantaged Communities. Disparity rates by linguistic isolation are lower for some sources, but notably high for industrial sources and the natural gas and petroleum sector.

Table 16: Difference in population-weighted exposure concentration to PM<sub>2.5</sub> by age category (units: µg/m<sup>3</sup>, relative percent difference)

	Average	Δ Age under 5	Δ Age under 18	Δ Women of child bearing age	Δ Age over 65	Δ Age over 85
Agriculture	1.37	2%	2%	2%	-6%	-5%
Construction	0.28	3%	1%	3%	-7%	-7%
Cooking	0.15	1%	-2%	5%	-8%	-7%
Elec. Gen	0.06	2%	0%	2%	-4%	0%
Fugitive Dust	0.21	5%	3%	3%	-7%	-10%
Industrial	1.64	2%	1%	4%	-8%	-6%
Miscellaneous	0.12	1%	-1%	5%	-8%	-5%
Nat. Gas & Petr.	0.22	2%	1%	4%	-8%	-7%
Off road Mob. SrCs	0.50	1%	-1%	5%	-8%	-4%
On road Mob. SrCs	1.65	3%	0%	5%	-9%	-5%
Residential	0.58	0%	-2%	3%	-4%	-1%
<b>Grand Total</b>	<b>6.78</b>	<b>2%</b>	<b>0%</b>	<b>4%</b>	<b>-8%</b>	<b>-5%</b>

Table 17: Difference in population-weighted exposure concentration to PM<sub>2.5</sub> by other socioeconomic status categories (units: µg/m<sup>3</sup>, relative percent difference)

	Average	Δ Less than HS education	Δ Linguistic Isolation	Δ Disadvantaged Communities
Agriculture	1.37	16%	9%	41%
Construction	0.28	11%	1%	13%
Cooking	0.15	16%	7%	21%
Elec. Gen	0.06	13%	6%	35%
Fugitive Dust	0.21	11%	-5%	15%
Industrial	1.64	22%	16%	59%
Miscellaneous	0.12	19%	13%	55%
Nat. Gas & Petr.	0.22	18%	16%	70%
Off road Mob. SrCs	0.50	16%	12%	52%
On road Mob. SrCs	1.65	18%	11%	53%
Residential	0.58	3%	6%	11%
<b>Grand Total</b>	<b>6.78</b>	<b>17%</b>	<b>11%</b>	<b>45%</b>

Similar tables – the absolute intake difference and relative percent difference by demographic group – are tabulated separately for each sector in Appendix E.

The interaction between race-ethnicity and income in total exposure concentration level is illustrated in Figure 11. The colored icon indicates the average exposure concentration for the given racial-ethnic group from sector and the gray icons indicate the exposure concentration at different income quintiles within that racial-ethnic group. Overall, we see that the distribution of exposure concentrations across income quintiles within a race-ethnicity is smaller than the distribution of exposure concentrations among races/ethnicities; White populations are less exposed to PM<sub>2.5</sub> regardless of income level, and Black populations are more exposed regardless of income level, as are Hispanic populations for every source except fugitive dust. This pattern is less consistent for the Asian population, in which higher income groups are less exposed than the population average while lower income groups are more exposed. For some minor sectors, the exposure concentration range by income is wide for some racial-ethnic groups.

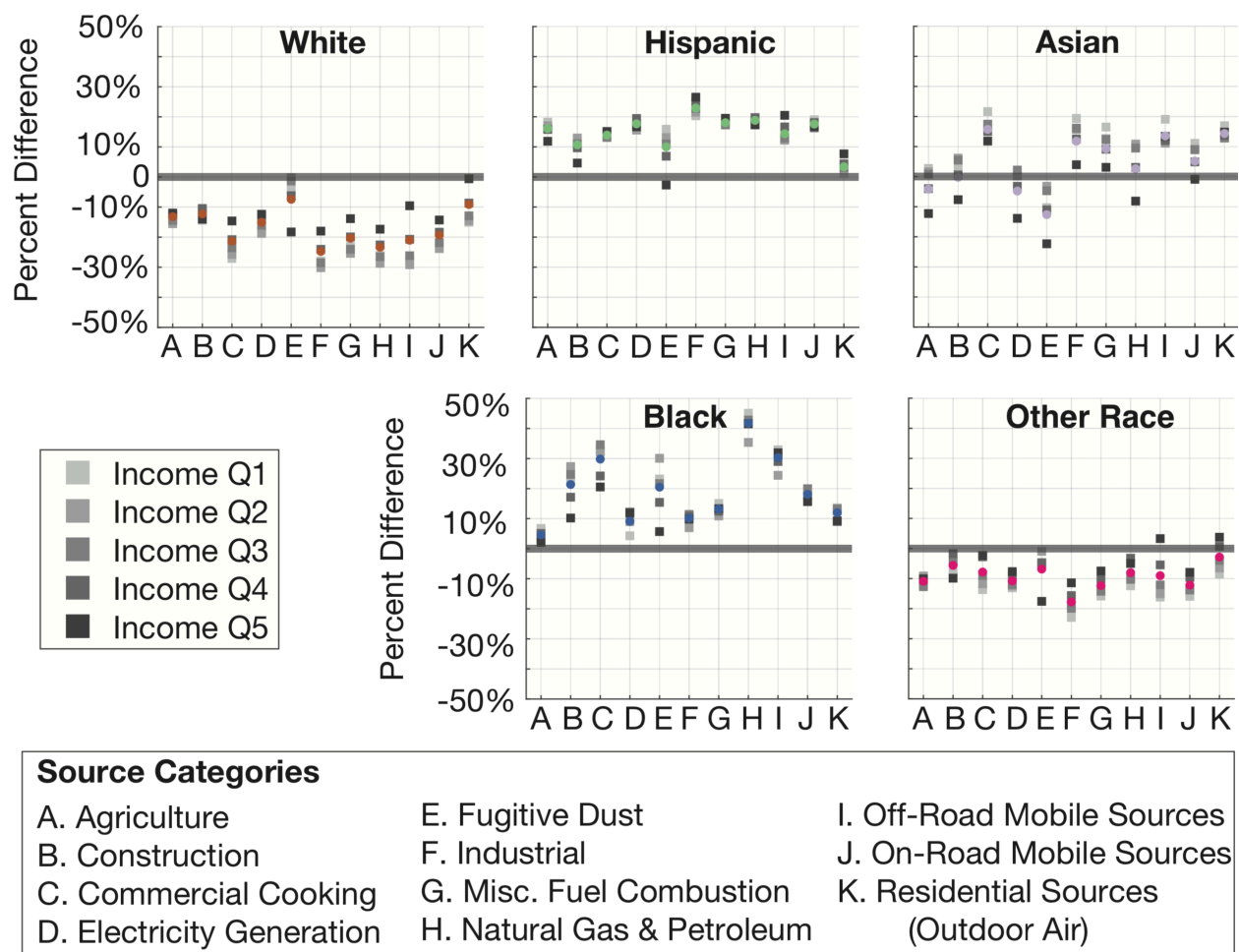
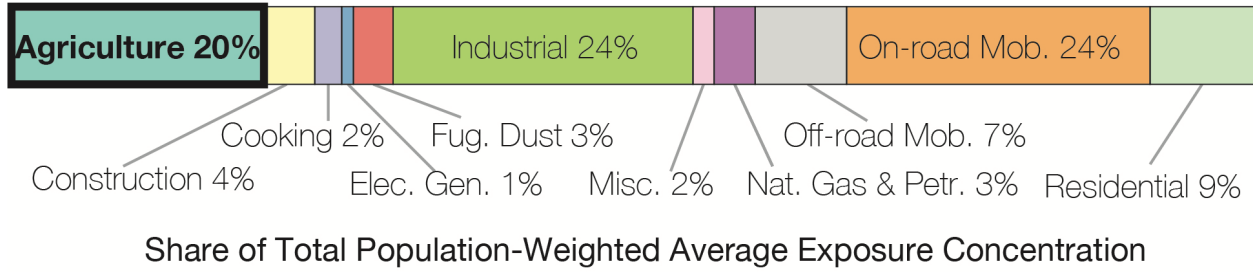


Figure 11: All-sector relative percent differences in population-weighted average PM<sub>2.5</sub> concentration compared to total population average, shown by race-ethnicity (colored circle icons) and by each income quintile in each racial-ethnic category (gray square icons).

## Agriculture



The agriculture sector contains 7 subcategories: fertilizer application, agriculture-specific industrial processes, livestock production, off-road mobile agricultural equipment, pesticide application, and tilling. PM<sub>2.5</sub>-related emissions in this overall category are dominated by ammonia (NH<sub>3</sub>). Agriculture is also a significant source of VOCs, NO<sub>x</sub>, and primary PM<sub>2.5</sub>. Agricultural emissions are modeled primarily as area sources based on land-use designations, with some livestock waste subcategories modeled as point sources.

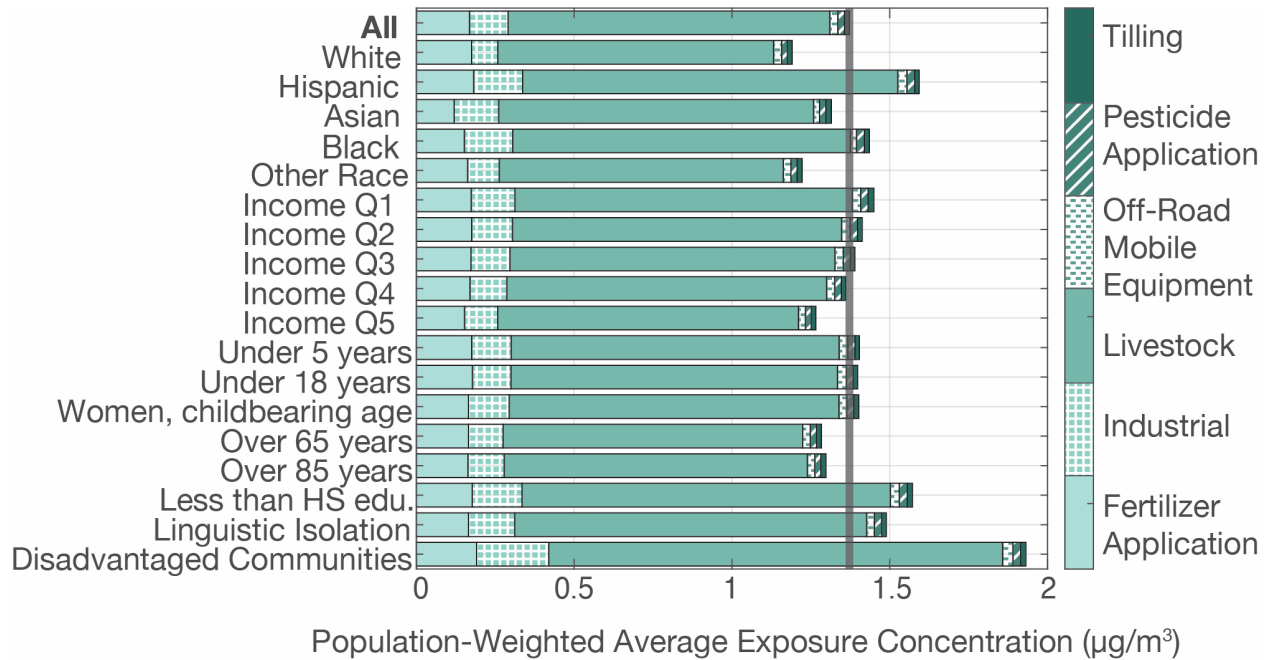


Figure 12: Agricultural sector: contribution of sector categories to population-weighted average exposure concentration for different demographic groups.

The agricultural sector is the third-largest contributor to population-weighted average exposure concentration (20%). The dominant source of PM<sub>2.5</sub> is livestock, followed by industrial processing and fertilizer application. Among races and ethnicities, the Hispanic group is most disproportionately exposed to agricultural PM<sub>2.5</sub>, with the greatest exposure concentration disparity resulting from livestock production. The highest relative disparity occurs among people of color from industrial agriculture

processes. Disparity by income category is minor, as is disparity by age. Among all demographic groups, disadvantaged communities experience the highest average exposure concentration from the agriculture sector.

Income quintiles within racial-ethnic groups play a stronger role in exposure concentration within the agricultural sector than in other sectors. Those in the highest income quintile for Hispanic, Asian, and black populations are markedly less exposed to agricultural sources than those in lower quintiles. This pattern does not occur within the white or “other race” populations.

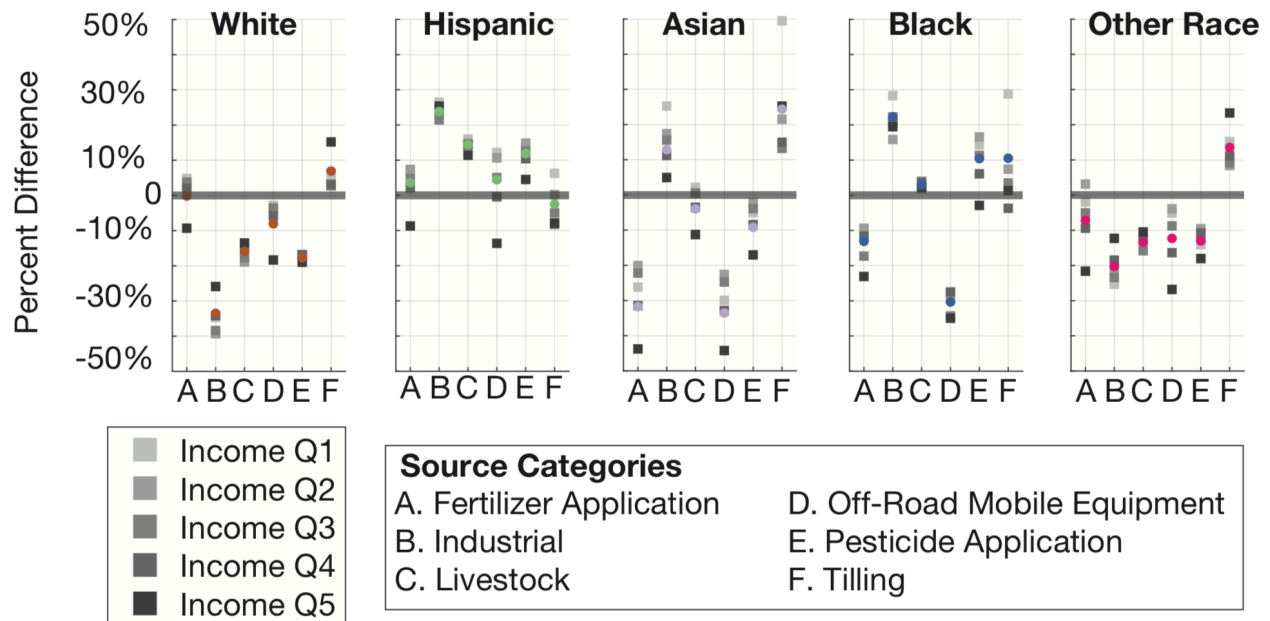
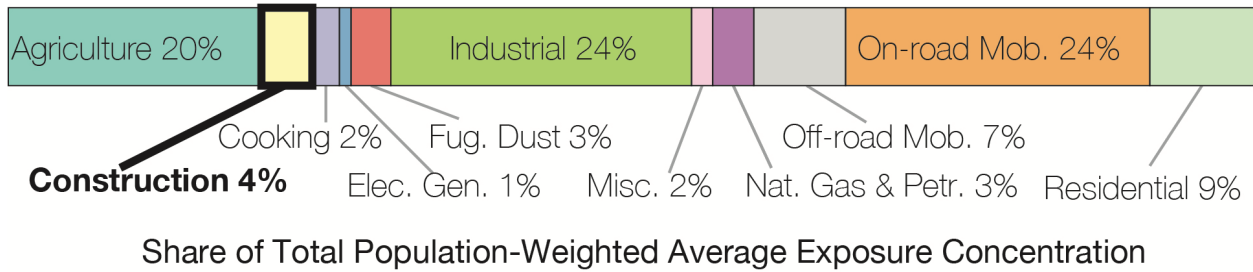


Figure 13: Agricultural sector: relative percent differences in population-weighted average  $PM_{2.5}$  concentration compared to total population average for categories.

Exposure concentration difference by racial-ethnic group is shown as colored circle icons, and exposure concentration for income quintiles within in each racial-ethnic category are shown as gray square icons.

## Construction



The construction sector is divided into five categories: off-road mobile construction equipment, fugitive emissions during road construction, fugitive dust from other construction activities, demolitions, and site preparation. The sector is a minor contributor to the population-weighted average exposure concentration (4%). The dominant source of exposure concentration within the construction sector is off-road mobile construction equipment, followed by fugitive dust from road construction and other sources. The contribution of site preparations and demolitions are sufficiently negligible that they are not visible in Figure 14. Black and Hispanic populations are more highly exposed than other races and ethnicities across all construction sector categories, with the exposure concentration disparity for the Black population greater than for any other demographic group. Exposure concentration is lower among higher income quartiles and the aged population, and higher for those with less than a high school education and Disadvantaged Communities.

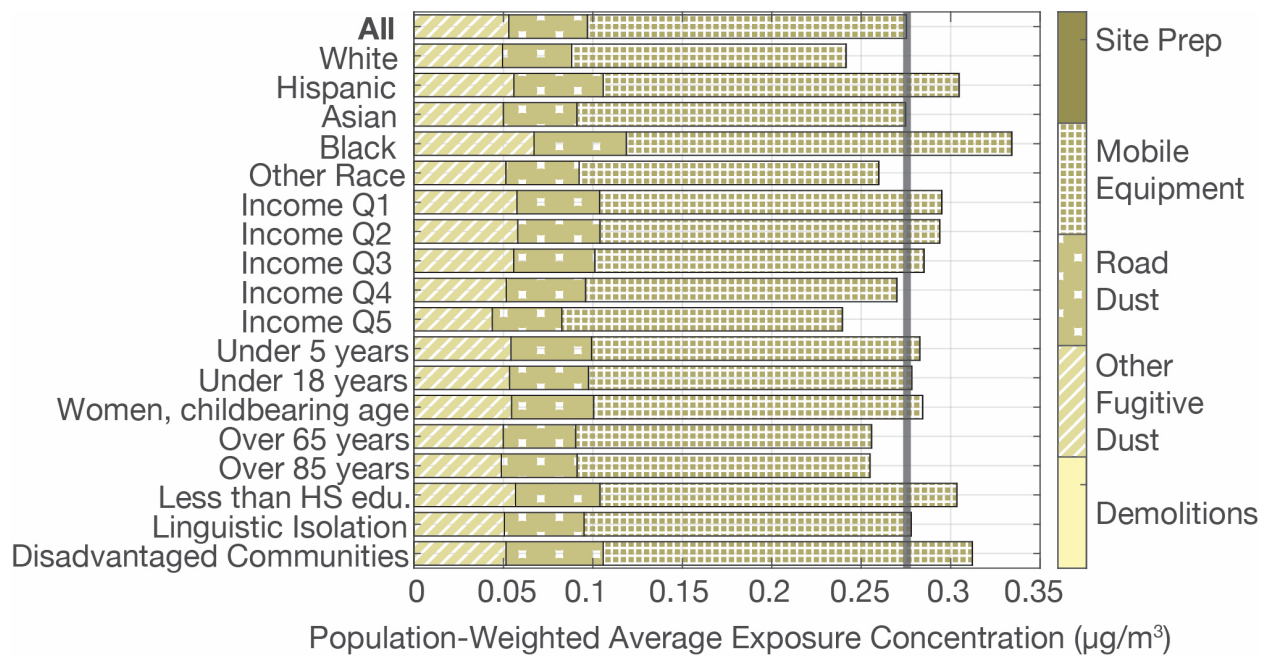


Figure 14: Construction sector: contribution of construction sector categories to population-weighted average exposure concentration for different demographic groups.

Within each racial-ethnic group, those in high-income categories are least exposed. Demolitions and site preparation caused high relative exposure concentration disparity for some race-income groups, but the absolute magnitude of this disparity is negligible.

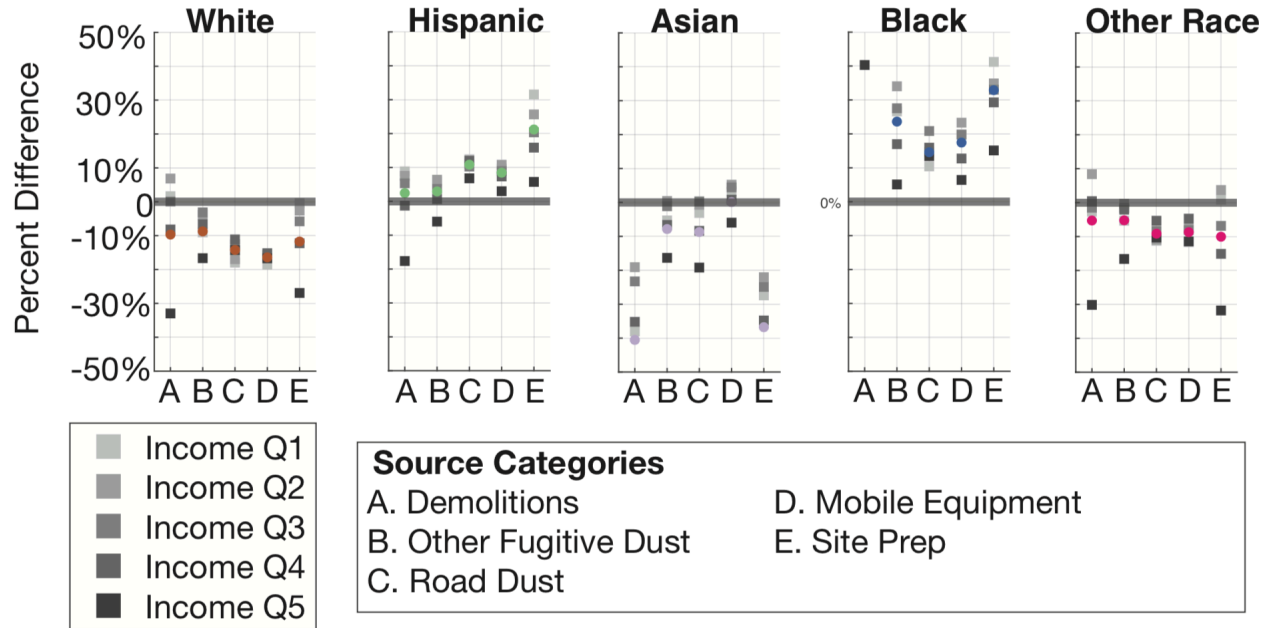
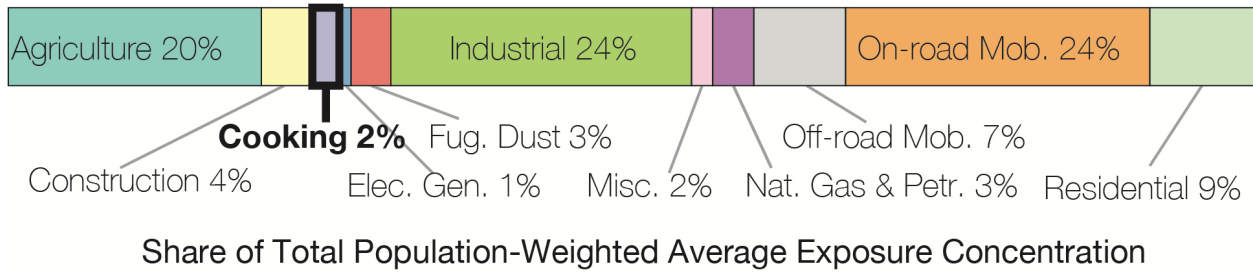


Figure 15: Construction sector: relative percent differences in population-weighted average  $PM_{2.5}$  exposure concentration compared to total population average for categories.

Exposure concentration difference by racial-ethnic group is shown as colored circle icons, and exposure concentration for income quintiles within in each racial-ethnic category are shown as gray square icons.

## Cooking



This category includes the contribution of commercial cooking emissions to ambient outdoor  $PM_{2.5}$  concentrations. This category includes two types of activities: charbroiling and frying. Cooking creates emissions of both primary  $PM_{2.5}$  and VOCs. Emissions in this category are modeled as an area source based on county-level assessment of the number of restaurants and the level of charbroiling and frying activity at each restaurant.

As a sector, cooking is a minor contributor to population-weighted average exposure concentration (2%), but its impacts are of a magnitude comparable to many individual categories within the industrial or off-road mobile sector. Cooking disproportionately affects Hispanic, Asian, and black populations, and causes comparable exposure concentration disparity for those with less than a high school education and Disadvantaged Communities.

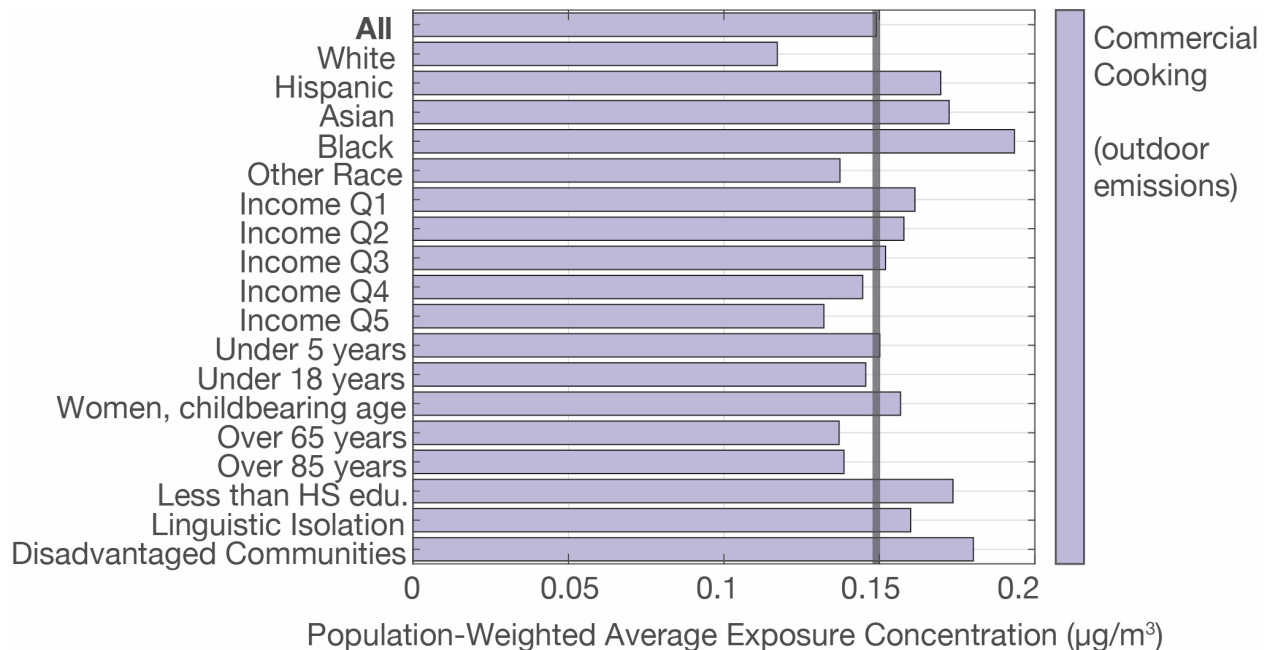


Figure 16: Cooking: contribution to population-weighted average exposure concentration for different demographic groups.

Higher income populations on the whole experience lower cooking-related  $PM_{2.5}$  exposure concentration, but income categories within racial-ethnic groups show less consistent effects: higher income groups in white and “other race” populations

experience higher exposure concentrations than other income groups, while the opposite is true for Asian and black populations.

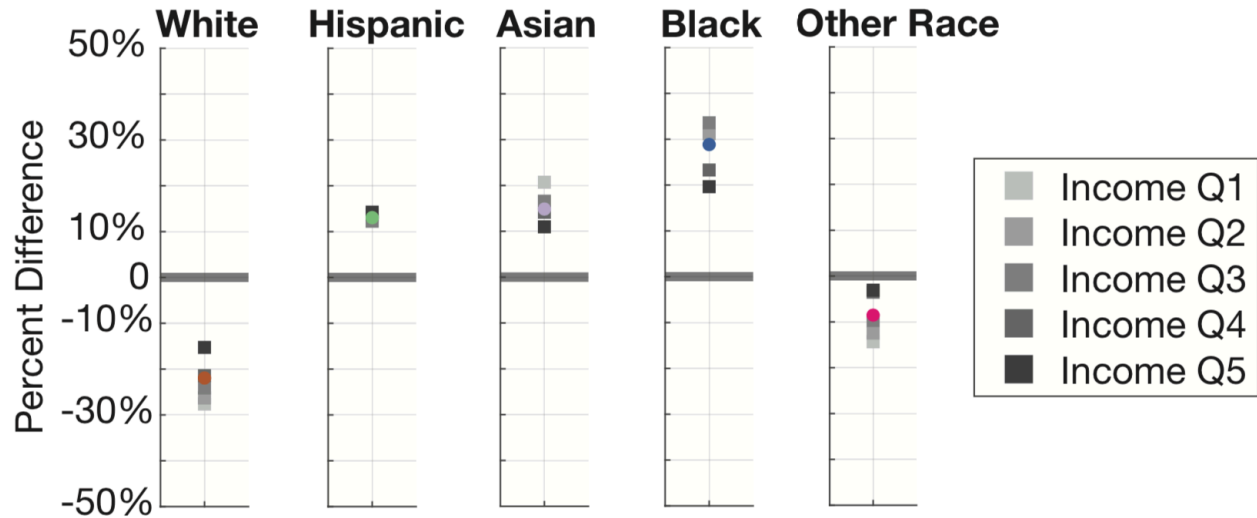
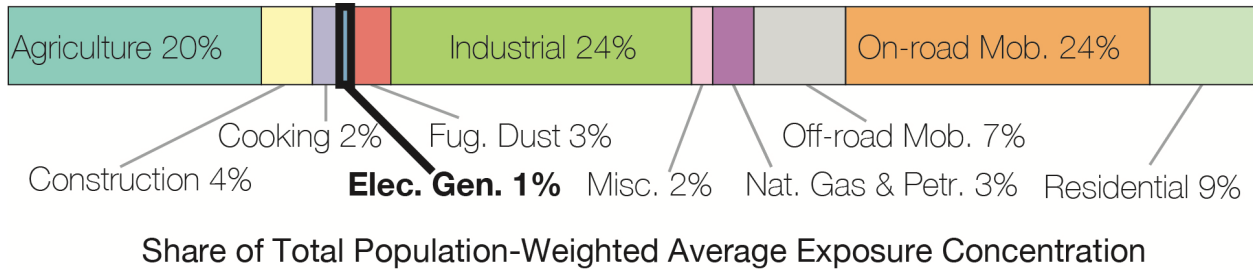


Figure 17: Cooking: relative percent differences in population-weighted average  $PM_{2.5}$  concentration compared to total population average.

Exposure concentration difference by racial-ethnic group is shown as colored circle icons, and exposure concentration for income quintiles within in each racial-ethnic category are shown as gray square icons.

## Electricity Generation



Electricity generation sources are categorized by the type of fuel used by the facility: coal (of varying grades), residual oil, distillate oil, natural gas, process gas, landfill gas, and various minor fuel types contained in an “other” category. Electricity generation facilities are point sources that emit both at ground-level and in elevated stacks.

The electricity generation sector is the smallest contributor to population-weighted average exposure concentration (1%). This result stands in contrast with patterns observed for the whole of the continental United States, as electricity generation in the eastern US tends to be more emissions intensive. Within the sector, natural gas electricity generation is the dominant source of exposure concentration, and results in higher exposure concentrations for Hispanic and black populations as well as Disadvantaged Communities.

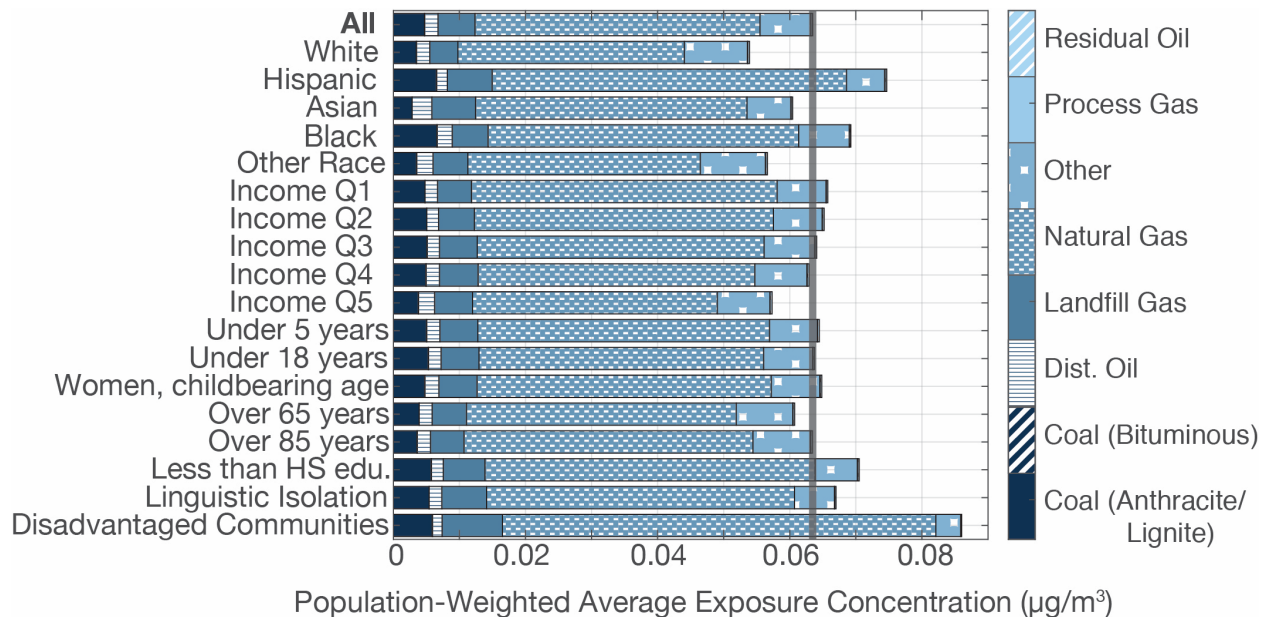


Figure 18: Electricity generation: contribution of sector categories to population-weighted average exposure concentration for different demographic groups.

As shown in Figure 19, PM<sub>2.5</sub> exposure concentrations from natural gas emissions, the highest-impact electricity generation source, shows much greater variation due to race/ethnicity than income level. Some other electricity-generating sources show high relative differences in exposure concentration for some categories (e.g., process gas), but contribute a negligible amount to total exposure concentration disparity.

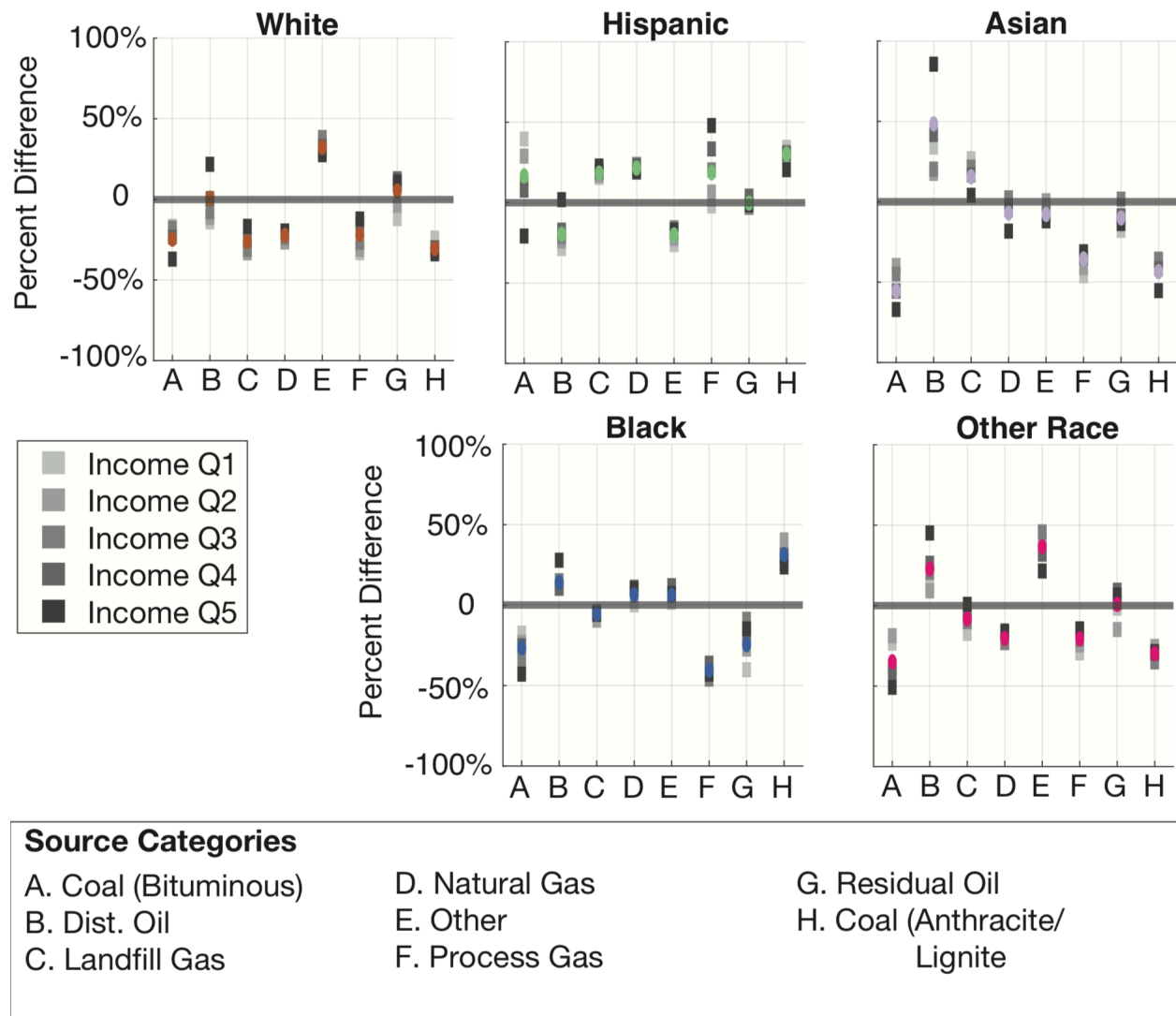
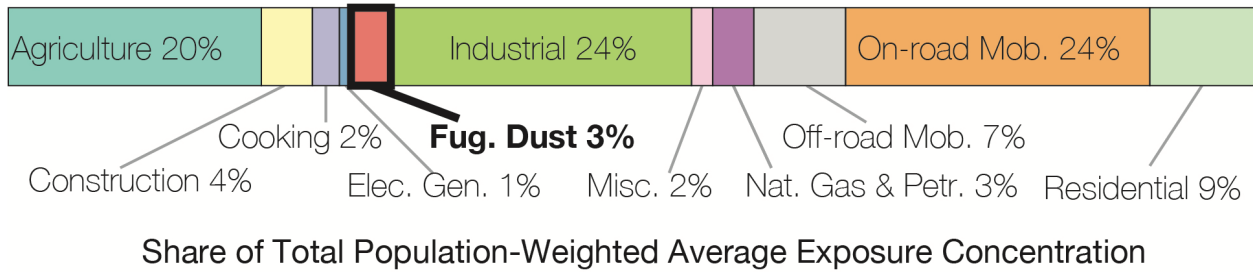


Figure 19: Electricity generation: relative percent differences in population-weighted average PM<sub>2.5</sub> concentration compared to total population average for categories.

Exposure concentration difference by racial-ethnic group is shown as colored circle icons, and exposure concentration for income quintiles within in each racial-ethnic category are shown as gray square icons.

## Fugitive Dust



Fugitive road dust includes resuspended primary PM<sub>2</sub> emissions from paved and unpaved roads and road sanding/salting. Fugitive dust from other sources, including construction and agriculture, are included within subsections of those sectors. Fugitive dust is a minor contributor to the population-weighted average exposure concentration (3%). This sector serves as a clear example of the importance of proximity to population exposure concentration: fugitive dust from paved roads contributes only 40% to total fugitive dust emissions but causes 80% of total exposure concentration from the category. Paved roads result in 10% higher exposure concentration for the Hispanic population and 20% higher exposure concentration for the black population, while unpaved roads result in 20% higher exposure concentration for the white population and lower exposure concentration among all other racial-ethnic groups. High income is associated with lower exposure concentrations across all races and ethnicities.

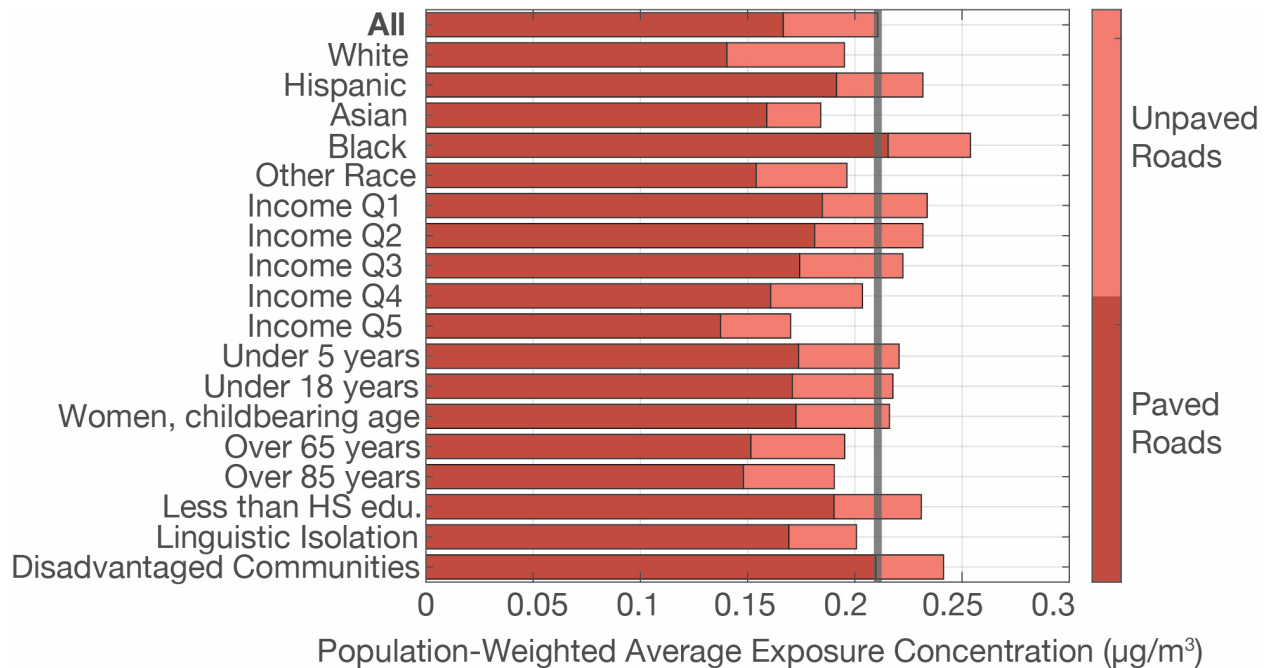


Figure 20: Fugitive dust: contribution of fugitive dust categories to population-weighted average exposure concentration for different demographic groups.

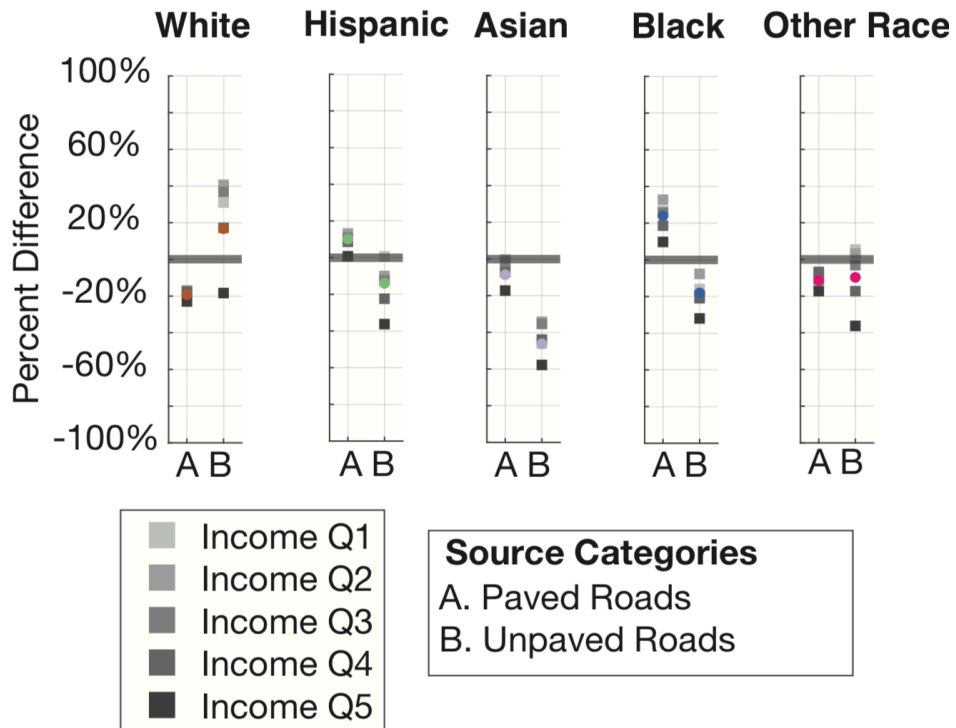
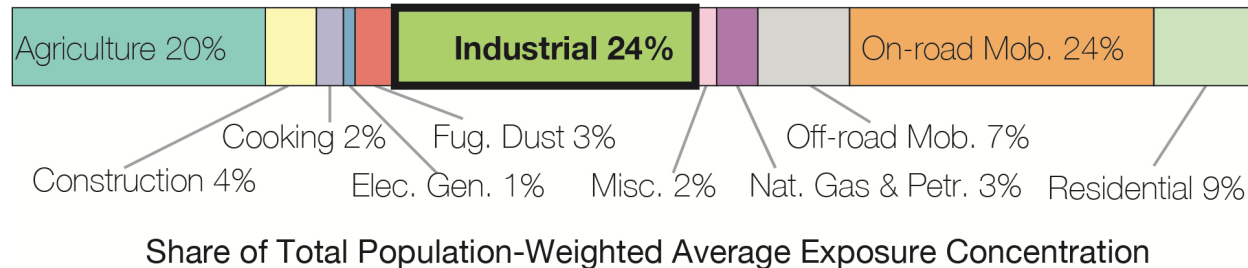


Figure 21: Fugitive dust: relative percent differences in population-weighted average  $PM_{2.5}$  concentration compared to total population average.

Exposure concentration difference by racial-ethnic group is shown as colored circle icons, and exposure concentration for income quintiles within in each racial-ethnic category are shown as gray square icons.

## Industrial Sources



Industrial emission sources include a variety of types of facilities and several different types of processes in the extraction, manufacturing, storage, and distribution of materials such as minerals, metals, biofuels, wood products, textiles, organic solvents, and cement. This category also includes emissions that result from the manufacture of secondary products derived from these materials. The 10 subcategories for industrial sources are organized broadly by the processes involved in industrial activity: surface mining and stone quarrying (non-metal); fuel combustion; metals processing; chemical and allied product manufacturing; solvent utilization; transport, storage and marketing of materials (TSM); waste disposal and incineration; and other miscellaneous industrial processes. Two specific materials of interest -- cement/concrete and cogeneration facilities -- are considered separately.

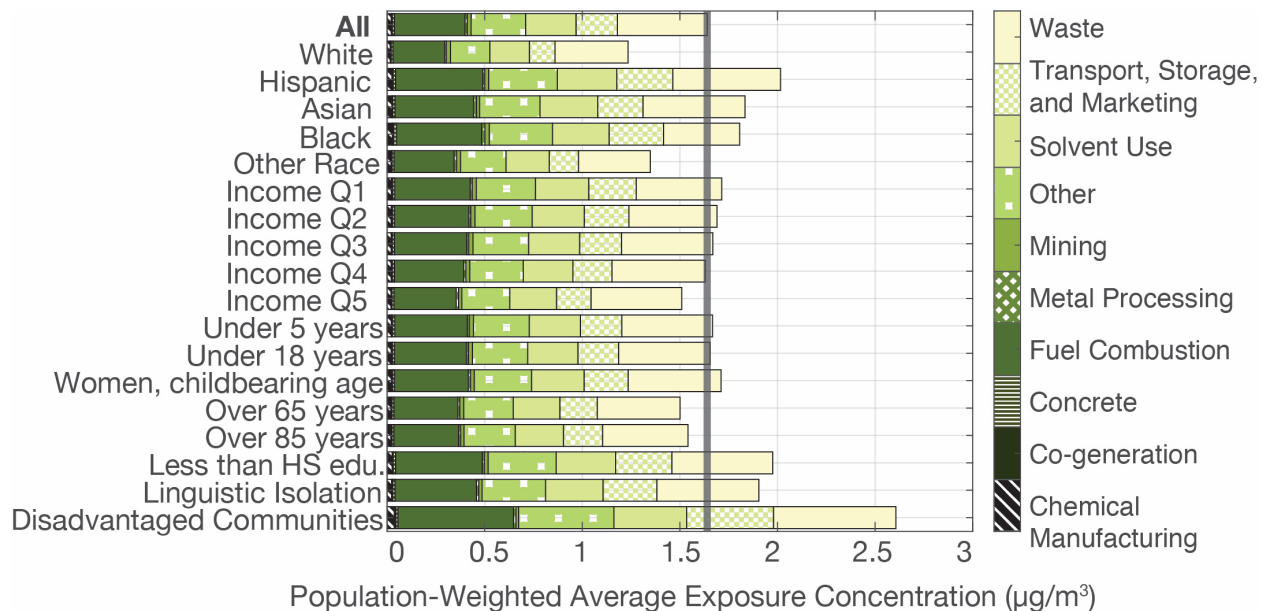
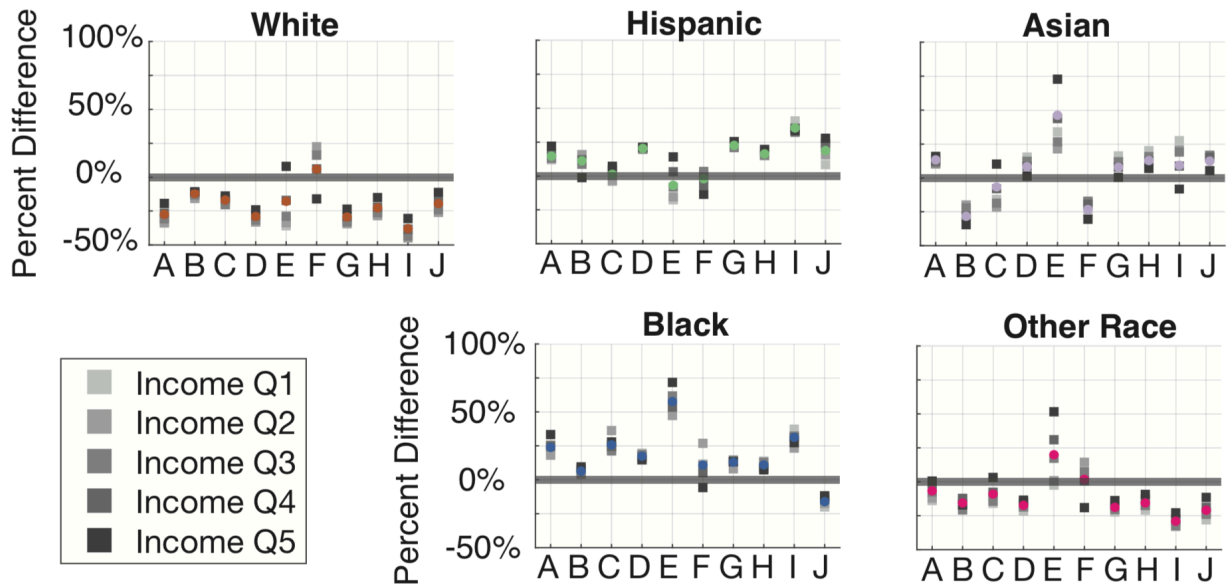


Figure 22: Industrial sector: contribution of industrial sector categories to population-weighted average exposure concentration for different demographic groups.

The industrial sector matches on-road mobile sources as the top contributor to population-weighted average exposure concentration (24%). Within the sector, the

category of waste disposal and incineration causes the largest impact, followed by fuel combustion, other activity, solvent utilization, and TSM. This sector results in substantial exposure disparity for Disadvantaged Communities, which experience average exposure concentrations 59% higher than the population as a whole. Chemical manufacturing, fuel combustion, and TSM result in 71%, 64%, and 111% higher exposure concentrations in Disadvantaged Communities. Pollution from the industrial sector results in 23% higher exposure concentration for the Hispanic population, 22% higher exposure concentration for those with less than a high school education, and 59% higher exposure concentration for Disadvantaged Communities. The absolute exposure concentration difference for these three categories is higher for the industrial sector than for any other sector, including on-road mobile sources. Asian and black populations and linguistically isolated populations are exposed >10% more than the population-weighted average.

The major sources of exposure concentration disparity in the industrial sector -- fuel combustion, waste disposal, TSM, and the other processes category -- are all elevated for Hispanic, Asian, and black populations, but the magnitude of the difference is consistently highest for the Hispanic population, lower for the black population, and least for the Asian population. The exception is waste disposal, for which the black population experiences lower than average exposure concentration. Several minor categories follow differing patterns: metals processing results in much higher relative exposure concentrations for Asian, black, and "other race" populations than for any other category, and surface mining results in higher exposure concentration for white, black, and "other race" populations. While patterns by income follow the typical decrease in exposure concentration with increase in income, the pattern is reversed for waste disposal and varies further for income categories within racial-ethnic groups.



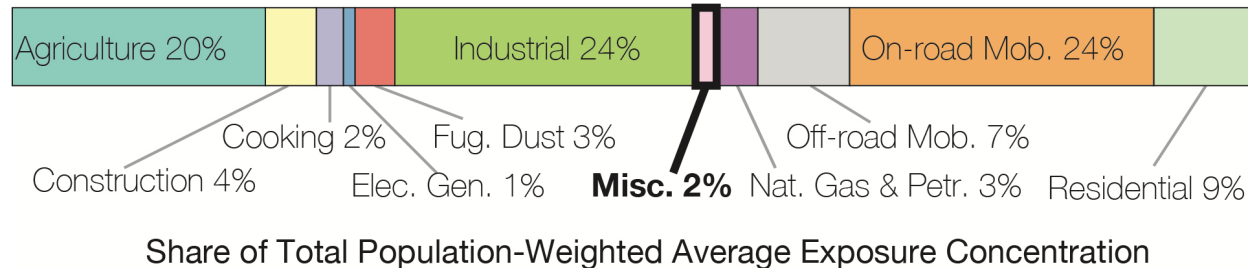
**Source Categories**

- A. Chemical Manuf.
- B. Co-generation
- C. Concrete
- D. Fuel Combustion
- E. Metal Processing
- F. Mining
- G. Other
- H. Solvent Use
- I. Transport, Storage, and Marketing
- J. Waste

Figure 23: Industrial sector: relative percent differences in population-weighted average  $PM_{2.5}$  concentration compared to total population average.

Exposure concentration difference by racial-ethnic group is shown as colored circle icons, and exposure concentration for income quintiles within in each racial-ethnic category are shown as gray square icons.

## Miscellaneous



This category includes various sources of fuel combustion that did not fit into other sectors: fuel combustion for commercial processes, fuel used in engine testing, and several generic/unspecified source categories. Miscellaneous emission sources are a minor contributor to population-weighted average exposure concentration (2%). These sources do not contribute to high rates of exposure disparity for most demographic groups, although Disadvantaged Communities experience 55% higher exposure concentrations from these sources than the average population. These sources cause moderately higher impacts among Hispanic, Asian, and black populations and lower-income groups, ranging from 9% to 18% higher. As shown in Figure 25, the variation among income groups within racial-ethnic categories is moderate for Asian and White communities but is small for the other categories.

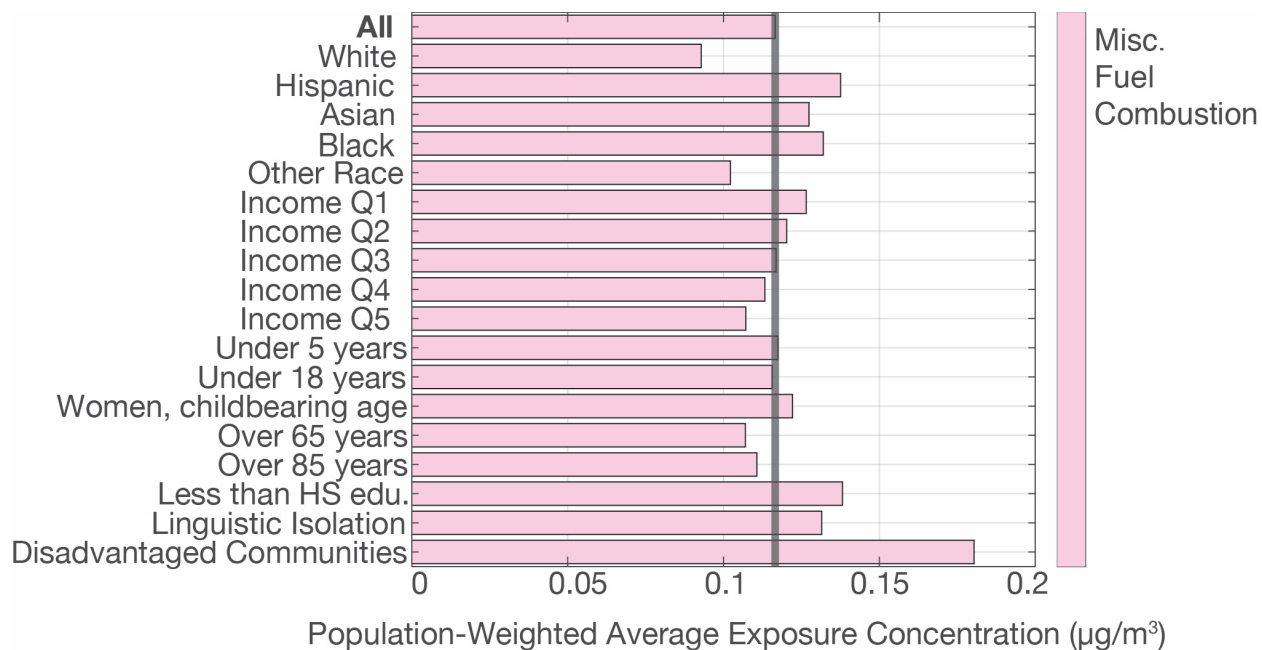


Figure 24: Miscellaneous sources: contribution to population-weighted average exposure concentration for different demographic groups.

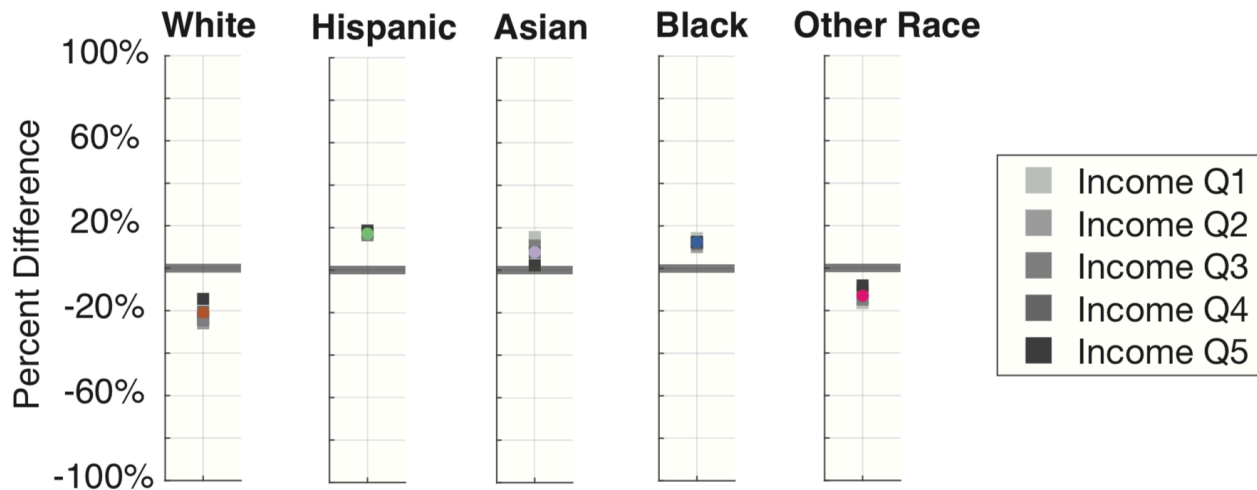
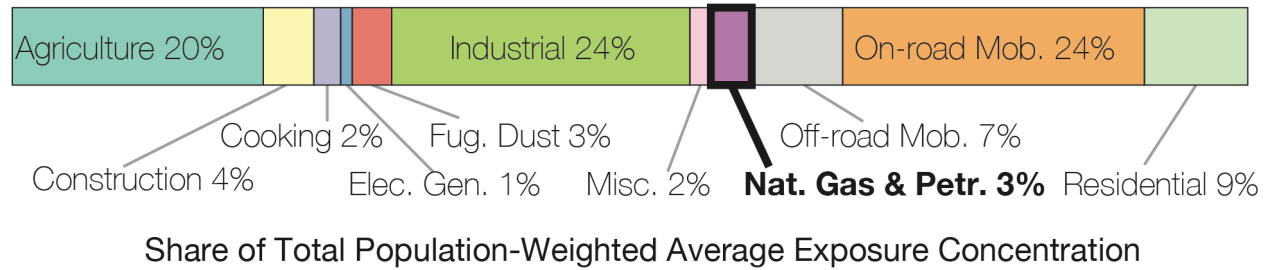


Figure 25: Miscellaneous sources: relative percent differences in population-weighted average  $PM_{2.5}$  concentration compared to total population average.

Exposure concentration difference by racial-ethnic group is shown as colored circle icons, and exposure concentration for income quintiles within in each racial-ethnic category are shown as gray square icons.

## Natural Gas and Petroleum



The natural gas and petroleum industry is considered separately from other industrial activity because it is a major contributor to VOC emissions and is of particular interest for environmental justice concerns. The categories included in this sector are oil and gas production; petroleum refining; petroleum transport, storage, and marketing (TSM); and asphalt manufacturing. This sector is a minor contributor to population-weighted average exposure concentration (3%), and compared with other industrial sector categories it ranks fifth. However, the relative exposure differences from this category are substantial. Disadvantaged communities experience 70% higher exposure concentrations from this category than the population as a whole, with 102% higher exposure from refinery operations. This sector also has a disproportionate impact on the black population and to a lesser degree the Hispanic population, as well as those with less than a high school education and the linguistically isolated population.

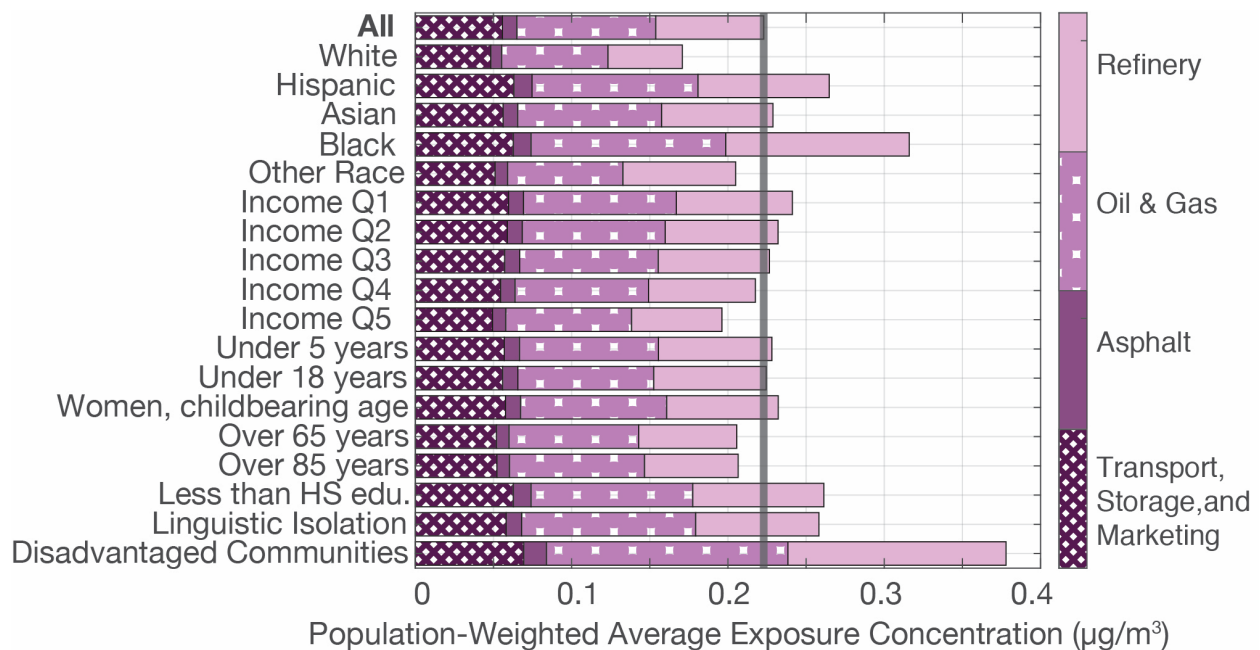


Figure 26: Natural gas and petroleum: contribution to population-weighted average exposure concentration for different demographic groups.

The relative impacts of the natural gas and petroleum industry are higher for the black population than any other, particularly from refinery activities. Counter-intuitively, exposure disparity from refinery operations is greater for higher-income sections of the black community, while the opposite is true for oil & gas development. More generally, exposure concentration patterns by income are inconsistent within and across racial-ethnic groups, with no consistent income patterns within the Hispanic and Asian populations.

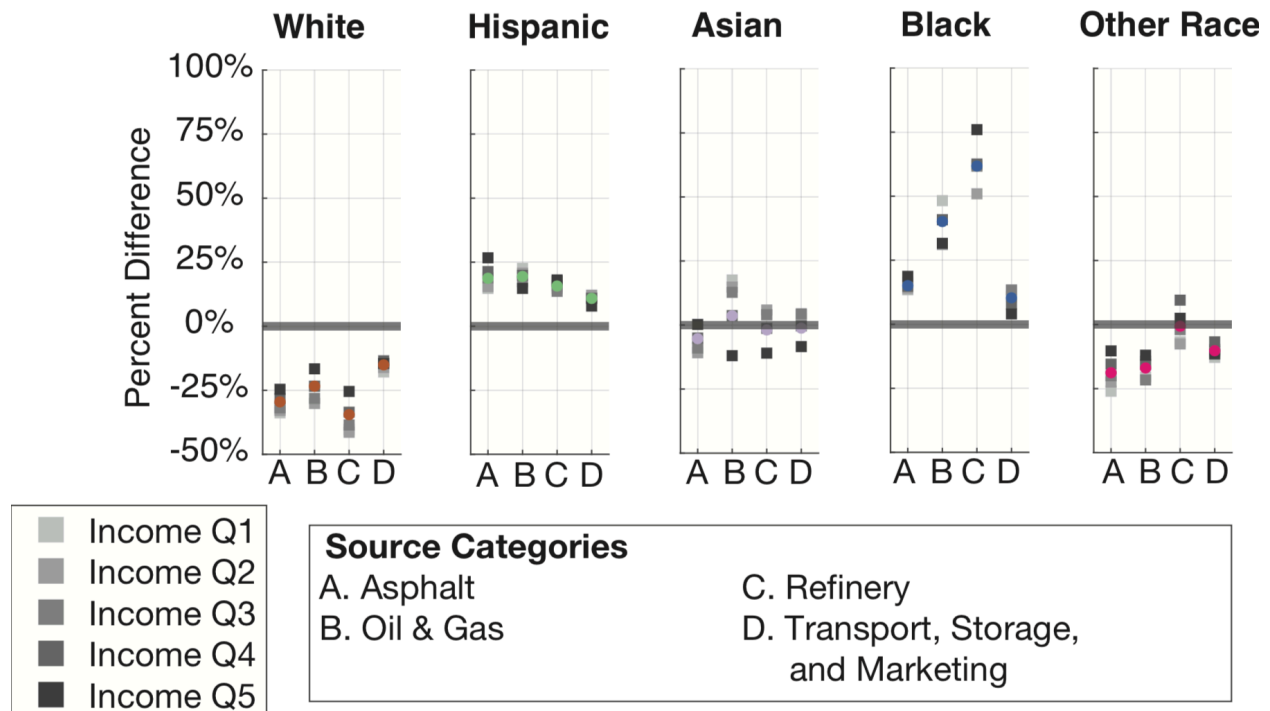
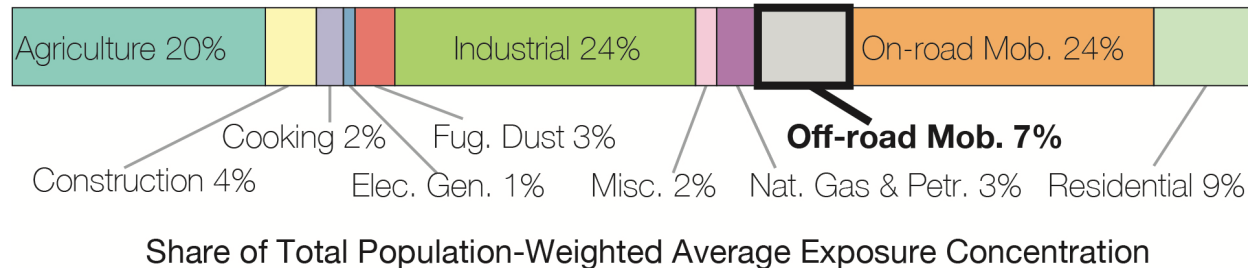


Figure 27: Natural gas and petroleum: relative percent differences in population-weighted average  $PM_{2.5}$  concentration compared to total population average.

Exposure concentration difference by racial-ethnic group is shown as colored circle icons, and exposure concentration for income quintiles within in each racial-ethnic category are shown as gray square icons.

## Off-Road Mobile Sources



This sector includes emissions from a diverse range of mobile equipment that operate off-road. They include three major means of passenger and goods transport – aircraft, marine, and rail – as well as a variety of industrial, commercial, and recreational equipment powered by diesel, gasoline, or an alternative fuel. Several categories of off-road mobile sources are accounted for in other sectors: equipment used for agriculture or construction are featured in their respective sections, and lawn and garden equipment are featured in the residential section.

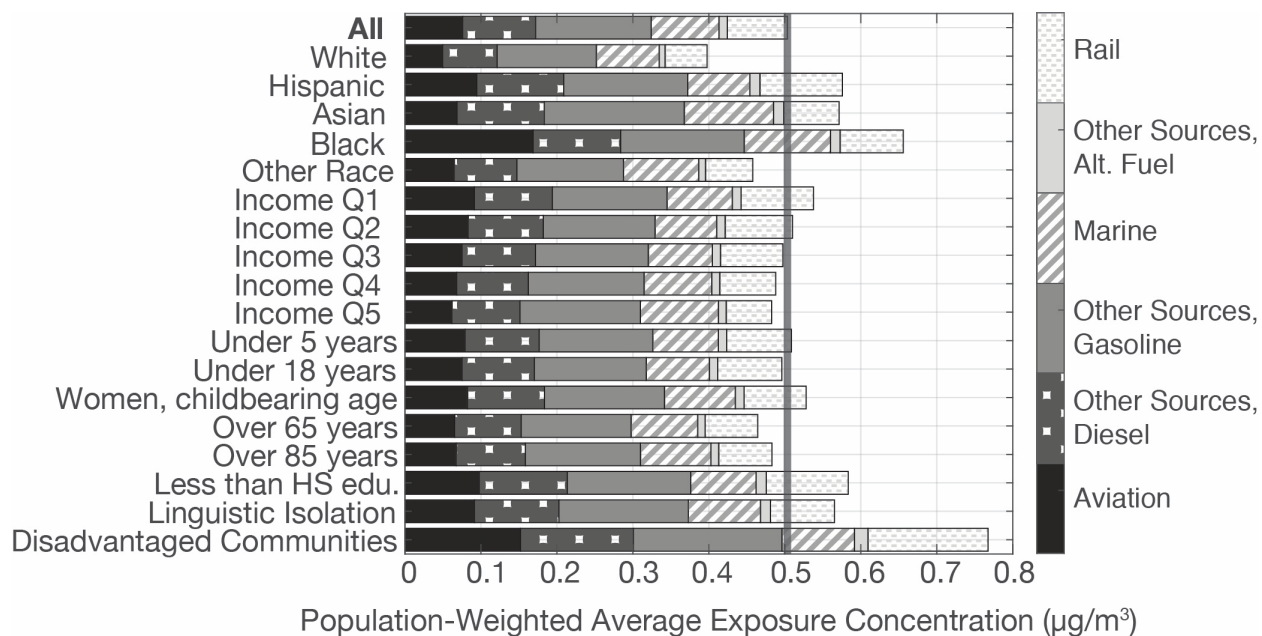


Figure 28: Off-road mobile sources: contribution to population-weighted average exposure concentration for different demographic groups.

Off-road mobile sources are the fifth-largest contributor to population-weighted average exposure concentration (7%). Emissions from off-road mobile sources are of comparable magnitude to on-road mobile sources, but the more remote location of off-road emissions decreases the resulting exposure concentration. Exposure concentrations are higher than average for Hispanic, Asian, and black populations. The difference for the Hispanic population is driven by rail emissions, while the difference for

the Asian population is driven by marine and gasoline vehicles, and the difference for the black population is driven by aircraft. High exposure concentration in Disadvantaged Communities is driven equally by rail and aircraft, followed by other diesel and gasoline sources. The variation in exposure disparity rates among income categories within racial-ethnic groups is small relative to differences between groups. Exposure concentrations from off-road sources are not consistently higher for low-income categories, and exposure concentrations from marine sources are higher for the highest income category across all racial-ethnic groups.

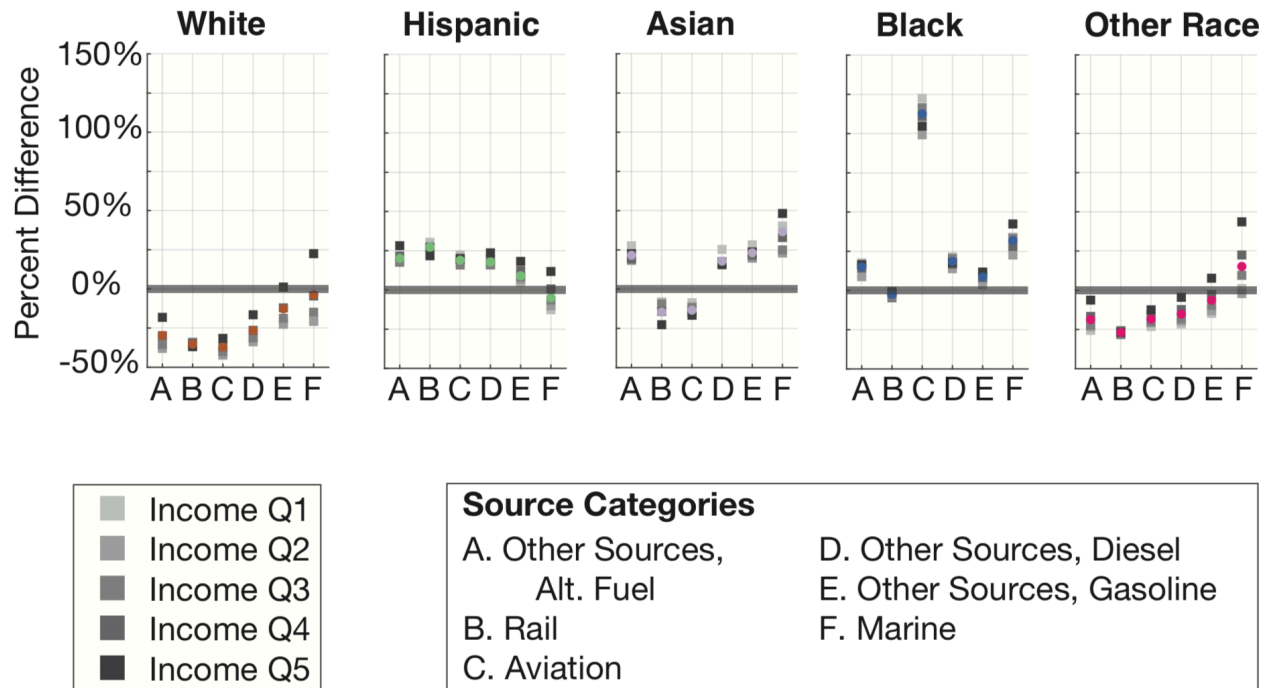
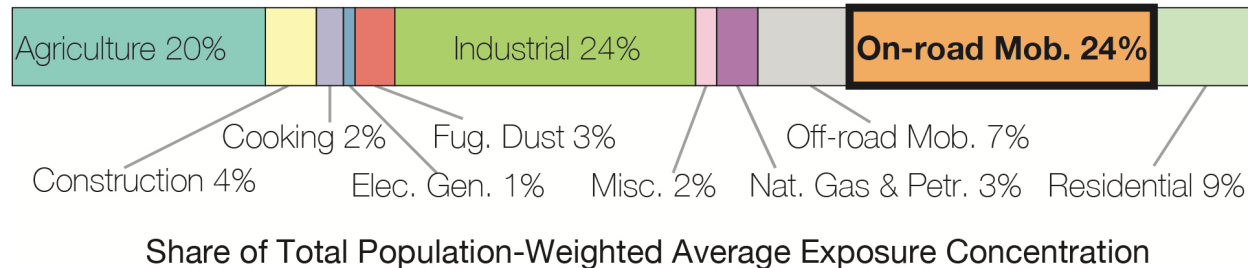


Figure 29: Off-road mobile sources: relative percent differences in population-weighted average  $PM_{2.5}$  concentration compared to total population average.

Exposure concentration difference by racial-ethnic group is shown as colored circle icons, and exposure concentration for income quintiles within in each racial-ethnic category are shown as gray square icons.

## On-Road Mobile Sources



On-road mobile sources include light-, medium- and heavy-duty vehicles used for passenger transport, goods transport, and municipal services. This sector accounts for tailpipe, brake, and tire-wear emissions from mobile sources as well as fugitive VOC emissions at fueling stations. On-road mobile sources are the largest contributor to NO<sub>x</sub> emissions in the modeling domain, and a major contributor to primary PM<sub>2.5</sub> and VOCs.

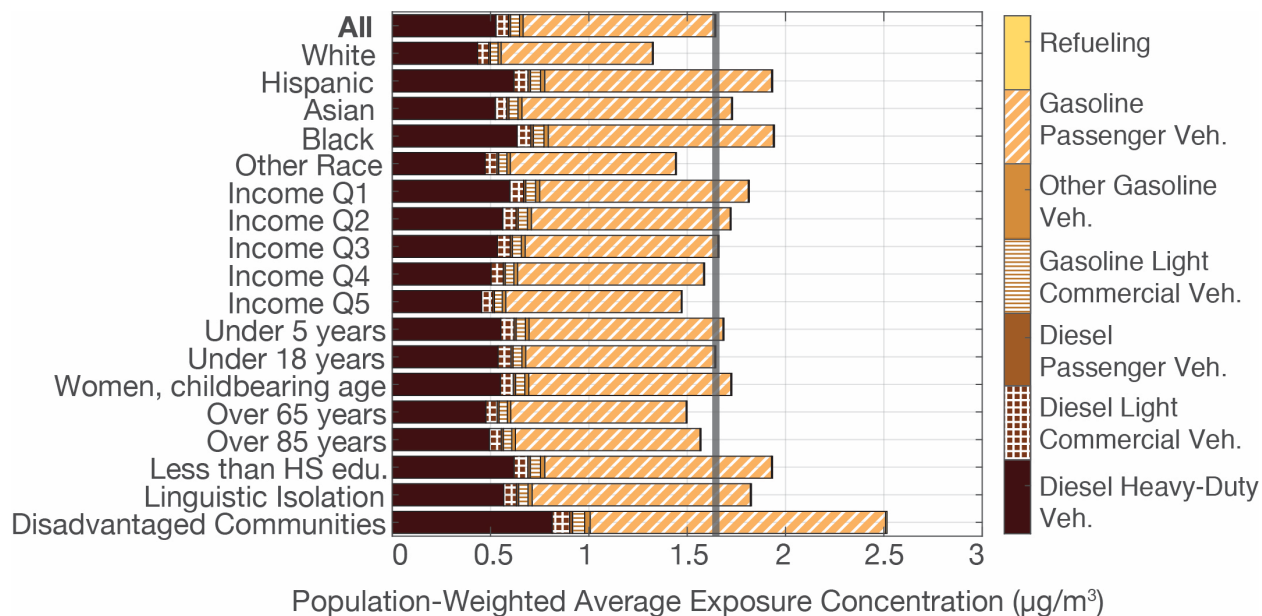


Figure 30: On-road mobile sources: contribution to population-weighted average exposure concentration for different demographic groups.

On-road mobile sources are matched with the industrial sector as the top contributor to population-weighted average exposure concentration (24%). Exposure concentration from this sector is strongly dominated by gasoline passenger vehicles and diesel heavy-duty vehicles. The average exposure concentration for Disadvantaged Communities is 53% higher than for the population as a whole. Both Hispanic and black populations experience approximately 20% higher exposure concentration from both of these categories compared with the population average. Asian populations experience 10% higher exposure concentration from gasoline passenger vehicles but slightly lower-than-average exposure concentration from diesel heavy-duty vehicles. Exposure

concentration is inversely related to income level among the population as a whole, but patterns are mixed for income categories within racial-ethnic groups.

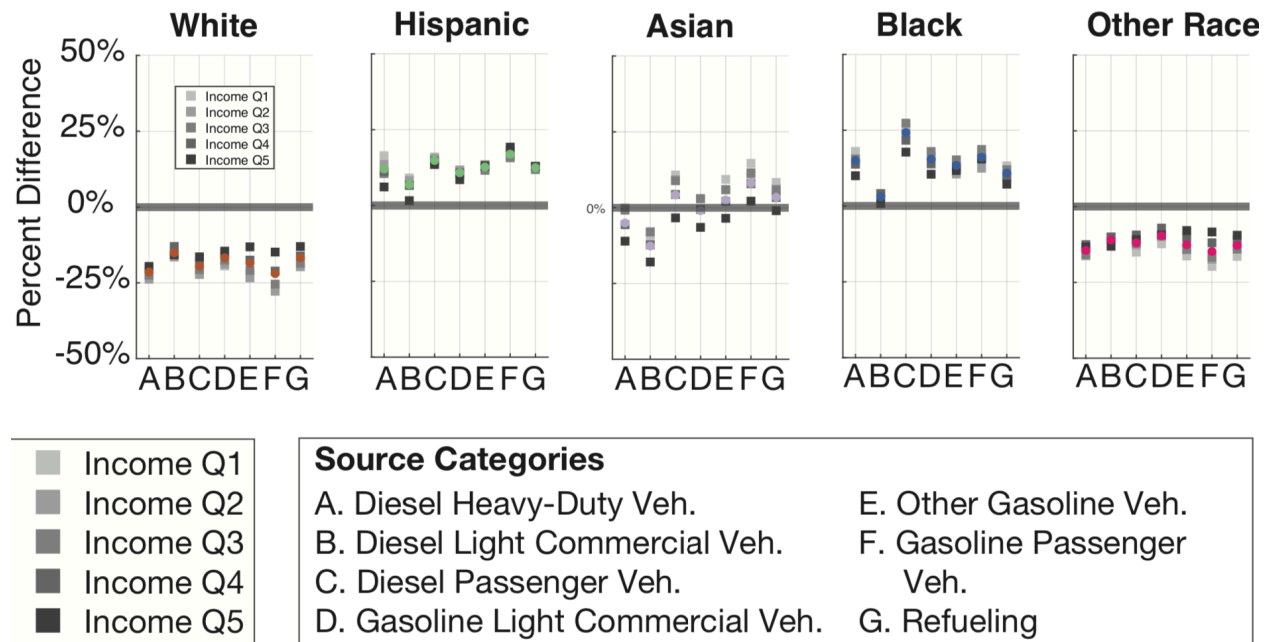
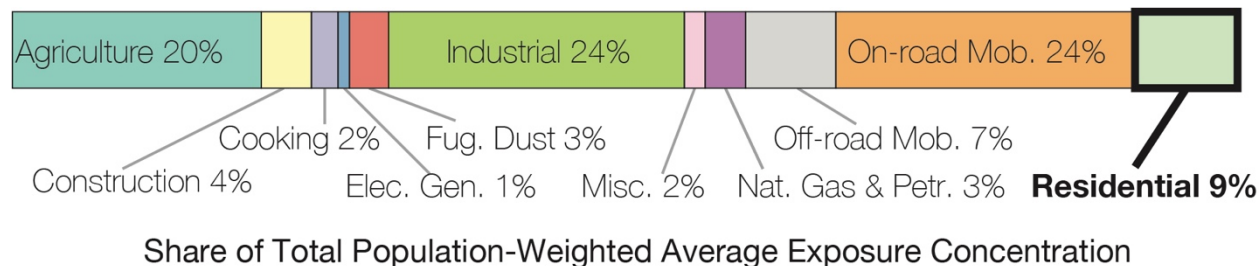


Figure 31: On-road mobile sources: relative percent differences in population-weighted average  $PM_{2.5}$  concentration compared to total population average.

Exposure concentration difference by racial-ethnic group is shown as colored circle icons, and exposure concentration for income quintiles within in each racial-ethnic category are shown as gray square icons.

## Residential Sources



Residential emissions sources include burning of wood, natural gas, and other fuels; residential solvent use; and lawn and gardening equipment. This sector is the fourth-largest contributor to population-weighted average exposure concentration (9%), but contributes less to exposure disparity than the other sectors. The dominant sources of exposure concentration within this category are residential natural gas use and wood fireplaces, followed by lawn & gardening equipment and solvent use. This sector results in 11% higher exposure concentrations for Disadvantaged Communities compared to the population as a whole, but some sources offset others: outdoor emissions from residential natural gas burning result in 43% higher exposure concentrations for Disadvantaged communities, while woodstoves result in substantially lower exposure. Overall, this sector has only a slightly higher impact for some racial-ethnic groups (Hispanic and Asian), but exposure concentration disparity varies substantially by emissions source category. As shown in Figure 33, natural gas, lawn & garden, and solvent use all disproportionately expose Hispanic and black populations, while the reverse is true for wood fireplace emissions.

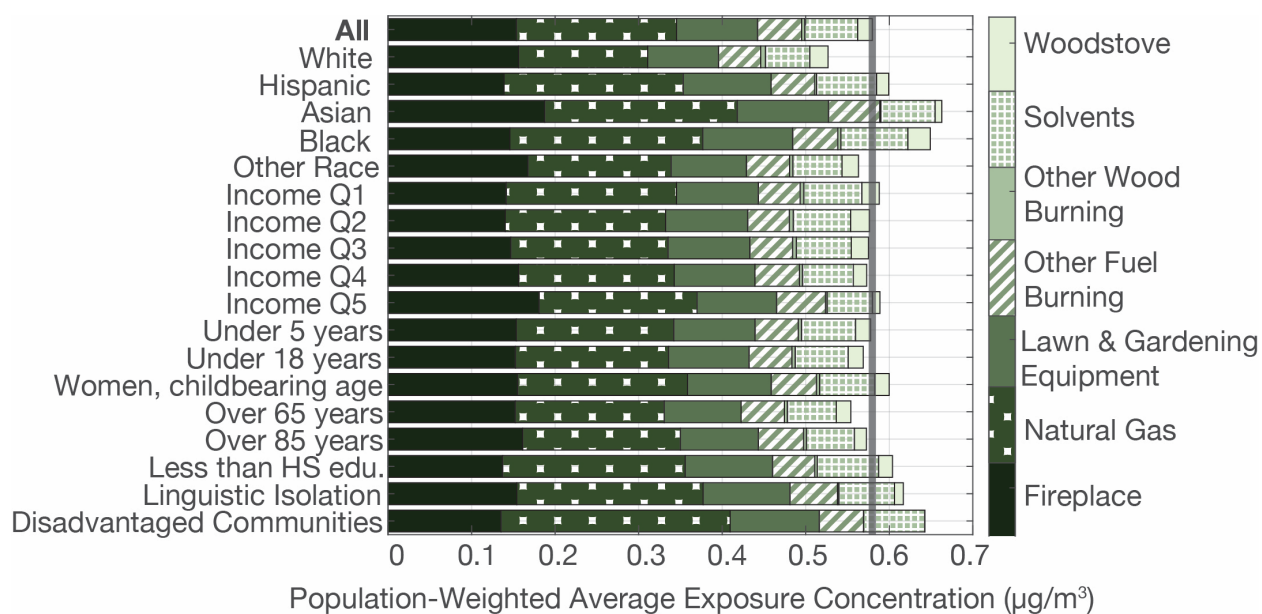


Figure 32: Residential sector: contribution to population-weighted average exposure concentration for different demographic groups.

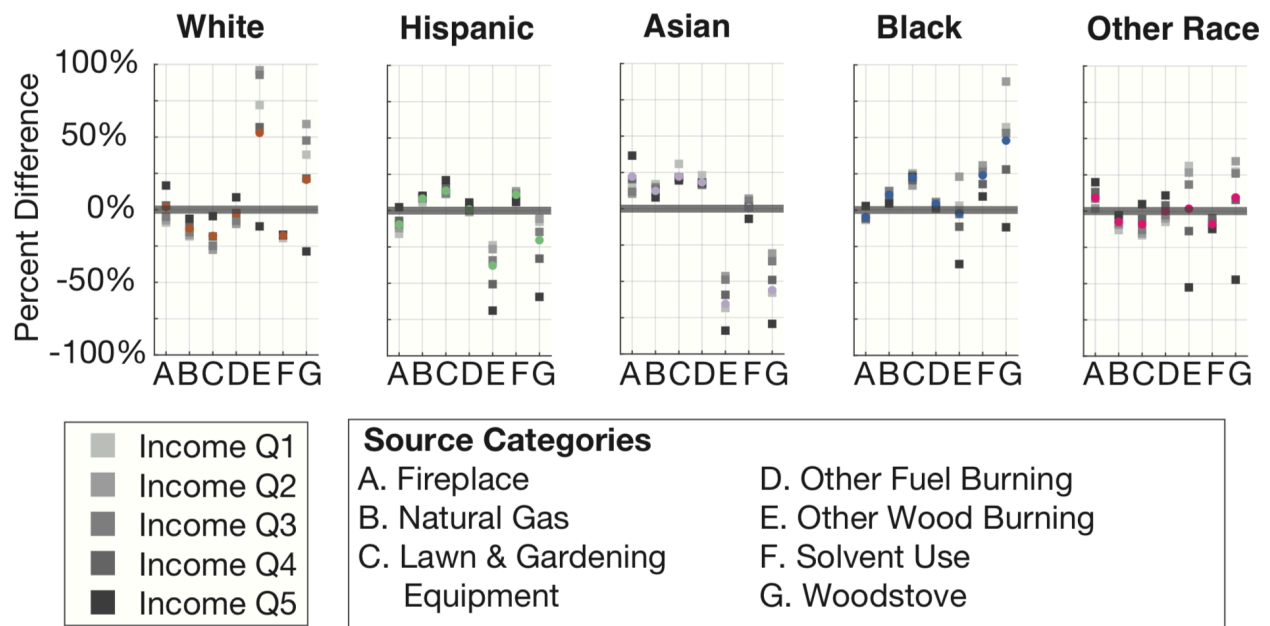


Figure 33: Residential sector: relative percent differences in population-weighted average  $PM_{2.5}$  concentration compared to total population average.

Exposure concentration difference by racial-ethnic group is shown as colored circle icons, and exposure concentration for income quintiles within in each racial-ethnic category are shown as gray square icons.

## Discussion

This report presents a new methodology for deriving source-specific EJ metrics for screening-level policy analysis. The reduced-complexity model we use provides several novel aspects to this analysis. First, it allows both high spatial resolution and broad geographic coverage. We see from the analysis of iFs that this high spatial resolution is important for detecting differences in intake and exposure concentration among different demographic groups due to small-scale variation in race-ethnicity and income levels, a finding that also been shown in other studies (Su et al. 2015, Paoletta et al. 2018). The geographic breadth of the modeling provides a spatial database of intake metrics that can be applied consistently across all regions of the state of California, in contrast to previous studies that used more geographically restricted modeling and only provided comparisons among a select group of regions. The computational efficiency of the reduced-form model also allows for many repeated model runs, enabling us to analyze intake and EJ impacts for a detailed and comprehensive set of emission sources. This level of detail reveals several source-specific patterns that would not have emerged from an analysis of broader emission categories, and it provides a set of source-specific iF values that can be applied in future studies connecting reductions in sector emissions with reductions in intake for different communities and demographic groups.

### Findings From the iF Spatial Database

The database of metrics available from this project can facilitate intake and EJ analysis, either simplified or highly detailed, by translating emissions changes into health-relevant metrics. For a rough approximation of state-wide intake changes resulting from state-level emission control measures, population-weighted iF values<sup>12</sup> can be multiplied with the proposed emission changes, in line with methods described by Humbert et al. 2011, giving the state-scale intake differences by race-ethnicity, income, etc. This calculation may be useful for a first-level estimate of impacts when the geographic distribution of emissions changes and specific target sector is unknown. For a state-wide reduction of emissions from a specific source category (e.g., waste disposal, industrial solvent use, on-road passenger vehicles, etc.), source-specific iF values<sup>13</sup> can be used to calculate the total expected reduction of PM<sub>2.5</sub> intake from a proposed emissions change. The EJ implications of that emissions reduction can be analyzed by considering the difference in per-capita intake changes among the demographic groups of interest.<sup>14</sup>

Another major analytical use of the iF database is to compare the efficiency of control strategies by source and by pollutant. The variation of iF among source categories reflects a substantial sector-to-sector difference in the potential to reduce PM<sub>2.5</sub> exposure through reductions of primary or precursor emissions: on-road mobile sources, construction, and outdoor emissions from commercial cooking and residential sources all have an outsized effect on PM<sub>2.5</sub> exposure concentrations due to their

---

<sup>12</sup> Appendix D, Table D2 – D3

<sup>13</sup> Table D10

<sup>14</sup> Age-, race-ethnicity-, and income-specific iF values by source category are not reproduced in print but are available in the accompanying spreadsheet described in Appendix F.

proximity to urban areas. In contrast, pollution associated with electricity generation and agriculture has a lower impact on exposure concentrations relative to emissions levels. Impacts of different sectors also vary by the share of pollution emitted as precursors in addition to primary PM<sub>2.5</sub>. Primary PM<sub>2.5</sub> contributes more to overall PM<sub>2.5</sub> intake than any other pollutants, but in combination precursor species account for the majority of PM<sub>2.5</sub> intake, given their significantly greater emissions rates. This balance is visually demonstrated at the broad level in Figure 9, which ranks sector categories and shows intake for the total population. A more detailed analysis of the state-wide exposure concentration change for specific demographic groups and subsectors can be conducted with the source- and demographic-specific iF values provided in the accompanying spreadsheet, and policymakers can pair these iF values with emission control cost estimates to identify cost-efficient options from an array of potential emission control strategies. However, intake and EJ metrics calculated from population- or emissions-weighted average values are broad estimates to be used as guideline values, and cost-effectiveness estimates of specific emission control measures should be verified with more complex modeling.

Some additional conclusions can be drawn from summary statistics and maps of the iF database, which broadly characterize spatial and pollutant-specific patterns: iF is consistently highest for primary PM<sub>2.5</sub> and lower for precursors, consistent with patterns reported in the literature. Considering the interquartile range of values (25<sup>th</sup> to 75<sup>th</sup> percentile values), we see population-weighted values vary by 200% to 400% between upper and lower quartiles, indicating the wide range of conditions in communities across California. Furthermore, emissions-weighted upper and lower quartiles span an order of magnitude, reflecting the fact that the emissions sources are not distributed in proportion to population density, leading to substantial variation in sector-specific iFs (Appendix D). This shows that a spatially explicit iF database provides a stronger basis for comparing sector impacts than archetypal or summary values. For regional-scale emission reductions it is more appropriate to use spatially explicit iF values included in the spatial database, following the example provided on pages 20-21 of the methods section.

In addition to more accurately representing sector impacts, using a model with high spatial resolution in highly populated areas is critical in the identification of environmental justice issues. Su et al. identified significant within-county and within-neighborhood variation in environmental risk from diesel PM exposure (Su et al., 2012). This pattern is not well characterized by population-weighted summary statistics of iF but appears clearly in iF maps of urban areas (Figure 7 and Figure 8). Ground-level iF for primary PM<sub>2.5</sub> – analogous to DPM – is highly sensitive to demographic heterogeneity, in line with the findings of Su et al. Furthermore, localized difference in iF across racial-ethnic categories is also apparent in elevated emissions of precursor species, although these have weaker gradients and less sensitivity to high-resolution population patterns. This shows how within a single county there may be highly effective emission reduction targets for EJ goals.

Although we only highlighted two pollutants in Los Angeles, the database could be used to look at other counties or air basins and consider a wider range of pollutants.

### Sector-Specific Environmental Justice Impacts

The fundamental finding of the sector-specific environmental justice analysis is that groups of lower socioeconomic status – non-white, low-income, low educational attainment, or linguistically isolated groups – systematically experience higher PM<sub>2.5</sub> exposure concentration from all emissions categories. This finding reinforces the conclusions of earlier studies and indicates that there are still major environmental justice issues to confront in PM<sub>2.5</sub> control strategies in California. A more detailed review of the results shows that the magnitude of exposure concentration disparity varies by source category. Two of the highest-impact sectors – industrial and on-road mobile sources – are also major contributors to exposure concentration disparity by race-ethnicity and income group. These are both clear targets for emission reductions measures, and the breakdown of impacts by subsector categories suggests possible reduction strategies within the sector. Some minor sectors show a high relative percent difference in exposure concentrations for low-income or non-white groups – these may also be useful targets, as a small emissions reduction would provide more benefits for exposure concentration equality. For many of these minor sectors, patterns vary substantially among demographic groups.

The findings of this study align with the results of earlier work, both in the overall magnitude of disparity and demographic patterns. Marshall et al. (2006) estimated that within the South Coast Air Basin, the white population experienced 15% lower DPM exposure, while Hispanic, Black, and Asian/Pacific Islander populations experienced 20%, 15%, and 10% higher exposure. Our findings are similar, even when including the population of the whole state and secondary PM in the calculation: 18% lower PM<sub>2.5</sub> exposure concentration among the white population, and 17%, 15%, and 6% higher exposure concentrations among Hispanic, Black, and Asian populations. Su et al. (2012) also observed significant patterns of inequality in DPM exposure for non-white communities. In contrast with our results, Su et al. observed that patterns of inequality in total PM<sub>2.5</sub> were much weaker. We find that non-diesel sources that predominately produce secondary PM<sub>2.5</sub> are among the largest contributors to exposure concentration disparity—for example, on-road gasoline vehicles, petroleum refining, transport and storage of industrial materials, and livestock production.

The relative importance of race-ethnicity vs. income in exposure concentration disparity is often considered in EJ studies. Su et al. (2012) found that patterns of inequality based on poverty level were similar to those based on race-ethnicity but noted that there is significant correlation between the two variables. We account for this correlation by dividing each racial-ethnic group by income level and noting how patterns differ when comparing the highest income quartile across all races vs. the lowest (Figure 11 and similar figures within subsector analyses). The broad conclusion is that while exposure concentration varies by income within a racial-ethnic group, the within-group variation is generally small compared to the differences among racial-ethnic groups; in other words, the high-income segment of a non-white group is typically still exposed to higher PM<sub>2.5</sub>

concentrations than the low-income segment of the white group. This generally matches findings that racial-ethnic divides in exposure still exist when controlling for income (Clark et al., 2017).

## Summary and Conclusions

This project demonstrates a new methodology for conducting a screening-level analysis to estimate the impacts in exposure concentration and EJ-relevant disparity levels from changes in both primary and precursor emissions from different sectors. While this report presents the central findings from this modeling work, this work also produced a highly detailed set of iF, intake and EJ metrics, available in the appendices and accompanying data files, that allow further investigation of the relative magnitudes of public health benefits of different control measures. Summary statistics of state-wide iF values – population- or emissions-weighted averages – provide the basis for comparing the efficiency of different control measures at reducing exposure concentration levels for different demographic groups. However, the spatial database of iF values provides a stronger basis for calculating the effects of regionally-targeted emissions reductions. Within the iF database we found strong spatial variation in iF for different demographic groups and for both primary and precursor species, suggesting that a high-resolution, spatially explicit database is required to adequately characterize exposure concentration differences among different populations.

The strength of this screening tool is to show how all major sectors contribute to exposure concentration disparity, to provide a comparison of the relative contribution to exposure concentration from different sources within a sector, and to compare levels of exposure concentration disparity among demographic groups. However, model limitations should be considered when interpreting these results. The concentration values presented do not represent total population exposure to PM<sub>2.5</sub> (see Appendix B). Because simplifying assumptions limit the precision of exposure concentration estimates, in cases where differences in modeled exposure concentration are very small, those differences may only reflect model uncertainty and not a meaningful pattern in exposure concentrations. The influence of secondary PM<sub>2.5</sub> is critical for comparing among sources, but due to uncertainties in secondary PM<sub>2.5</sub> formation rates, the relative impact of sources dominated by single precursor species (e.g., agriculture) should be interpreted with care. This tool is not designed to definitively quantify PM<sub>2.5</sub> exposure concentration but instead to complement other research tools, aiding policy development by identifying potential high-impact targets for emission control and suggesting fruitful avenues for more complex modeling.

In applying a reduced-complexity model to the 2014 emissions inventory, we find significant disparity in PM<sub>2.5</sub> exposure concentration by race, income category, and other socioeconomic indicators. We find that the major sources of PM<sub>2.5</sub> exposure concentration within the domain – the industrial sector and on-road mobile sources– are also the major sources of exposure concentration disparity by race and income. There is no single culprit for exposure concentration disparity: among major emissions sectors, different emissions categories have differential effects by racial-ethnic, income, or other

grouping. Some minor categories also have outsized impacts on single demographic groups. This suggests that (1) a cross-sector approach to emission control is necessary to address EJ issues, and (2) particular groups may find it beneficial to identify specific localized sources within a sector category that pollute their community.

## Recommendations for Further Research

The iF spatial database and source-specific impact estimates created for this project provide a rich, complex source of information that can be analyzed among many dimensions beyond the state-wide source ranking analysis chosen for this report. The source-specific EJ metrics described here are applicable at the state level; the creation of region-specific sets of EJ metrics was beyond the scope of this report. However, the spatial database of iF values provides the means to create a similar ranking of sources from a regional emissions inventory; region-specific analyses may reveal that local patterns of exposure concentration disparity vary from those observed in the state as a whole. Although the population data used to calculate iF would not be limited to the given region, and thus the total intake values would be overestimated, the source rankings and relative rates of disparity would be generally indicative of more localized conditions. Additionally, the Source-Receptor matrix created for this report is available by request and may be used to directly model concentration changes. Taking advantage of the spatial aspect of the tool, future use may also include generating maps of per-capita statistics to identify regions of the state where sources contribute most to exposure concentration disparity or exposure concentrations in particular communities.

Other future steps for this model may include an update to the baseline CTM input, addressing the change in secondary  $PM_{2.5}$  formation rates that occur as a result of reductions in emissions of precursor species. As an extension, sensitivity of the model to large or small perturbations in precursor emissions could be informed by a limited set of additional CTM runs with varied emissions inputs.

## References

- Apte, J. S., Bombrun, E., Marshall, J. D., & Nazaroff, W. W. (2012). Global intraurban intake fractions for primary air pollutants from vehicles and other distributed sources. *Environmental Science & Technology*, 46(6), 3415–3423. <https://doi.org/10.1021/es204021h>
- Bell, M. L., Dominici, F., Ebisu, K., Zeger, S. L., & Samet, J. M. (2007). Spatial and Temporal Variation in PM<sub>2.5</sub> Chemical Composition in the United States for Health Effects Studies. *Environmental Health Perspectives*, 115(7), 989–995. <https://doi.org/10.1289/ehp.9621>
- Bennett, D. H., McKone, T. E., Evans, J. S., Nazaroff, W. W., Margni, M. D., Jolliet, O., & Smith, K. R. (2002). Defining intake fraction. *Environmental Science & Technology*, 36(9), 206A-211A. <https://doi.org/10.1021/es0222770>
- Burnett, R. T., Pope III, C. A., Ezzati, M., Olives, C., Lim, S. S., Mehta, S., ... Cohen, A. (2014). An integrated risk function for estimating the global burden of disease attributable to ambient fine particulate matter exposure. *Environmental Health Perspectives*, 122(4), 397–403. <https://doi.org/10.1289/ehp.1307049>
- Clark, L. P., Millet, D. B., & Marshall, J. D. (2017). Changes in transportation-related air pollution exposures by race-ethnicity and socioeconomic status: Outdoor nitrogen dioxide in the United States in 2000 and 2010. *Environmental Health Perspectives*, 125(9). Retrieved from <https://doi.org/10.1289/EHP959>
- Cushing, L. J., Wander, M., Morello-Frosch, R., Pastor, M., Zhu, A., & Sadd, J. (2016). *A preliminary environmental equity assessment of California's cap-and-trade program* (p. 18). USC Dornsife Program for Environmental and Regional Equity. Accessed 5 September 2019, < <https://dornsife.usc.edu/PERE/enviro-equity-CA-cap-trade> >
- Evans, J. S., Wolff, S. K., Phonboon, K., Levy, J. I., & Smith, K. R. (2002). Exposure efficiency: An idea whose time has come? *Chemosphere*, 49(9), 1075–1091.
- Fantke, P., Jolliet, O., Apte, J. S., Hodas, N., Evans, J. S., Weschler, C. J., ... McKone, T. E. (2017). Characterizing aggregated exposure to primary particulate matter: Recommended intake fractions for indoor and outdoor sources. *Environmental Science & Technology*, 51(16), 9089–9100. <https://doi.org/10.1021/acs.est.7b02589>
- Faust, J., August, L., Bangia, K., Galaviz, V., Leichty, J., Prasad, S., ... Zeise, L. (2017). *CalEnviroScreen 3.0: Update to the California Communities Environmental Health Screening Tool*. Retrieved from Office of Environmental Health Hazard Assessment website: <https://oehha.ca.gov/media/downloads/calenviroscreen/report/ces3report.pdf>
- Gilmore, E. A., Heo, J., Muller, N. Z., Tessum, C. W., Hill, J., Marshall, J., & Adams, P. J. (2019). An inter-comparison of air quality social cost estimates from reduced-complexity models. *Environmental Research Letters*. <https://doi.org/10.1088/1748-9326/ab1ab5>
- Greco, S. L., Wilson, A. M., Spengler, J. D., & Levy, J. I. (2007). Spatial patterns of mobile source particulate matter emissions-to-exposure relationships across the United States. *Atmospheric Environment*, 41(5), 1011–1025. <https://doi.org/10.1016/j.atmosenv.2006.09.025>

- Hauschild, M. Z., Goedkoop, M., Guinée, J., Heijungs, R., Huijbregts, M., Jolliet, O., ... Pant, R. (2013). Identifying best existing practice for characterization modeling in life cycle impact assessment. *The International Journal of Life Cycle Assessment*, 18(3), 683–697. <https://doi.org/10.1007/s11367-012-0489-5>
- Humbert, S., Manneh, R., Shaked, S., Wannaz, C., Horvath, A., Deschênes, L., ... Margni, M. (2009). Assessing regional intake fractions in North America. *Science of the Total Environment*, 407(17), 4812–4820.
- Humbert, S., Marshall, J. D., Shaked, S., Spadaro, J. V., Nishioka, Y., Preiss, P., ... Jolliet, O. (2011). Intake fraction for particulate matter: Recommendations for life cycle impact assessment. *Environmental Science & Technology*, 45(11), 4808–4816. <https://doi.org/10.1021/es103563z>
- Krewski, D. (2009). Evaluating the effects of ambient air pollution on life expectancy. *New England Journal of Medicine*, 360(4), 413–415. <https://doi.org/10.1056/NEJMe0809178>
- Laden, F., Schwartz, J., Speizer, F. E., & Dockery, D. W. (2006). Reduction in Fine Particulate Air Pollution and Mortality. *American Journal of Respiratory and Critical Care Medicine*, 173(6), 667–672. <https://doi.org/10.1164/rccm.200503-443OC>
- Lai, A. C. K., Thatcher, T. L., & Nazaroff, W. W. (2011). Inhalation transfer factors for air pollution health risk assessment. *Journal of the Air & Waste Management Association*, 50(9), 1688–1699. <https://doi.org/10.1080/10473289.2000.10464196>
- Lamancusa, C., Parvez, F., & Wagstrom, K. (2017). Spatially resolved intake fraction estimates for primary and secondary particulate matter in the United States. *Atmospheric Environment*, 150, 229–237. <https://doi.org/10.1016/j.atmosenv.2016.11.010>
- Lobscheid, A. B., Nazaroff, W. W., Spears, M., Horvath, A., & McKone, T. E. (2012). Intake fractions of primary conserved air pollutants emitted from on-road vehicles in the United States. *Atmospheric Environment*, 63, 298–305. <https://doi.org/10.1016/j.atmosenv.2012.09.027>
- Marshall, J. D. (2008). Environmental inequality: Air pollution exposures in California's South Coast Air Basin. *Atmospheric Environment*, 42(21), 5499–5503. <https://doi.org/10.1016/j.atmosenv.2008.02.005>
- Marshall, J. D., & Behrentz, E. (2005). Vehicle self-pollution intake fraction: Children's exposure to school bus emissions. *Environmental Science & Technology*, 39(8), 2559–2563. <https://doi.org/10.1021/es040377v>
- Marshall, J. D., Granvold, P. W., Hoats, A. S., McKone, T. E., Deakin, E., & Nazaroff, W. W. (2006). Inhalation intake of ambient air pollution in California's South Coast Air Basin. *Atmospheric Environment*, 40(23), 4381–4392. <https://doi.org/10.1016/j.atmosenv.2006.03.034>
- Marshall, J. D., & Nazaroff, W. W. (2004). *Using intake fraction to guide ARB policy choices: The case of particulate matter*. Sacramento, California: California Air Resources Board. Accessed 5 September 2019 <https://depts.washington.edu/airqual/reports/MARSHALL%20and%20NAZAROFF%20-%20IF%20and%20PM.doc>

- Marshall, J. D., & Nazaroff, W. W. (2002). *Risk Assessment of Diesel-Fired Back-up Electric Generators Operating in California*. Oakland, California: Environmental Defense. Accessed 11 November 2019  
<https://depts.washington.edu/airqual/reports/MARSHALL%20and%20NAZAROFF%20-%20Diesel%20BUGs%20Health%20Risk%20Assessment.pdf>
- Marshall, J. D., Swor, K. R., & Nguyen, N. P. (2014). Prioritizing environmental justice and equality: Diesel emissions in Southern California. *Environmental Science & Technology*, 48(7), 4063–4068. <https://doi.org/10.1021/es405167f>
- Marshall, J. D., Teoh, S.-K., & Nazaroff, W. W. (2005). Intake fraction of nonreactive vehicle emissions in US urban areas. *Atmospheric Environment*, 39, 1363–1371. <https://doi.org/10.1016/j.atmosenv.2004.11.008>
- Meng, Y.-Y., Rull, R. P., Wilhelm, M., Lombardi, C., Balmes, J., & Ritz, B. (2010). Outdoor air pollution and uncontrolled asthma in the San Joaquin Valley, California. *Journal of Epidemiology and Community Health*, 64(2), 142–147. <https://doi.org/10.1136/jech.2009.083576>
- Nguyen, N. P., & Marshall, J. D. (2018). Impact, efficiency, inequality, and injustice of urban air pollution: Variability by emission location. *Environmental Research Letters*, 13(2), 024002. <https://doi.org/10.1088/1748-9326/aa9cb5>
- Patel, M. M., Hoepner, L., Garfinkel, R., Chillrud, S., Reyes, A., Quinn, J. W., ... Miller, R. L. (2009). Ambient metals, elemental carbon, and wheeze and cough in New York City children through 24 months of age. *American Journal of Respiratory and Critical Care Medicine*, 180(11), 1107–1113. <https://doi.org/10.1164/rccm.200901-0122OC>
- Schiferl, L. D., Heald, C. L., Nowak, J. B., Holloway, J. S., Neuman, J. A., Bahreini, R., ... Murphy, J. G. (2014). An investigation of ammonia and inorganic particulate matter in California during the CalNex campaign. *Journal of Geophysical Research: Atmospheres*, 119(4), 1883–1902. <https://doi.org/10.1002/2013JD020765>
- Su, J. G., Jerrett, M., Morello-Frosch, R., Jesdale, B. M., & Kyle, A. D. (2012). Inequalities in cumulative environmental burdens among three urbanized counties in California. *Environment International*, 40, 79–87. <https://doi.org/10.1016/j.envint.2011.11.003>
- Tainio, M., Holnicki, P., Loh, M. M., & Nahorski, Z. (2014). Intake fraction variability between air pollution emission sources inside an urban area. *Risk Analysis*, 34(11), 2021–2034. <https://doi.org/10.1111/risa.12221>
- Tessum, C., Hill, J. D., & Marshall, J. D. (2017). InMAP: A model for air pollution interventions. *PLOS ONE*, 12(4), e0176131. <https://doi.org/10.1371/journal.pone.0176131>
- Tessum, C. W., Hill, J. D., & Marshall, J. D. (2015b). Twelve-month, 12 km resolution North American WRF-Chem v3.4 air quality simulation: Performance evaluation. *Geoscientific Model Development*, 8, 957–973. <https://doi.org/10.5194/gmd-8-957-2015>
- Xu, J., Jin, T., Miao, Y., Han, B., Gao, J., Bai, Z., & Xu, X. (2015). Individual and population intake fractions of diesel particulate matter (DPM) in bus stop microenvironments. *Environmental Pollution*, 207, 161–167. <https://doi.org/10.1016/J.ENVPOL.2015.09.005>

## Glossary of Terms, Abbreviations, and Symbols

<b>Abbreviation Used</b>	
CTM	Chemical Transport Model
DPM	Diesel particulate matter
EJ	Environmental Justice
iF	Intake Fraction
NEI	US EPA National Emissions Inventory
NH <sub>3</sub>	Ammonia
NO <sub>x</sub>	Oxides of nitrogen
PM <sub>2.5</sub>	Fine particulate matter (particles with an aerodynamic diameter ≤ 2.5 μm)
RCM	Reduced-complexity model
SOA	Semi-volatile organic aerosol
SO <sub>2</sub>	Sulfur dioxide
SO <sub>x</sub>	Oxides of sulfur, including sulfur dioxide
TSM	Transport, storage, and marketing
VOC	Volatile organic compound